

The search for myco-hormones in the metabolome of the model
organism *Sordaria macrospora* via LC-MS/MS.

A Thesis Submitted to the Committee on Graduate Studies in Partial

Fulfillment of the Requirement for the Degree of

Master of Science

In the

Faculty of Arts and Science

Trent University

Peterborough, Ontario, Canada

© Copyright by Kimberly Molina-Bean

Environmental and Life Sciences M.Sc. Graduate Program

January 2024

Abstract

The search for myco-hormones in the metabolome of the model organism *Sordaria macrospora* via LC-MS/MS.

Kimberly Molina-Bean

Fungi are a diverse group of organisms that play crucial roles in various ecological processes and have immense economic importance. Understanding the intricate mechanisms underlying fungal growth and development is fundamental to harnessing their potential and exploring their applications in different fields. Signalling molecules, such as hormones, have been identified as key regulators in fungal physiology, orchestrating intricate processes and modulating biological responses to the environment. Phytohormones, commonly associated with plants, have been proposed as potential myco-hormones due to their production in a wide variety of fungi. Metabolomic analyses were performed via LC-MS/MS to investigate the role of phytohormones, specifically cytokinins (CKs) and indole-3-acetic acid (IAA), along with lipids and energetic metabolites such as organic acids during the growth and development of the model fungus *Sordaria macrospora*. The results revealed a clear switch between CK ribosides and CK free bases during the ascosporegenesis stage, with increased levels of cZ and iP and decreased levels of iPR and cZR. A similar pattern was observed in the mutant strain *smgpil* but demonstrating higher levels of CK free bases and increased fruiting body formation compared to the wild type. These findings provide insights into the regulation of phytohormones especially during fungal fruiting body development. In terms of IAA, the levels increased during the transition to sexual development in all strains, with the *per5* mutant, unable to produce lipids via the cytosol, demonstrating a higher concentration than

the wild type. The interplay between energetic metabolites and IAA suggests a potential role in the transition to sexual development. Additionally, the dose-dependent effects of exogenous CK application were investigated, showing the potential of low concentrations, from 1 to 10 μM , of CKs in promoting biomass accumulation or sexual development. Furthermore, gene editing in *S. macrospora* was proposed as a future direction to explore the functions of CKs and other metabolites during fungal development. Overall, this research contributes to our understanding of phytohormone-mediated processes in fungi and opens avenues for future investigations in fungal biology.

Keywords: fungi, sexual development, phytohormone, cytokinin, auxin, myco-hormone, metabolomics, lipidomics, LC-MS

Acknowledgments

I would like to express my gratitude to all the individuals who have supported and guided me throughout this thesis journey. Their contributions and encouragement have been invaluable, and I am deeply grateful for their presence in my life.

First and foremost, I am deeply thankful to my thesis supervisor, **Dr. Neil Emery**. His unwavering support, scientific expertise, and invaluable guidance have been fundamental in shaping this research. I am truly grateful for the opportunities he has provided me, both as an international undergraduate student and as an MSc student in his lab. Without his mentorship, this thesis would not have been possible.

I extend my thanks to **Dr. Anna Kisiala** and **Dr. Erin Morrison**, members of my committee who contributed with their knowledge and insights to my research. Their expertise, guidance, and motivation were instrumental in shaping this thesis. I am grateful for their support and the valuable discussions we had throughout the thesis process.

I would like to acknowledge **Dr. Minou Nowrousian** and **Dr. Stefanie Pöggeler** for generously providing the fungal strains, including the mutants, for my analysis. Their generous assistance and prompt responses have been immensely helpful, their contributions were essential to the success of this research.

I am grateful to **MITACS** for their financial support through the MITACS Globalink Program, which provided me with the opportunity for a research internship, and the MITACS Fellowship Program, which supported my MSc degree. Their funding has been instrumental in facilitating this academic journey.

A special thanks to all the members of the Emery lab, including **Zeynab Azimychetabi, Megan Aoki, Mark Seegobin, Erin Morrison, Anna Kisiala, Ainsely Lewis, Vedanti Ghatwala, Ewart Smith, Stacy James, Peter Andreas, Malaika Persaud, Daniel Palberg, Dev Seneviratne, Imesha Perera, Emma Kaszecki, Nourhene Grich, and Thien Nguyen.** Your collaboration, assistance, and shared passion have made this research experience both productive and enjoyable.

I am deeply appreciative of my friends who have been a source of encouragement, laughter, and support throughout this thesis process. **Zeynab Azimychetabi** and **Megan Aoki**, your assistance with my work and your friendship have made this journey taste the most enjoyable, thank you for being my sunshine, for the best memories, and for your unconditional support. **Mark** and **Carolyn Seegobin**, your warm, sweet, and welcoming home has provided me with comfort and support when I needed it the most. **Diana Chavez**, your unwavering friendship and advice have been invaluable to me. **Smolly Coulson**, thank you for your technical advice, guidance, and to provide me with material during my experiments, but also for all the memories, for listening to me, and for sharing your laugh with me, I feel grateful for sharing gold time with you. To my “changos”, **Maya Peters, Julia Vanderhorst, Shiqi Huang, and Charles Cumberland**, your friendship, positive energy, and shared memories have brought joy to this thesis journey.

A special thank you goes to the Emery family, **Neil, Laurence, Frances, Elise**, and especially to **Jill Emery** for her friendship, warm welcome, and positive energy. Their kindness and support meant a lot to me during this period.

I would like to express my gratitude to all my family for their unconditional love and unwavering support. To my brothers, **Juan Molina-Bean** and **Myron Molina-Bean**,

thank you for your technical assistance and for being a source of advice, scolding, and motivation throughout this thesis journey. To my aunt **Yolis Bean-Quezada**, my second mom, thank you for always listening, providing financial support, and offering me unconditional love. To my uncle **Felipe Molina-Bravo**, thank you for your constant motivation and valuable advice have been instrumental in helping me overcome challenges and strive for excellence throughout the thesis journey. To my best friend and boyfriend, **Jesus Anaya-Lupercio**, thank you for being there for me, always offering me your support, hugs, and advice even from a distance, your presence has been a constant source of strength and encouragement.

Finally, but not least, I would like to thank my mother, **Carmen Bean-Quezada**, who has been my mountain and my inspiration. Your love, guidance, and unwavering belief in me have been invaluable. I am grateful for all the sacrifices you have made and for always being there for me, especially during this thesis. I am truly blessed to have you as my mother.

-DEDICATION

To my beloved dad, Juan Enrique Molina-Bravo. You and my mom were always by my side, supporting me and my siblings in all our academic and sports endeavors, no matter how far away we were. You were the one who encouraged me to pursue my MSc in Canada and were providing me with everything I needed to succeed. Other than being my best friend you taught me to never give up, to pursue my dreams, and that a life without happiness is not life. Your words and teachings have always been in my heart, reminding me to live a life filled with love and determination. This thesis is dedicated to you, as a tribute to your unwavering belief in education as the greatest inheritance one can receive. Your memory lives on through us, and I am forever grateful for the love and guidance you bestowed upon us.

Contents

Abstract.....	ii
Acknowledgments.....	iv
List of tables.....	x
List of Figures.....	xi
1. CHAPTER ONE - General introduction	1
1.1 IMPORTANCE OF FUNGI.....	1
1.2 RESEARCH CONTEXT.....	2
1.3 PHYTOHORMONES.....	3
1.3.2 Auxins.....	6
1.3.1 Cytokinins.....	7
1.4 METABOLOMICS.....	8
1.4.1 LC-MS targeted approach.....	10
1.4.2 LC-MS untargeted approach.....	10
1.4.3 LC-MS semi-targeted approach.....	11
1.4.4 LC-MS metabolomic approach in this thesis.....	11
1.5 A model multicellular fungus: <i>SORDARIA MACROSPORA</i>	13
1.5.1 <i>S. macrospora</i> Life Cycle.....	14
1.5.2 <i>Sordaria macrospora</i> mutant strains.....	16
1.6 HYPOTHESIS AND OBJECTIVES.....	25
CHAPTER 2: The metabolomes of the <i>S. macrospora</i> wild type and developmental mutants	28
2.1 INTRODUCTION.....	28
2.1.1 Targeted Analysis of Phytohormones.....	29
2.1.2 -Semi-targeted Metabolomics of Energy compounds (EnM).....	32
2.1.3 Untargeted Lipidomics.....	36
2.2 MATERIALS AND METHODS.....	40
2.3 RESULTS.....	49
2.3.1 Endogenous Phytohormones in <i>Sordaria macrospora</i>	49
2.3.2 Semi-targeted analysis of the Energy metabolome (EnM) in <i>S. macrospora</i> wild type.....	57
2.3.3 Lipidomics of <i>S. macrospora</i>	66
2.4 DISCUSSION.....	78
2.4.1 An overview of the metabolome of <i>S macrospora</i>	78
2.4.1 Production of cytokinins by <i>S. macrospora</i>	81

2.4.2 Cytokinin and metabolites	83
2.4.4 Auxins and lipids.....	86
2.4.5 Auxins and the energy metabolome	87
2.4.6 Lipidomics in <i>S. macrospora</i>	90
2.5 CONCLUSIONS.....	92
CHAPTER 3 – The effects of cytokinins on <i>S. macrospora</i> growth and development 94	
3.1 INTRODUCTION	94
3.2 METHODS	96
3.3 RESULTS.....	101
3.4 DISCUSSION	106
CHAPTER 4- Conclusions and future work.....	111
REFERENCES	117
APPENDIX I	145

List of tables

Table 1. Endogenous production of cytokinins in fungi	27
Table 2. Strains used in this study. The table describes the phenotype, developmental stage, and genotype of the <i>S. macrospora</i> strains used in this study. Also the number of inoculated discs per petri dish according to the harvesting stage. The grey cells represent the final developmental stage of the strain.....	42
Table 3. Liquid chromatography parameters for phytohormones, Energetic metabolites (EnM), and lipid analysis.....	45
Table 4. Mass spectrometry parameters for phytohormones, Energetic metabolites (EnM), and lipids.....	46
Table 5. Relative abundance within each class of lipids (mass tolerance of 10 ppm) across the life cycle of <i>S. macrospora</i> wild type (Stages 2 to 5) and per5 strain (Stage 3’). In this representation, red indicates a higher abundance, while blue signifies a lower abundance within the lipid class.	68
Table 6. Pathways that were significantly changing (Enrichment $p < 0.05$) across the life cycle of <i>S. macrospora</i> . the comparison was done with the next stage (W2, W3, W4, and W5, representing wild-type strain in the different stages, E3 represents the strain per 5 after 6 days post-inoculation). Data analyzed with MetaboAnalysis .	77
Table 7. Effects of exogenous cytokinin treatment in fungi.	110

List of Figures

- Figure 1. Fungal CK biosynthesis via tRNA degradation pathways proposed by Morrison et al. (2017). 1. tRNA isopentenyl transferase; 2. cis-hydroxylase; 3. 5'ribonucleotide phosphohydrolase; 4. adenosine nucleosidase; 5. CK phosphoribohydrolase 'Lonely guy'; 6. purine nucleoside phosphorylase; 7. adenosine kinase; 8. adenine phosphoribosyltransferase.....8
- Figure 2. Schematic representation of *S. macrospora* life cycle.18
- Figure 3. Metabolic pathways analyzed as the Energy Metabolome (EnM).The blue circle represents glucose, which initiates the glycolysis pathway after several catalytic reactions glucose is converted into Acetyl-CoA, which can enter either the TCA cycle or participate in the biosynthesis of lipids, including fatty acids and sterols.Fatty acids undergo β -oxidation to produce Acetyl-CoA, which enters the TCA cycle to produce energy. The TCA cycle includes organic acids such as citrate, α -Ketoglutarate, Succinate, Fumarate, Malate, and Oxaloacetate. This cycle generates molecules of NADH, FADH₂, and ATP to fuel the electron transport chain. The Glyoxylate pathway is an alternative pathway of the TCA cycle. Alongside glycolysis and the TCA cycle, the biosynthesis of amino acids take place, utilizing organic acid as precursors.(Koivistoinen, 2013; Ljungdahl & Daignan-Fornier, 2012; Peraza Reyes & Berteaux-Lecellier, 2013; Tao et al., 2017; L. Wang et al., 2011; Yang et al., 2020; K. Zhang et al., 2013; S. Zhang et al., 2020).....36
- Figure 4. A) Schematic representation of the methodology for the analysis of phytohormones, metabolites, and lipids in the *S. macrospora* strains, B) Schematic representation of the life cycle of *S. macrospora* (image obtained from Teichert et al. (2020)), in this study day 2, 4, 6, and 8 corresponded to stages 1, 2, 3, and 4, respectively.49

Figure 5. Production of cytokinins in different stages of *S. macrospora*. The strains were cultured in Sordaria macrospora minimum media and harvested at each stage until their developmental last developmental stage, with an additional stage included (2 more days). The strains Spt3 (S) and Smagt4 (M) exhibit stagnation in the first stage; Pro1 (P) and Pro11 (R) in the second stage; Per5 (E) in the third stage; and Smgpi1 (G) is characterized by excessive fruiting body production. **A)** In vitro production of the iP type and **A.1)** cis-Zeatin type by *S. macrospora* wildtype and mutants at different developmental stages. The x-axis represents the developmental stages: 1 vegetative mycelium, 2 protoperithecium, 3 young perithecium, 4 mature perithecium, and 5 tissue collected 12dpi. The y-axis represents the concentration in pmol/mg. The error bars represent the standard deviation (SD±) for 4 biological replicates (n=4). The small tissue icons in the graphs represent the developmental stagnation of each strain. The stages of the strains were confirmed using an inverted microscope. **B)** Microscope images showing the different developmental stages (1 to 4) of *S. macrospora* wildtype. **C)** Microscope images showing the last developmental stage of *S. macrospora* mutants.53

Figure 6. Production of the auxin indole acetic acid (IAA) in the *S. macrospora* strains at the different developmental stages. The strains were cultured in Sordaria macrospora minimum media and harvested at each stage until their developmental last developmental stage, with an additional stage included (2 more days). The strains Spt3 (S) and Smagt4 (M) exhibit stagnation in the first stage; Pro1 (P) and Pro11 (R) in the second stage; Per5 (E) in the third stage; and Smgpi1 (G) is characterized by excessive fruiting body production. The x-axis represents the developmental stages: 1 vegetative mycelium, 2 protoperithecium, 3 young perithecium, 4 mature perithecium, and 5 tissue collected 12dpi. The y-axis

represents the concentration in pmol/mg. The error bars represent the standard deviation (SD±) for 4 biological replicates (n=4).....56

Figure 7. Organic acids (OAs) detected with LC-MS/MS in *S. macrospora*. The fungus was grown in Sordaria Minimal Media (SMM) for 12 days. The x-axis represents the developmental stages: 1 vegetative mycelium, 2 protoperithecium, 3 young perithecium, 4 mature perithecium, and 5 tissue collected 12dpi. The y- axis represents the relative abundance according to the recovery of the labeled internal standards ([¹⁵N] or [¹³C] labelled aminoacids). The error bars represent Standard Error (SE ±) for 4 biological replicates. The graphs are color-coded, with black bars representing OAs associated with the tricarboxylic acid (TCA) cycle and glycolysis, white (glyoxylate) a variation of the TCA cycle, the orange precursor is phosphoenolpyruvate, the pink precursor is pyruvate and blue other metabolites. *Shikimate was confirmed only with MS1.58

Figure 8. Amino acids detected with LC-MS/MS in *S. macrospora* across different developmental stages. The fungus was grown in Sordaria Minimal Media (SMM) for 12 days. The x-axis of the graphs represents the developmental stages: 1 vegetative mycelium, 2 protoperithecium, 3 young perithecium, 4 mature perithecium, and 5 tissue collected 12dpi. The y- axis represents the relative abundance according to the recovery of the labeled internal standards ([¹⁵N] or [¹³C] labelled aminoacids). The error bars represent Standard Error (SE ±) for 4 biological replicates. The graphs are color-coded based on the organic acid precursors derived from *Saccharomyces cerevisiae* glycolysis metabolism (Ljungdahl & Daignan-Fornier, 2012; Takpho et al., 2018; Yang et al., 2020). The orange bars represent amino acids originating from phosphoenolpyruvate, blue bars represent amino acids derived from 3-phosphoglycerate, yellow bars represent amino acids derived

from α -ketoglutarate, green bars represent amino acids derived from oxaloacetate, pink bars represent amino acids derived from pyruvate and grey bars represent proteinogenic amino acids. * means data confirmed only with MS1 analysis.61

Figure 9. Nucleosides, nucleotides, and nucleobases (NNNs) detected with LC-MS/MS in *S. macrospora* across different developmental stages. The fungus was grown in Sordaria Minimal Media (SMM) for 12 days. The x-axis of the graphs represents the developmental stages: 1 vegetative mycelium, 2 protoperithecium, 3 young perithecium, 4 mature perithecium, and 5 tissue collected 12dpi. The y- axis represents the relative abundance according to the recovery of the labeled internal standards ($[^{15}N]$ or $[^{13}C]$ labelled aminoacids). The error bars represent Standard Error (SE \pm) for 4 biological replicates. The graphs are color-coded based on the molecule, red represents the nucleosides, pink the nucleotides, and grey and green the nucleobases. cyclic adenosine monophosphate (cAMP), and 5'-Deoxy-5'-Methylthioadenosine (MTA). *MTA was confirmed only with MS1.....63

Figure 10. Sugars detected with LC-MS/MS in *S. macrospora* across different developmental stages. The y-axis represents the normalized peak areas. The x-axis of the graphs represents the developmental stages: 1 vegetative mycelium, 2 protoperithecium, 3 young perithecium, 4 mature perithecium, and 5 tissue collected 12dpi. The y- axis represents the relative abundance according to the recovery of the labeled internal standards ($[^{15}N]$ or $[^{13}C]$ labelled aminoacids). The error bars represent Standard Error (SE \pm) for 4 biological replicates. The sugar trehalose (TRE) and sucrose are isomers, as well as fructose and glucose. The isomers were scored together. * Ribose-5-phosphate was confirmed only with MS165

Figure 11. Other small molecules analyzed with LC-MS/MS in *S. macrospora* across different developmental stages. The x-axis of the graphs represents the developmental stages: 1 vegetative mycelium, 2 protoperithecium, 3 young perithecium, 4 mature perithecium, and 5 tissue collected 12dpi. The y- axis represents the relative abundance according to the recovery of the labeled internal standards ($[^{15}N]$ or $[^{13}C]$ labelled aminoacids). The error bars represent Standard Error (SE \pm) for 4 biological replicates. *Mevalonate was confirmed only with MS1.66

Figure 12. Analysis for lipidomic of *S. macrospora*, comparison in A) stage 2 and stage 3 wildtype and B) stage 3 for wild type and the strain per5. 1) PCA score plot, 2) Volcano plot ($p < 0.1$ and $FC > 2$ or < -2), and 3) Heatmap (t-Test) for the top 150 top feature.75

Figure 13. An example for CellProfiler analysis workflow using exogenous Kinetin Riboside $0.1 \mu\text{M}$ treatment added at 0 day post-inoculation (dpi) in *S. macrospora*. The image was obtained with an inverted microscope (magnitude (4X) after 8 dpi. A) Color to Gray module, the original image was converted to gray scales, B) ImageMath module, to invert the gray intensities, C) Identification of protoperithecium, D) identification of young perithecium, E) removing holes of mature perithecium and F) Identification of mature perithecium. 101

Figure 14. Schematic representation of the methodology employed for exogenous cytokinin treatments. In experiment 1, the growing media consisting of liquid Sordaria Minimal Media (SMM) was supplemented with either $0.1 \mu\text{M}$ cis-Zeatin (cZ) or Kinetin Riboside (KR) at 0 days post inoculation (dpi), and after 5 dpi (stage 3), liquid SMM without hormones was added to the media. In experiment 2, liquid SMM was added at 0 dpi, and after 5 dpi, liquid SMM supplemented with different concentrations ranging from 0.01 to $100 \mu\text{M}$ of cytokinins (cZ, KR, isopentenyl-adenine (iP), and iP-ribose (iPR)) was

introduced. The control group received liquid SMM without any cytokinin supplementation at both 0 and 5 dpi. Tissue weight and fruiting body counts were recorded after 8 dpi to evaluate the effects of the treatments.102

Figure 15. Effects of cis-Zeatin (cZ) or kinetin riboside (KR) on the growth of *S. macrospora* growth. The fungus was grown in Sordaria Minimal Media (SMM) for 8 days, the media was supplemented, with cZ or KR at 0.1 μ M. **A)** Tissue weight in grams per petri dish, with SE (\pm) for 4 replicates. **B)** Relative number of fruiting bodies, including those ranging from protoperithecium to mature perithecium, with SE (\pm) for 6 images per 4 replicates103

Figure 16. Effect of cytokinins in *Sordaria macrospora* growth. The fungus was grown in Sordaria Minimal Media (SMM) for 8 days, the media was supplemented, after 5 days of growth, with cis-Zeatin (cZ)- Kinetin Riboside (KR), isopentenyladenine (iP), and isopentenyl adenine riboside (iPR) at different concentrations ranging from 0.01 to 100 μ M. **A)** Tissue weight in grams per petri dish, with SD (\pm) of 4 replicates., **B)** Relative number of fruiting bodies including from protoperithecium to mature perithecium, with SE (\pm) for 6 images per 4 replicates. The blue line represents the average of the control in all the graphs. ...105

Figure 17. Schematic representation of the results in this thesis. **A)** The upper section depicts the findings described in Chapter 2, the metabolome analysis of *S. macrospora*. Liquid chromatography mass spectrometry was employed to analyze metabolites during the four stages of the fungus life cycle, with an additional fifth stage to study the accumulation of fruiting bodies. The blue squares in the figure represent the relative abundance of metabolites throughout the life cycle, with lighter blue squares indicating lower relative abundance and darker blue squares representing higher abundance. Key organic acids from

the TCA cycle, such as citrate/isocitrate and malate, are the representative of TCA cycle in this figure. IAA- indoleacetic acid; CK riboside -cytokinin ribosides including cZR and iPR; CK free basses including cZ and iP.116

1. CHAPTER ONE - **General introduction**

1.1 IMPORTANCE OF FUNGI

Fungi, as a eukaryotic kingdom, play a crucial role in various ecosystems and have garnered significant scientific interest. They are characterized by their ability to produce spores for dispersal, possess chitinous cell walls, and lack mobility (Margulis & Chapman, 2009). Fungi can be found in diverse environments worldwide, ranging from jungles and forest soils to extreme habitats such as deserts, hot springs, oceans, and even the air. They coexist with animals, bacteria, and plants, contributing to the complexity and resilience of ecosystems (Sheldrake, 2020).

One of the key factors enabling fungi to thrive in different environments is their remarkable capacity to form various tissues, including mycelium, fruiting bodies (commonly known as mushrooms), and spores. These structures enable fungi to efficiently transport nutrients and water, establish beneficial or adverse interactions with other organisms such as animals, plants, and bacteria, and even form symbiotic associations, as seen in lichens with algae or bacteria (Bates et al., 2011; Nanjundappa et al., 2019; Voglmayr et al., 2011; Xue et al., 2017; Zhou et al., 2021).

Apart from their ecological significance, fungi have also found numerous applications in improving human welfare. For instance, fungi have been extensively studied in the field of medicine because of their ability to produce various compounds with

antioxidant, anticarcinogenic, anti-inflammatory, antibiotic, and neuroprotective properties (He et al., 2017; Sevindik, 2020). With their high nutritional value, edible mushrooms are gaining recognition as a source of protein, healthy lipids, and dietary fiber (Wang et al., 2019). Fungi have also been harnessed for the production of enzymes used in manufacturing of detergents, textiles, and dairy products (Schimpf & Schulz, 2016; Y. Wang et al., 2018; Wen et al., 2005). Furthermore, fungi contribute to ecosystem remediation through their ability to produce bioactive and degradation compounds, making them valuable in bioremediation efforts (Kim et al., 2005; Kumar & Dwivedi, 2019).

Finally, fungi are hugely influential in agriculture and hold significant potential for the industry, acting as bio-fertilizers, bio-control agents against crop pests and pathogens, and facilitators of soil pollution mitigation (Homrahud et al., 2016; Martínez-Medina et al., 2014). Therefore, understanding the intricate cellular communication mechanisms of fungi within their environment and the organism itself is essential for harnessing their full potential in these diverse application areas.

1.2 RESEARCH CONTEXT

Cellular communication in fungi must be mediated, at least partially, by signaling molecules, including hormones, which may trigger specific reactions based on the immediate needs of the cells. Hormones are small molecules produced in minute (normally in the range of fmol or pmol/g FW, depending on the tissue and species (Simura et al. 2018)), circulating within an organism to bind to specific cell surface receptors and initiate amplified cellular responses (Combarous & Nguyen, 2019). Hormones have been

extensively studied in the context of development and regulation in other complex organisms. For example, human growth hormones regulate metabolism and postnatal growth, while steroids orchestrate the development and morphogenesis of insects (Lu et al., 2019; Niwa & Niwa, 2014). In plants, phytohormones regulate all key processes such as flowering, growth, senescence, and immune responses (Tran & Pal, 2014).

Surprisingly, the exploration of any hormones produced by fungi and their associated effects on fungal growth and development remains largely unexplored. Understanding the role of hormones in fungi could shed light on their cellular communication mechanisms and unlock new avenues for studying fungal biology, as well as for developing practical applications in various fields.

Therefore, this thesis aims to investigate the presence and potential roles of hormones in fungi, with a particular focus on their potential effects on fungal growth and development. By exploring the hormones and associated cellular chemistry within fungi, I hope to gain insights into their communication strategies and shed light on their diverse interactions with the environment and other organisms. Accordingly, the thesis is divided into different metabolite identification and profiling strategies: targeted phytohormones, semi-targeted analyses of energy metabolites and an overview of untargeted, metabolomic features, which will be narrowed in this thesis to the subset of lipid compounds that make up the lipidome. This will be performed using a model genetic fungus, *Sordaria macrospora*, and several of its mutants that arrest development at different life cycle stages.

1.3 PHYTOHORMONES

Phytohormones are diverse compounds produced in specific tissues and organs, and they act in low concentrations to regulate physiological processes at various stages of plant life. These hormones orchestrate fundamental processes such as seed germination, root and shoot growth, flowering, fruit development, and senescence (Chanclud & Morel, 2016; Pal et al., 2023). Additionally, they play crucial roles in mediating plant responses to biotic and abiotic stresses, including pathogen attacks, nutrient availability, light quality, temperature fluctuations, and drought (Zhao et al., 2021).

Major classes of phytohormones include auxins, cytokinins (CKs), gibberellins (GAs), abscisic acid (ABA), ethylene, jasmonic acid (JA), and salicylic acid (SA). Each hormone class exhibits distinct chemical properties and exerts specific effects on plant growth and development. For instance, auxins are involved in cell elongation and tropic responses, cytokinins regulate cell division and differentiation, GAs control stem elongation and seed germination, ABA governs seed dormancy and stress responses, ethylene influences fruit ripening and senescence, JA and SA are critical in plant defense against pathogens and stress (Pal et al., 2023; Zhao et al., 2021).

Fungi are recognized for their ability to produce phytohormones, which serve as a crucial strategy for fungal interactions with host plants (Chanclud & Morel, 2016). The specific roles and effects of fungal phytohormones can vary depending on factors such as the plant-fungus interaction, the particular hormone involved, and the timing and concentration of hormone exposure. For instance, fungal phytohormones like ABA, auxins, and CKs are produced by fungi to facilitate pathogenesis by suppressing plant defense mechanisms (Chanclud et al., 2016; Kunkel & Harper, 2018; Lozano-Juste et al., 2019; Morrison et al., 2017). However, the same phytohormones can be used by fungi to promote

plant growth and enhance defense responses (Bean et al., 2022; Chanclud & Morel, 2016; Lozano-Juste et al., 2019; Xu et al., 2013).

Despite that fungal CKs are believed to be produced to modulate plant physiology for the benefit of the fungus (Gautam et al., 2022; Hinsch et al., 2016; Kind et al., 2018; Morrison et al., 2017), fungi possess the ability to produce phytohormones even in the absence of direct interaction with living plants. For instance, it has been discovered that saprotrophs, which derive nutrients by decomposing organic matter, also produce CKs (Table 1). This suggests that the production of these hormones by fungi may have effects beyond their role in plant-fungus interactions.

Furthermore, studies have demonstrated that plant phytohormones can influence fungal development. Researchers have conducted experiments where they applied exogenous phytohormones to the growth media. The outcomes of these studies indicate that the effects of phytohormones on fungal growth are both dose-dependent and species-specific. For example, Liu et al. (2016) found that the growth-promoting effects of 5 mM of the auxin indole-3-acetic acid (IAA) were observed only in *Saccharomyces* yeast strains that naturally produced higher amounts of IAA, whereas higher 5 mM IAA had inhibitory effects on the other 24 *Saccharomyces* strains that naturally produced lower amounts of IAA concentrations. Similarly, in *Neurospora crassa* low concentrations of CKs ranging from 1-40 μ M were found to restore fertility in mutant strains, which were normally highly infertile (Lee, 1961). On the other hand, in the fungus *Pleurotus ostreatus*, a concentration of 50 μ M of the CK isopentenyladenine (iP) in the growth media increased the fungal diameter, while a concentration of 500 μ M inhibited fungal growth (Grich 2020).

Thus, the intricate relationship between fungi and phytohormones opens new avenues of exploration to unravel the complex dynamics of fungal growth and development.

Among the various phytohormones, IAA and CKs are particularly intriguing. Both IAA and CKs play essential roles in plant cell elongation and differentiation (Chanclud & Morel, 2016). In plants, growth and cell division are confined to specialized regions known as meristems, located in both shoots and roots. Remarkably, plants possess the ability to undergo differentiation, dedifferentiation, and redifferentiation. The orchestration of these processes relies on a combination of hormonal and genetic factors. Phytohormones can have both independent and dependent effects on various aspects of plant growth and differentiation (Ai et al. 2020). In fungi, vesicles transport cell wall-synthesizing enzymes and accumulate in the Spitzenkörper, guiding tip membrane fusion. The Spitzenkörper, alongside cell end markers and related proteins, dictates fusion sites and growth direction during exocytosis. Vesicle and cytoskeleton dynamics play pivotal roles in processes like maintaining cell integrity, hyphal branching, and morphogenesis. When hyphae differentiate for reproduction or interspecies interactions, cellular machinery can be reprogrammed through new protein synthesis or activity modifications. While transcriptome analysis in some fungi is well studied, the direct link to fungal morphogenesis remains unknown (Riquelme et al., 2018).

1.3.2 Auxins

In plants, auxins are hormones derived from indole, and the major active form is indole-3-acetic acid (IAA), which is produced through the hydrolysis of indole-3-acetamide. Interestingly, fungi also produce auxins, although the biosynthesis pathways

may vary among different species. For instance, the fungi *Fusarium sp.* was reported to synthesize IAA from tryptophan (Tsavkelova et al., 2012), while *Ustilago maydis* and *Leptosphaeria maculans*, plant pathogens, were found to produce IAA from indole-3-pyruvate (Leontovyčová et al., 2020; Reinke et al., 2008).

1.3.1 Cytokinins

Cytokinins are an adenine-derived diverse group of phytohormones with isoprenoid or aromatic side chains. The isoprenoid group is categorized into different types based on the side chain structure, such as dihydrozeatin (DZ), trans-zeatin (tZ), cis-zeatin (cZ), and isopentenyladenine (iP), along with their derivatives. The types of cytokinins present in an organism can provide insights into their biosynthesis origins. For example, tZ and DZ types are typically produced through de novo biosynthesis, while cZ, and 2-methylthiolated CKs (2MeS) are derived from tRNA degradation (Figure 1), and iP types can be generated through both pathways (Sakakibara, 2006).

Interestingly, fungal species have been found to produce CKs, particularly cZ and iP types, as documented in Table 1. Recent studies have shed light on the involvement of the tRNA pathways (Figure 1) and the presence of an enzyme for inactivating CKs called cytokinin oxidase/dehydrogenase (CKX), in the metabolism of CKs by fungi (Morrison et al., 2015; Trdá et al., 2017). These findings suggest that fungi possess mechanisms to synthesize and regulate CK levels, potentially influencing their own growth and development as well as their interactions with other organisms.

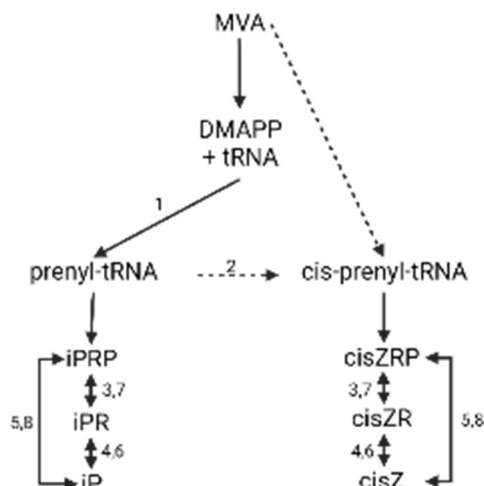


Figure 1. Fungal CK biosynthesis via tRNA degradation pathways proposed by Morrison et al. (2017). 1. tRNA isopentenyl transferase; 2. cis-hydroxylase; 3. 5'ribonucleotide phosphohydrolase; 4. adenosine nucleosidase; 5. CK phosphoribohydrolase 'Lonely guy'; 6. purine nucleoside phosphorylase; 7. adenosine kinase; 8. adenine phosphoribosyltransferase.

1.4 METABOLOMICS

Metabolomics is the field of study that focuses on analyzing and understanding the complete set of metabolites present in a biological sample at a specific time. Metabolites are small molecules involved in various biological processes, including amino acids, organic acids, hormones, vitamins, nucleobases, and lipids. As a result, metabolomics examines any changes occurring within the organism, distinguishing it from other omics disciplines such as genomics, which focuses on studying gene function. Therefore, to comprehensively understand a biological system, metabolomics is considered complementary to genomics, transcriptomics (the study of gene to messenger RNA), and proteomics (which investigates proteins, the products of messenger RNA) (Kosmidis et al., 2013).

Metabolomics often employs liquid chromatography-mass spectrometry (LC-MS), to enable a comprehensive profiling of metabolites and the detection of low-abundance molecules based on the different physicochemical properties of each class of molecules. For instance, LC-MS metabolomics has been used to identify hormones from different tissues, biofluids, and cell cultures, from plants (Nguyen et al., 2021) microorganisms (Aoki, Kisiala, et al., 2019a; Bean et al., 2022), and animals (Aoki, Seegobin, et al., 2019b).

The immense diversity of metabolites and their wide range of chemical properties pose significant challenges for data analysis in metabolomics. Due to the complexity and abundance of metabolites, it is practically impossible to analyze all of them simultaneously. Therefore, researchers must carefully choose or create strategies to selectively target and analyze specific subsets of metabolites in order to gain meaningful insights from the data. By employing targeted or untargeted approaches, researchers can effectively study the metabolome and uncover valuable information about the metabolic processes and pathways underlying biological systems.

In metabolomics, a feature is a signal indicating the presence of a compound detected by LC-MS. Identification of features involves three levels of confidence. Level 1 is high confidence, achieved by matching mass spectra and retention time with standards. Level 2 is tentative identification, using additional techniques like MS/MS. Level 3 is putative characterization at the compound class level (Reisdorph et al., 2020). These levels ensure reliable annotation and classification of metabolites in metabolomics studies and can be achieved according to the approach to be used.

1.4.1 LC-MS targeted approach

Targeted metabolomics focuses on the identification and quantification of a specific set of pre-defined metabolites. This approach involves the selection of a known set of target compounds based on prior knowledge or specific research objectives (Roberts et al., 2012; Want, 2018) In targeted metabolomics, LC-MS is used to measure the abundance or concentration of these pre-determined metabolites in a sample. The LC separates the metabolites based on their physicochemical properties, such as size, polarity, or charge, while the MS detects and quantifies the metabolites based on their mass-to-charge ratio (m/z). Targeted metabolomics is particularly useful when studying specific metabolic pathways or investigating the response of organisms to certain stimuli (Roberts et al., 2012).

To quantify and confirm metabolites, various techniques are utilized, with the addition of a labeled internal standard (IS) being the most common approach. The IS is a molecule that shares similar physicochemical properties with the target metabolite and is added at a known concentration for accurate quantification, achieving a high level of confidence (level 1). However, this technique has its limitations, primarily due to its cost and the vast complexity of the metabolome. It becomes impractical to have an internal standard available for all metabolites in the sample.

1.4.2 LC-MS untargeted approach

On the other hand, untargeted metabolomics aims to comprehensively analyze a global set of metabolites detectable in a biological sample for group comparison and, subsequently, bio-markers discovery. This approach allows for the exploration of a wide

range of metabolites, including known and unknown molecules, in a holistic manner. In untargeted metabolomics, LC-MS is used to separate and detect as many metabolites as possible, generating a complex dataset containing multiple peaks representing different metabolites (Lelli et al., 2021; Want, 2018). These peaks are then subjected to data analysis, including peak alignment, feature extraction, and statistical analysis, to identify significant differences between samples and potentially discover novel biomarkers or metabolic pathways (Lelli et al., 2021; Martínez-Medina et al., 2014). Therefore, the level of confidence achieved can be both level 2 and 3.

1.4.3 LC-MS semi-targeted approach

Finally, in semi-targeted metabolomics, a selection of specific metabolites of interest is predetermined based on prior knowledge or research objectives, in a similar manner to that of targeted metabolomics. These compounds may include known biomarkers, metabolites from specific pathways, or compounds with biological significance. However, this technique can detect a broader range of metabolites that may be present even when they were not specifically targeted for quantification (Malm et al., 2021), leading to a confidence level of 2. This semi-targeted profiling provides a more comprehensive view of the metabolome, allowing for the potential discovery of unexpected metabolites that could be biologically relevant.

1.4.4 LC-MS metabolomic approach in this thesis

In this study, a combination of targeted, semi-targeted, and untargeted metabolomics approaches will be employed to investigate specific aspects of fungal metabolism. The targeted technique will be applied to analyze and quantify

phytohormones, which are signaling molecules involved in various growth and developmental processes. By focusing on phytohormones, I can gain insights into their roles in fungal physiology and explore potential connections between these signaling molecules and fungal growth.

Furthermore, the energetic pathways, such as the tricarboxylic acid (TCA) cycle, will be studied using a semi-targeted approach. The TCA cycle is a key metabolic pathway involved in energy production and the generation of important metabolites (Tao et al., 2017). By applying a semi-targeted approach, we can examine specific metabolites and intermediates within the TCA cycle and other related pathways and thereby gain insights into how energy production and utilization are regulated during different stages of fungal development.

In addition to the targeted and semi-targeted analyses, the lipidome will be studied using an untargeted approach. Lipids, a diverse group of biomolecules that are insoluble in water, play crucial roles in cellular structure, energy storage, and signaling (Bieberich, 2018; Peraza Reyes & Berteaux-Lecellier, 2013; Savidov et al., 2018). However, the study of lipids in fungal growth and development is not well explored. Therefore, by employing an untargeted analysis, I can comprehensively explore the diversity and abundance of lipids present in the fungal system. This untargeted exploration will allow me to identify lipid species, assess their changes across different growth stages or conditions, and potentially uncover novel lipid-based signaling molecules or metabolic pathways that contribute to fungal development.

1.5 A model multicellular fungus: *SORDARIA MACROSPORA*

The study of fungal organisms has contributed to our understanding of eukaryotic cell biology. Fungi can exist as either multicellular or unicellular organisms. Unicellular fungi, known as yeast, have been extensively studied, with *Saccharomyces cerevisiae* being the most well-known yeast species that has provided insights into eukaryotic cell pathways (Kück et al., 2009). On the other hand, multicellular fungi offer the opportunity to investigate cell differentiation at different developmental stages. The life cycle of multicellular fungi typically involves two main stages: vegetative and reproductive. During the vegetative stage, cell differentiation processes and tissue formation occur, while the reproductive stage is primarily focused on spore propagation by fruiting bodies through meiotic or mitotic divisions (Kück et al., 2009).

Sordaria macrospora, a filamentous fungus in the phylum of Ascomycota, is an excellent fungus for studying different signaling pathways in a multicellular eukaryotic organism. It is a microscopic fungus that can form fruiting bodies called perithecia, and its reproductive stage can involve both sexual and asexual propagation (Teichert et al., 2020). The complete life cycle of *S. macrospora*, from spore germination to mature perithecium, takes only 7 days, which is considered relatively fast for a fungus. Moreover, *S. macrospora* is a homothallic fungus, meaning it does not require a mating partner to initiate all steps of meiosis (sexual reproduction). But it can also fuse with an opposite mating partner for sexual reproduction (Kück et al., 2009). Furthermore, *S. macrospora* has been studied as a genetic model organism for more than 25 years where several mutants (more than 100) of *S. macrospora* have been obtained through ultraviolet (UV) exposure, outcrossing with

different species, X-ray mutagenesis, and plasmid transformation (Lord & Read, 2011; Teichert et al., 2020). Most of the mutants are characterized by the ability to block growth and development at different life stages. These factors collectively contribute to a more efficient and focused investigation of energy metabolism, hormonal regulation, and growth processes in fungi, ultimately enhancing our understanding of these fundamental biological processes.

1.5.1 *S. macrospora* Life Cycle

Stage 1, from day 0 to 2, mycelium growth and ascogonium formation, the beginning of the sexual reproduction

The life cycle of *S. macrospora* begins with spore germination (Figure 2). When the spore is inoculated under favorable conditions, a germ tube emerges through the germ pore, elongating with the assistance of cell protoplasts (Hock & Bahn, 1976). As the germ tube elongates, it is referred to as a hypha. The hyphae develop septa, which are pore-delimited regions that allow for the flow of nutrients, signaling molecules, organelles, and vacuoles throughout the hyphae (Hock et al., 1978; Lord & Read, 2011).

To facilitate hyphal branching, the principal hyphae produce lateral branches where mitochondria and vacuoles migrate, forming a branching structure called mycelium. The mycelium exhibits linear growth in length and branching, resulting in circular expansion (Hock & Bahn, 1976). Subsequently, the hyphal tips from the mycelium network can either fuse with another hyphal tip or collide with each other to initiate the formation of the ascogonium (Figure 2).

When two hyphal tips fuse, it allows for the sharing of nutrients, organelles, and, in the case of mycelium from a different organism, genetic information (Hock & Bahn, 1976). The ascogonium tissue represents the first stage in fruiting body formation, which occurs approximately three days after germination. Initially, these cells remain sterile. The formation of the ascogonium involves the hyphae adopting a hook-shaped structure. To maintain optimal nutrient flow, only one ascogonium is formed in the parental hyphae's vicinity (Hock & Bahn, 1976). The parental hyphae can be submerged in agar, grow on the agar surface, or be aerial hyphae (Lord & Read, 2011).

Stage 2, from day 2 to 4, protoperithecium formation

The protoperithecia stage follows the agglomeration of additional hyphae, originating from either the ascogonium coil or parent hyphae. At this stage, the protoperithecia begins to assume a spherical shape (Hock & Bahn, 1976; Lord & Read, 2011). Self-fertilization occurs during this stage, and two distinct cell types can be observed: ascogonial cells and pseudoparenchymatous peridial cells (Lord & Read, 2011). The pseudoparenchymatous cells surround the ascogonial cells.

Once the protoperithecia reaches a width of approximately 50 μm while maintaining its spherical shape, it starts to produce fringe hyphae resembling tiny hairs (Lord & Read, 2011). These fringe hyphae emerge radially from the main body. The protoperithecia stage becomes visible to the naked eye around four days after inoculation. At this point, four cell types can be identified: peridium, centrum pseudoparenchyma, fringe hyphae, and ascogonium (Lord & Read, 2011). The fruiting body begins to develop in a polarized flask-shaped form (Figure 2).

Stage 3, from day 4 to 6, immature perithecium formation

Around day five after germination, the transition from protoperithecia to immature perithecium occurs (Hock & Bahn, 1976). The neck becomes distinguishable from the flask-shaped structure, and the central ascogonium is no longer visible (Lord & Read, 2011). This marks the initiation of the ascus, a bag-like structure where spores are formed. At this stage, the ascus lacks pigmentation and does not contain spores, while the hymenial paraphyses start to emerge from the basal region. Within the immature perithecium, the centrum pseudoparenchyma is present, filled with extracellular matrices. The outer pigmented wall of the peridium cells differentiates from the fruiting body's exterior (Hock & Bahn, 1976; Lord & Read, 2011).

Stage 4, from day 6 to day 8, mature perithecium and spore release

By day six, the fruiting body is fully visible, acquiring a flask-shaped structure with an oscillate pore region at the top of the neck. The ascus begins to form eight aligned spores, each containing two nuclei resulting from the partition of the protoplast. Mature spores possess a pigmented cell wall (Lord & Read, 2011). On day seven to eight, the spores are released through the neck pore to initiate a new life cycle.

1.5.2 *Sordaria macrospora* mutant strains

In the study of *S. macrospora*, genetic analysis has played a crucial role in understanding the morphological processes, particularly during the reproductive stage. By investigating gene expression related to cellular differentiation, over 100 mutants of *S. macrospora* have been generated and characterized. These mutants can be categorized into four types based on their specific phenotypic characteristics (Kück et al., 2009) and are categorized in Figure 2.

1. Asc mutants: These mutants are unable to progress beyond the ascogonium stage, which is the initial stage of fruiting body formation. Consequently, these mutants are sterile and fail to develop perithecia. Only five asc mutants have been identified so far (Kück et al., 2009).

2. Pro mutants: Approximately 45 mutants fall into this category, and they exhibit defective protoperithecia formation. These mutants are unable to transition to the perithecium stage, rendering them sterile (Kück et al., 2009).

3. Per mutants: Similar to the Pro mutants, around 45 mutants belong to this group. While the perithecial body can be observed in these mutants, it is not well-formed, and they are unable to produce mature ascospores (Kück et al., 2009).

4. Pile mutants: These mutants typically retain fertility but display abnormalities in melanin pigmentation, particularly in the ascospores. Additionally, they exhibit a significantly lower germination rate compared to the wildtype, and the spatial arrangement of the perithecia is disrupted (Kück et al., 2009).

Various molecular approaches such as genomics, transcriptomics, and proteomics have been employed to gain further insights into the genetic regulation of *S. macrospora* life cycle. These techniques have enabled the identification of gene expression patterns during different phases of the fungus life cycle. In this study, I will be working with one or two mutants from each type.

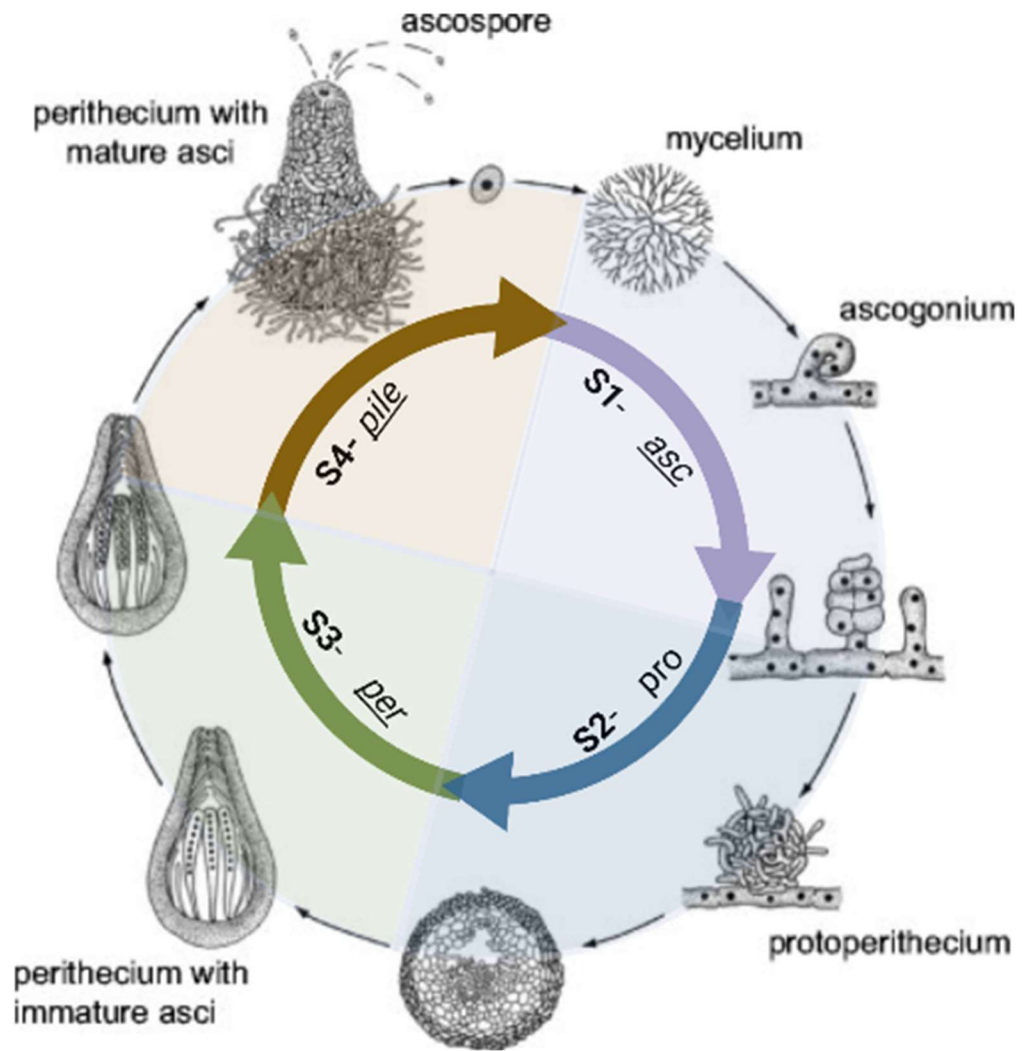


Figure 2. Schematic representation of *S. macrospora* life cycle. Stage one (S1) ascogonium (asc) formation; Stage two (S2) protoperithecium (pro) formation, Stage three (S3) immature perithecium (per); Stage four (S4) mature perithecium (pile) and spore release. The image was adapted from (Kück et al., 2009) using Biorender.com

1.5.2a Asc- strains used

spt3 -S-

Spt3 gene encodes a subunit of the Spt-Ada-Gcn5 acetyltransferase (SAGA) complex, which is a conservative complex found in fungi, plants, and humans. SAGA is known to regulate gene expression and functions as a transcriptional coactivator, chromatin

promoter-proximal modifier, and DNA repair and signaling factor (Herbst et al., 2021). In yeast, SAGA is composed of 19 subunits and has been described as a cofactor of the RNA polymerase II regulator (G. Liu et al., 2019). These subunits are organized into four modules: HAT, DUB, TAF, and SPT.

The deletion of the *spt3* gene in *S. macrospora*, generated by transforming the deletion cassette, leads to several notable effects. Additionally, the transcriptome undergoes drastic changes, and the mutant exhibits sterile and few non-pigmented protoperithecia formations (Lütkenhaus et al., 2019; Teichert et al., 2020). In the $\Delta spt3$ mutant of *S. macrospora*, around 20 categories of genes are upregulated, while 15 categories are downregulated. The upregulated processes primarily include metabolic, oxidoreduction, catalytic, and cytoplasmic processes. On the other hand, the downregulated processes are mainly related to oxidoreduction, oxidoreductase activity, heme binding, transmembrane transport, and carbohydrate metabolic processes (Lütkenhaus et al., 2019).

Given that the *spt3* mutant not only fails to form fruiting bodies but also exhibits defects in vegetative growth, it is logical that multiple processes are affected. In comparison to the deletion of other genes like *asm3* and *asm2* (which result in defective perithecium formation), the *spt3* mutant shows a broader range of regulated processes (Lütkenhaus et al., 2019). However, the specific causal relationship between the changes in gene expression and the growth defects in the fungus remains unknown and requires further investigation.

Smatg4 -M-

Autophagy, a conserved mechanism for recycling cytosolic material during stress and cellular differentiation, plays a crucial role in fungal development, prolonged cell

survival under starvation, and pathogenicity (Bérangère et al., 2005; Pollack et al., 2009; Xiao-Hong et al., 2007). In filamentous fungi like *S. macrospora*, the core autophagy (ATG) genes regulate the initiation, nucleation, expansion of the phagophore membrane, autophagosome completion, docking and fusion with the vacuolar membrane, and degradation/recycling processes (Teichert et al., 2020).

The ubiquitin- like (Ubl) system, a major autophagy pathway, employs more than half of the core ATG genes in yeast. It involves ATG8 and ATG12, which undergo conjugation through different enzymatic reactions. ATG12's C-terminal group is activated by the E1 enzyme Atg7, while Atg8 is synthesized with an extra C terminus that is later removed by Atg4 for its activation (Nakatogawa, 2013). In yeast, autophagy signals regulate the transcription of ATG8. Under favorable conditions, the Ume6-Sin3-Rpd3 complex binds to ATG8, but during starvation, the complex disassembles via ume6 phosphorylation, resulting in upregulation of ATG8. This process leads to the conjugation of ATG8 with PE (phosphatidylethanolamine), which is crucial for autophagosome hemi fusion and other autophagy-related structures (Nakatogawa, 2013).

S. macrospora, like other filamentous fungi, possesses most of the core ATG genes involved in the Ubl system but lacks genes required for selective autophagy. The deletion of the *smatg4* gene in *S. macrospora* disrupts fruiting body formation and impairs growth and ascospore germination, while hyphal fusion remains unaffected. Studies have demonstrated that *Smatg4*, along with *Smatg8*, is crucial for non-selective autophagy and selective pexophagy, suggesting their role in maintaining energy levels and promoting multicellular development under non-starvation conditions in *S. macrospora* (Teichert et al., 2020; Voigt & Pöggeler, 2013).

1.5.2b Pro -strains

pro1-P-

Transcription factors play a crucial role in regulating gene expression by binding to DNA. In *S. macrospora*, the transcription factor gene *pro1* encodes a C_6 zinc finger transcription factor (Masloff et al., 1999). This gene is involved in the regulation of approximately 400 genes, including around 30 genes crucial for fruiting body morphogenesis, which depend on proper *pro1* expression (Steffens et al., 2016). Deletion of *pro1* leads to the formation of defective protoperithecia, and mutants affected by *pro1* exhibit the same phenotype, being blocked at the protoperithecia stage (Masloff et al., 1999; Steffens et al., 2016).

The *pro1* gene regulates three main signaling pathways: the NOX complex, MAPK modules, and HAM pathway, which are responsible for the regulation of ROS (reactive oxygen species), pheromone, and cell fusion signaling, respectively. These pathways are crucial for fruiting body formation and ascospore germination. Therefore, *pro1* serves as a key regulator of genes required for the spatiotemporal coordination of cell differentiation. However, further studies are needed to fully understand the mechanism by which *pro1* functions (Steffens et al., 2016).

pro11-R-

WD40 repeat domains are protein domains characterized by a β -propeller structure that plays a crucial role in various cellular processes. These domains serve as essential subunits within multiprotein complexes involved in diverse functions such as G protein-coupled receptor (GPCR) signaling, DNA damage detection and repair, the ubiquitin-

proteasome system (UPS), cell growth and division, epigenetic regulation of gene expression and chromatin organization, and immune system responses (Schapira et al., 2017).

The *pro11* gene in *S. macrospora* encodes a protein that consists of three distinct structural domains. These domains include a coiled-coil region, a putative calmodulin binding site, and a C-terminal domain comprising seven WD40 repeats (Pöggeler & Kück, 2004). The C-terminal domain shares notable similarity with mammalian WD40 proteins, including stratin, SG2NA, and zinedin. In *S. macrospora*, this protein's function may be associated with the regulation of cytokinesis, vesicular traffic, and endocytosis processes (Pöggeler & Kück, 2004).

Interestingly, the deletion of the *pro11* gene in *S. macrospora* does not hinder vegetative growth. However, it resulted in reduced protoperithecium size and impaired protoperithecium formation. Moreover, this mutant strain was unable to undergo the transition to mature fruiting (Pöggeler & Kück, 2004). These findings suggest that the Pro11 protein, with its WD40 repeat-containing C-terminal domain, plays a critical role in the reproductive development and transition to fruiting in *S. macrospora*.

1.5.2c Per strain

per5-E-

ATP citrate lyase (Acl) is an enzyme that plays a crucial role in the conversion of citrate to oxaloacetate and acetyl-CoA, which are metabolic products of the Krebs cycle,

the main energy-yielding metabolic pathway in cells (Verschueren et al., 2019). Acetyl-CoA serves as a key regulatory molecule in both catabolic and anabolic fatty acid and sterol pathways. Acl is involved in lipid metabolism in animals and some fungi. Lipids, particularly fatty acids, are essential for various cellular processes, including the synthesis of biomembranes, hormones, and secondary messengers. In addition, lipid pathways are involved in pollen formation in plants, morphogenesis in animals, and the regulation of circadian rhythms, growth, and pheromone factors in certain fungal species (Nowrousian et al., 1999a; Pfitzner et al., 1987)

The *per5* mutant of *S. macrospora* exhibits a sterile phenotype and is unable to complete the development of perithecial bodies. This mutant can only form the ascus without mature spores. The deleted gene in the *per5* mutant shows significant homology to eukaryotic Acl. Acl activity was tested in the wild-type *S. macrospora*, and the highest enzymatic activity was observed 48 hours after inoculation. However, the *per5* mutant did not show any Acl activity. These results indicate that Acl is involved in the transition from vegetative to sexual growth (at 48 hours after inoculation) and the overall process of fruiting body formation (Nowrousian et al., 1999).

In *S. macrospora*, Acl is not only present in the cytosol but also in the cytoplasm. The proposed Acl1 protein in *S. macrospora* is approximately 50-kDa smaller than animal Acl but similar to Acl proteins found in other filamentous fungi, such as *A. niger* (Pfitzner et al., 1987). Acl has been demonstrated to be a key regulator in the maturation of mycotoxins in *Fusarium* and fruiting body development in *S. macrospora* (Nowrousian et al., 1999a; Sakamoto et al., 2013). Additionally, the existence of a yet-unidentified signal that regulates *acl* gene expression has recently been proposed (Nowrousian et al., 1999a).

The *per5* mutant of *S. macrospora* and the characterization of Acl provide valuable insights into the role of lipid metabolism and Acl in the sexual development and fruiting body formation of the fungus. Further investigations are needed to unravel the specific mechanisms by which Acl influences these processes and to identify the signaling pathways involved in the regulation of *acl* gene expression.

1.5.2d Pile strain

smgpi1 -G

The stratin-interacting phosphatases and kinases (STRIPAK) complex is a conserved eukaryotic complex that plays a role in various cellular and developmental processes (Frey, Lahmann, et al., 2015). This complex is formed around the trimeric protein phosphatase 2A (PP2A) (Frey, Reschka, et al., 2015). In *S. macrospora*, the main subunits of the STRIPAK complex are PRO11, PP2AA, PP2AC1, PRO22, MOB3, and PRO45 (Frey, Lahmann, et al., 2015). These subunits function as a PP2A regulatory subunit, PP2A scaffolding subunit, PP2A catalytic subunit, cell size control, vesicular trafficking, and membrane anchoring, respectively. MOB3/phocein homologues are involved in endocytotic processes and are found in filamentous fungi and animals but not in yeast (Frey, Reschka, et al., 2015). The deletion of the *Smmob3* gene in *S. macrospora* leads to sterility and hyphal fusion deficiency. The N-terminus of SmMOB3, which contains a conserved mob domain, interacts with the C-terminus of PRO11 as a kinase regulator (Bloemendal et al., 2012).

In addition to its role in the STRIPAK complex, *SmMOB3* is involved in the glycosylphosphatidylinositol (GPI) anchor attachment process. GPI-anchored proteins are

localized in the plasma membrane or cell wall and their attachment occurs in the endoplasmic reticulum (ER). Interestingly, the GPI anchor in *S. macrospora* can interact with the SmMOB3 subunit, thereby regulating hyphal fusion and fruiting body formation (Frey, Lahmann, et al., 2015). The deletion of the *Smgpil* gene in *S. macrospora* leads to an increased number of fruiting bodies but a decrease in their size, while the *Smmob3* mutant is unable to form fruiting bodies and undergo hyphal fusion (Frey, Lahmann, et al., 2015). However, when the *Smgpil* mutant is combined with the *Smmob3* mutant, the hyphal fusion and fruiting body formation are restored. Despite these observations, the specific functions of *smmob3* and *smgpil* in a fungal system remain largely unknown (Frey, Reschka, et al., 2015).

1.6 HYPOTHESIS AND OBJECTIVES

In this thesis, I aim to address the lack of knowledge about developmental myco-hormones by investigating potential growth and development regulators in fungi, by employing different metabolomic approaches with the *S. macrospora* model fungus. I will explore the role of phytohormones as candidate myco-hormones and employ LC-MS-based metabolomics of *Sordaria macrospora* and six mutant strains to identify and characterize these molecules in the fungus *S. macrospora*. By unraveling the regulatory mechanisms underlying fungal growth and development, this study aims to contribute to our understanding of fungal biology and open new avenues for the improvement of agriculture, industry, and biotechnology fungal systems.

My overall hypothesis was that fungi use signaling molecules as hormones to organize their development. I will address this hypothesis by profiling two types of hormones, CKs and IAA throughout the *S. macrospora* life cycle.

I hypothesize that phytohormones can act as myco-hormones. I predict that clear changes in hormones would be identifiable during developmental switches. I further hypothesize that those changes will be disrupted in the mutant strains specific to that stage of development.

I hypothesize that energetic metabolomics will change in a manner consistent to phytohormones according to *S. macrospora* needs in the developmental processes.

I hypothesize that lipids may act either as hormones themselves or through support of as yet unknown hormone agents. I predict that lipidomic profiles will reflect the needs of different stages of development and that some lipids may be identified that have abrupt changes that are consistent with candidate hormones.

Table 1. Endogenous production of cytokinins in fungi

Fungus specie	Life style	Division type	Detected phytohormones CKs	Concentration range	Reference
<i>Pyrenophora brassicae</i>	Hemibiotroph	ascomycetes	iPR and ZR	125 pmol/g-FW	(Murphy et al. 1997)
<i>Ventura inaequalis</i>	Hemibiotroph	ascomycota	iP and ZR	105.9 and 264 pmol/g- FW	(Murphy et al. 1997)
<i>Cladosporium fulvum</i>	Biotrophs	ascomycetes	ZR and iP	20 and 32 pmol/g- FW	(Murphy et al. 1997)
<i>Lentinus tigrinus</i>	Saprotrophic	basidomyces	Z	~20 µg/ml (of media culture)	(Özcan and Topcuoğlu, 2001)
<i>Laetiporus sulphureus</i>	Saprotrophic	basidomyces	Z	~9 µg/ml (of media culture)	(Özcan and Topcuoğlu, 2001)
Yeast	N/A	basidomycetes and ascomycetes	Z	NA	(Streletskii et al. 2019)
<i>Leptosphaeria maculans</i>	Hemibiotroph	ascomycetes	cZ, iP (mostly)	20 and 6 pmol/ g- DW	(Trdá et al. 2017)
<i>Trichoderma ssp.</i>	Saprotrophic and biotrophic	ascomycetes	cZ, iP, cZR, iPR, DZ	from 0.7 to 50 pmol/g	(Bean et al. 2022)
<i>Piriformospora indica</i>	Biotrophic - endophyte	basidomycota	cZ, iP, iPR, cZR	~50 and 160 pmol/ DW-g (cZ and iP)	(Vadassery et al. 2008)
<i>Rhizopogon luteolus</i>	Ectomycorrhizal	basidomycetes	Z, ZR, and iP	N/A	(Cole, Jameson, and Mcwha, 1982)
<i>Boletus elegans/ Suillus grevillei</i>	Ectomycorrhizal	basidomycetes	Z, ZR, and iP	N/A	(Cole, Jameson, and Mcwha, 1982)
<i>Laccaria bicolor</i>	Ectomycorrhizal	basidomycetes	iPR, iP, ZR and Z	from 10 to 1000 pmol/g	(Kraigher et al. 1991)
<i>Thelephora terrestris</i>	Ectomycorrhizal	basidomycetes	iPR, iP, ZR and Z	from 10 to 1000 pmol/g	Kraigher et al. 1992
<i>Ustilago maydis</i>	Saprophytic phase and pathogenic growth	basidomycetes	iP, iPR, cZ, cZR, DZ, and DZR	300, 5, and 90 pmol/g-FW (cZR, DZ, and iPR)	(Bruce, Saville, and Emery, 2011)
<i>P. ostreatus</i>	Saprotrophic	basidomycetes	iP, cZ, iPR, cZR, iPNT, and cZNT	~ 50 to 3500 pmol/g of TOTAL CKs	(Grich, 2020)
<i>Amanita bisporigera</i>	Ectomycorrhizal	basidomycetes			
<i>Hygrophorus sp.</i>	Ectomycorrhizal	basidomycetes			
<i>Hygrocybesp</i>	Ectomycorrhizal	basidomycetes			
<i>Phellinus ignarius</i>	Wood-root	basidomycetes			
<i>Oxyporus populinus</i>	Wood-root	basidomycetes			
<i>Ganoderma applanatum</i>	Wood-root	basidomycetes			
<i>Piptoporus betulinus</i>	Wood-root	basidomycetes			
<i>Bjerkandera adusta</i>	Saprotrophic	basidomycetes			
<i>Lycoperdon perlatum</i>	Saprotrophic	basidomycetes			
<i>Hypsizygus ulmarius</i>	Saprotrophic	basidomycetes	iP, iPR, cZ, cZR , and ABA	the strains produce around 24 - 210 pmol/g total CK content	(Morrison et al. 2015)
<i>Pleurotus ostreatus</i>	Saprotrophic	basidomycetes			
<i>Mycena leaiana</i>	Saprotrophic	basidomycetes			
<i>Exidia glandulosa</i>	Saprotrophic	basidomycetes			
<i>Trichaptum bifforme</i>	Saprotrophic	basidomycetes			
<i>Tyromyces chioneus</i>	Saprotrophic	basidomycetes			
<i>Trametes versicolor</i>	Saprotrophic	basidomycetes			
<i>Clitocybula abundans</i>	Saprotrophic	basidomycetes			
<i>Hymenopellis sp</i>	Saprotrophic	basidomycetes			
<i>Hygrocybe miniata</i>	Saprotrophic	basidomycetes			
<i>Trametes pubescens</i>	Saprotrophic	basidomycetes			
Ectomycorrhizal live in symbiosis in the rhizosphere (usually do not penetrate the host)					
Endophyte an organism (such as a bacterium or fungus) living within a plant (Merriam-Webster, n.d.)					
Biotrophics derive their nutrition from living host cells					
Necrotrophic fungi that obtain their nutrients from host tissues which they have killed					
Hemibiotrophs initially live as biotrophs shifting to a necrotrophic mode of nutrition as infection progresses (Murphy et al. 1997)					
Saprotrophs get nutrients by processing decayed (dead) organic matter					

CHAPTER 2: The metabolomes of the *S. macrospora* wild type and developmental mutants

2.1 INTRODUCTION

Fungi, as a diverse kingdom of eukaryotic cells, exhibit unique characteristics such as spore production, chitinous cell walls, and the lack of mobility (Margulis & Chapman, 2009). They are ubiquitous, found in various environments including: forests, deserts, oceans, and in coexistence with other organisms. The ability of fungi to form different tissues and structures, like mycelium and fruiting bodies, allows them to thrive and interact with animals, plants, bacteria, and even to form symbiotic relationships as lichens (Bates et al., 2011; Margulis & Chapman, 2009; Nanjundappa et al., 2019; Zhou et al., 2021). Beyond their ecological significance, fungi play a vital role in benefiting human welfare. They are utilized in medicine for their production of bioactive compounds, serve as a nutritional food source, contribute to the production of various products, and aid in agricultural practices by acting as bio-fertilizers and bio-control agents (Xue et al., 2017). To enhance fungal products and understand their communication, studying cellular signaling molecules, including hormones, becomes crucial.

Hormones are small molecules that regulate specific cell functions within an organism by circulating and binding to cell surface receptors, which leads to amplified cellular responses (Combarrous & Nguyen, 2019). Interestingly no “myco-hormones” have been described that are specific for fungal growth and development (Sheldrake, 2020; Grich, 2020). Therefore, this study aims to bridge the gap in our understanding of fungal

hormonal signaling, opening new possibilities for harnessing the potential of fungi and expanding our knowledge of their biology.

In the search for myco-hormones for fungal growth and development, we will investigate the metabolome of the model fungus *Sordaria macrospora* at various developmental stages using Liquid Chromatography-Mass Spectrometry (LC-MS). This approach will involve targeted metabolomics to analyze phytohormones, semi-targeted metabolite profiling of energetic pathways, and untargeted lipid metabolomics (aka lipidomics). By employing these techniques, we will gain valuable insights into the metabolic changes associated with candidate myco-hormones and their impact on fungal development.

2.1.1 Targeted Analysis of Phytohormones

Phytohormones have the potential to act as myco-hormones, influencing fungal growth and development. Phytohormones are diverse compounds that regulate physiological processes in plants at various stages of their life, such as: seed germination, growth, flowering, fruit development, and responses to biotic and abiotic stress (Pal et al., 2023). Major classes of phytohormones include auxins, cytokinins (CKs), gibberellins, abscisic acids (ABA), ethylene, jasmonic acid, and salicylic acid. Each of these have many well-known roles in plant growth and development.

Previous studies demonstrated that fungi produce phytohormones to interact with host plants, affecting defense mechanisms or promoting plant growth and defense. Phytohormones are also thought to affect hyphal growth, elongation, spore formation, and sexual development in fungi (Chanclud & Morel, 2016). It is important to mention that

some studies have demonstrated that phytohormones can impact fungal development in a dose-dependent and species-specific manner (Kind et al., 2018; Lee, 1961; Y.-Y. Liu et al., 2016). Understanding the interaction between fungi and fungal phytohormones may reveal insights into fungal growth and development, particularly the roles of IAA and CKs, which are important for plant cell differentiation and elongation.

CKs are a diverse group of adenine-derived phytohormones that have either isoprenoid or aromatic side chains. Isoprenoid CKs can be biosynthesized through two different pathways: the *de novo* pathway, which includes dihydrozeatin (DZ), *trans*-zeatin (tZ), and isopentenyladenine (iP) and their derivatives; and, the mevalonate or tRNA pathway, which includes *cis*-zeatin (cZ), 2-methylthiolated CKs (2MeS), and iP types (Sakakibara, 2006).

Probably because of their well-known roles in plants, researchers primarily attributed fungal-produced CKs as a mechanism for interacting with living plants (Gautam et al., 2022; Hinsch et al., 2016; Kind et al., 2018; Morrison et al., 2017). For instance, the plant pathogen *Plasmiodiosphora brassicae* produces CKs during plant infection, inducing local cell division in the root cortex to create a meristematic area. This area serves as a source of nutrients and energy for the pathogen (Devos et al., 2006). Interestingly, fungi, regardless of their nutrition mode (e.g., saprotrophs that derive nutrients from decaying organic matter), also produce CKs (Table 1).

The production of CKs in fungi varies from 5 to 300 pmol/g of fresh weight, depending on the CK type, the species tested, and the developmental stage (Bean et al., 2022; Bruce et al., 2011; Morrison et al., 2015; Trdá et al., 2017; Grich, 2020) (Table 1). For instance, the fungus *P. ostreatus* produced the lowest concentrations of total CKs

(~1000 pmol/g dry weight) after 7 days of incubation compared to the day 21 and 24 after incubation (~2000 pmol/g dry weight) (Grich, 2020).

Previous studies have predominantly detected cZ and iP type CKs in fungi (Table 1), indicating the existence of a common tRNA pathway (Morrison et al. 2015; Figure 2). Additionally, the presence of cytokinin oxidase/dehydrogenase (CKX), an enzyme that irreversibly inactivates CKs, has been observed in fungi (Trdá et al., 2017).

In exogenous applications, CKs have demonstrated different physiological effects on fungal growth, which depend on the type and dosage of CKs. For example, Gryndler et al. (1998) tested different concentrations of CKs ranging from 0.1 to 100 μ M in the fungus *Glomus fistulosum* and found inhibitory effects at concentrations above 10 μ M. In another study, a non-endogenous CK, kinetin, restored fertility in mutant infertile strains of *Neurospora crassa* at concentrations of 2 to 20 μ M (Lee, 1961). Recent studies involving exogenous treatments of CKs showed alterations in fungal metabolism when 100 μ M of 6-benzylaminopurine (6-BAP) was added to the media, particularly affecting energetic pathways such as glycolysis, sucrose metabolism, and oxidative phosphorylation (Anand et al., 2022). These findings suggest the CKs might be involved in fungal cell signaling.

In plants, auxins are hormones derived from indole, and the major active form is indole-3-acetic acid (IAA), which is produced through the hydrolysis of indole-3-acetamide. Interestingly, fungi also produce auxins, although the biosynthesis pathways may vary among different species. For instance, the fungi *Fusarium sp.* was reported to synthesize IAA from tryptophan (Tsavkelova et al., 2012), while in *Ustilago maydis* and *Leptosphaeria maculans*, IAA comes from indole-3-pyruvate (Leontovyčová et al., 2020; REINEKE et al., 2008). The concentration of IAA in fungi varies from 50 to 20000 pmol/g

FW, depending on the species and culture media composition (Leontovyčová et al., 2020). Exogenous applications of auxins demonstrated improved hyphal growth in the human pathogen *Candida albicans* (Rao et al., 2010), growth in yeast (Y.-Y. Liu et al., 2016) and inhibition in conidial germination in *Neurospora crassa* (Nakamura et al., 1978). However, the mechanism of action of fungal IAA is not well understood in fungal development.

2.1.2 -Semi-targeted Metabolomics of Energy compounds (EnM)

Metabolomics aspires to study the global change of all metabolites of the cell's immediate needs in response to external factors. Energy availability and its use plays a fundamental role in fungal growth, development, and reproduction. For instance, it is well known that sexual reproduction requires more energy compared to vegetative growth (Kück et al., 2009; Peraza Reyes & Berteaux-Lecellier, 2013). In *S. macrospora*, different developmental stages require distinct metabolic programs and energy demands. By identifying the energy sources and pathways involved, one can gain insights into the underlying metabolic “rewiring” and the role of candidate myco-hormones in coordinating these developmental processes.

Therefore, the metabolites chosen in this study are the organic acids that participate in the TCA cycle, glyoxylate pathways, and other pathways that are involved in the metabolism of amino acids and lipids in fungi. We define these as the Energy metabolome (EnM).

The TCA cycle is a central metabolic pathway that occurs in the mitochondria of eukaryotic cells, including fungi (Tao et al., 2017). It plays a vital role since it oxidizes acetyl-CoA derived from various carbon sources, such as sugars, fatty acids, and amino

acids. The cycle consists of a series of enzymatic reactions that result in the production of energy-rich molecules, such as NADH and FADH₂ s well as the waste product, CO₂ (Figure 3)(Koivistoinen, 2013; Tao et al., 2017; K. Zhang et al., 2013).

The TCA cycle starts with the entry of acetyl-CoA, which combines with oxaloacetate to form citrate, followed by a series of enzymatic reactions, including: isomerization, decarboxylation, and dehydrogenation. These reactions produce intermediate molecules, such as α -ketoglutarate, succinyl-CoA, succinate, fumarate, and malate, ultimately regenerating oxaloacetate to start another cycle. The TCA cycle generates reducing equivalents (NADH and FADH₂) that fuel the electron transport chain for ATP production through oxidative phosphorylation (Koivistoinen, 2013; Tao et al., 2017; K. Zhang et al., 2013).

The glyoxylate pathway is an alternative metabolic route that branches off from the TCA cycle. It is essential in organisms, including fungi, that utilize acetate or fatty acids as a primary carbon source. The pathway allows the net synthesis of carbohydrates from two molecules of acetyl-CoA, bypassing the CO₂-releasing steps of the TCA cycle (Figure 3)(Peraza Reyes & Berteaux-Lecellier, 2013; Tao et al., 2017) .

In the glyoxylate pathway, two key enzymes, isocitrate lyase and malate synthase, enable the conversion of isocitrate to succinate and glyoxylate, which is then utilized to synthesize malate. This pathway allows fungi to bypass the decarboxylation steps of the TCA cycle, conserving carbon and enabling the synthesis of carbohydrates that can be utilized for growth and energy production (Peraza Reyes & Berteaux-Lecellier, 2013; Tao et al., 2017).

Fungi possess various pathways involved in the metabolism of amino acids, which serve as important building blocks for protein synthesis and as a source of carbon and nitrogen. These pathways are described in brief below:

- **Amino Acid Biosynthesis:** Fungi can synthesize amino acids through specific biosynthetic pathways. For example, the biosynthesis of amino acids like proline, serine, and threonine involves multiple enzymatic reactions, utilizing intermediates from central metabolic pathways such as glycolysis and the TCA cycle (Ljungdahl & Daignan-Fornier, 2012; Yang et al., 2020).
- **Amino Acid Catabolism:** Fungi possess pathways for the catabolism of amino acids to generate energy and metabolic intermediates. Amino acids can be deaminated to produce α -keto acids, which can enter the TCA cycle or be utilized in other metabolic pathways. For instance, the catabolism of alanine generates pyruvate, while the breakdown of glutamate produces α -ketoglutarate (Ljungdahl & Daignan-Fornier, 2012; Sherry et al., 2015).

Fungal lipid metabolism involves the synthesis, degradation, and utilization of lipids for energy storage, membrane composition, and signaling. Key pathways include:

- **Fatty Acid Biosynthesis:** Fungi synthesize fatty acids through a series of enzymatic reactions, including the formation of acetyl-CoA from different carbon sources, elongation of fatty acid chains, and desaturation to introduce double bonds. Fatty acids serve as building blocks for the synthesis of complex lipids, such as phospholipids and triacylglycerols (Peraza Reyes & Berteaux-Lecellier, 2013; L. Wang et al., 2011).

- β -Oxidation: Fungal cells can break down fatty acids via β -oxidation, which occurs in the mitochondria and peroxisomes. β -Oxidation involves a cyclic series of reactions that sequentially remove two-carbon units from the fatty acid chain, producing acetyl-CoA, NADH, and FADH₂, which can be further utilized in energy production through the TCA cycle and oxidative phosphorylation (Peraza Reyes & Berteaux-Lecellier, 2013; L. Wang et al., 2011).
- Sterol Biosynthesis: Sterols, such as ergosterol, are important components of fungal cell membranes and play crucial roles in membrane fluidity and integrity. Fungi possess specific pathways for the biosynthesis of sterols, involving enzymatic reactions that convert intermediates derived from acetyl-CoA into sterol molecules (L. Wang et al., 2011).

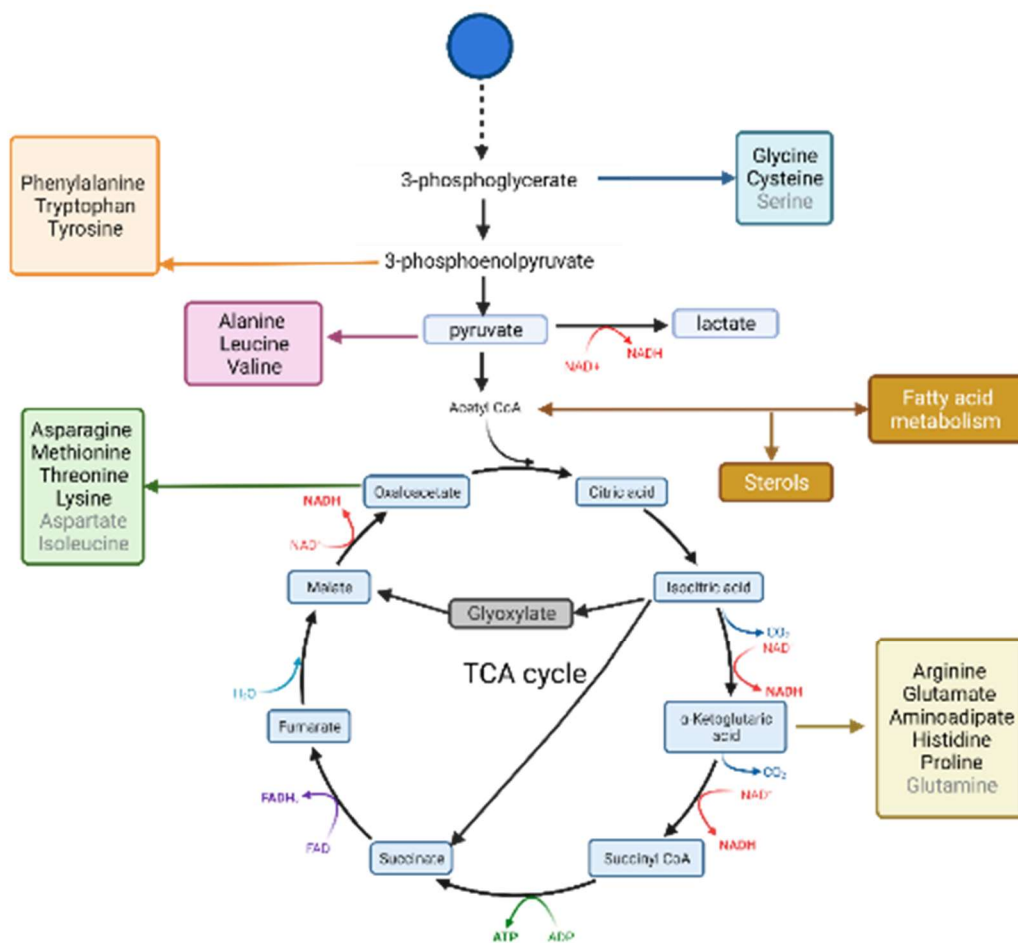


Figure 3. Metabolic pathways analyzed as the Energy Metabolome (EnM). The blue circle represents glucose, which initiates the glycolysis pathway after several catalytic reactions glucose is converted into Acetyl-CoA, which can enter either the TCA cycle or participate in the biosynthesis of lipids, including fatty acids and sterols. Fatty acids undergo β -oxidation to produce Acetyl-CoA, which enters the TCA cycle to produce energy. The TCA cycle includes organic acids such as citrate, α -Ketoglutarate, Succinate, Fumarate, Malate, and Oxaloacetate. This cycle generates molecules of NADH, FADH₂, and ATP to fuel the electron transport chain. The Glyoxylate pathway is an alternative pathway of the TCA cycle. Alongside glycolysis and the TCA cycle, the biosynthesis of amino acids take place, utilizing organic acid as precursors. (Koivistoinen, 2013; Ljungdahl & Daignan-Fornier, 2012; Peraza Reyes & Berteaux-Lecellier, 2013; Tao et al., 2017; L. Wang et al., 2011; Yang et al., 2020; K. Zhang et al., 2013; S. Zhang et al., 2020)

2.1.3 Untargeted Lipidomics

Lipids are a diverse group of organic compounds that are characterized by their insolubility in water. Lipids are organized into eight main classes: fatty acids, glycolipids (glycerolipids and glycerophospholipids), sphingolipids, prenol lipids, polyketides,

saccharolipids, and sterols and their derivatives (Fahy et al., 2009). They serve as a major source of energy in the body and are involved in important physiological processes, including hormone production, vitamin absorption, and cell membrane function. (Ahmed et al., 2023; Bieberich, 2018; Niu et al., 2020; Rush et al., 2020; Savidov et al., 2018; Sejdiu & Tieleman, 2020)

In terms of cell membranes, lipids play a crucial role in their structure, formation, integrity, and regulation. Phospholipids, such as phosphatidylcholine (PC), phosphatidylethanolamine (PE), and phosphatidylserine (PS), are the major constituents of cell membranes (De Craene et al., 2017). These phospholipids consist of fatty acid chains, glycerol, and phosphate groups esterified to organic molecules like choline, ethanolamine, or serine (Xie, 2019). The saturation levels of fatty acids within lipids can influence the fluidity and flexibility of cell membranes, affecting their functionality and overall cell performance (Ballweg et al., 2020).

When studying myco-hormones, understanding the role of lipids and their analysis becomes crucial. Lipids, especially those in cell membranes, contribute to the formation of protein receptors on the cell surface. G-protein-coupled receptors (GPCRs), transmembrane receptors involved in signal transduction, play a crucial role in coordinating cell transport, metabolism, growth, and fungal survival, reproduction, and virulence (Gao et al., 2021). Phosphatidylinositol and cholesterol, for instance, have been shown to bind specific GPCRs based on charge and conformational states (Sejdiu & Tieleman, 2020). Changes in lipid composition or saturation levels can impact the functioning of these protein receptors, subsequently affecting fungal response to candidate myco-hormones or other signaling molecules (Sejdiu & Tieleman, 2020)

Lipids also serve as an energy storage mechanism, undergoing β -oxidation catabolism to provide energy to cells. In fungi, lipid production and storage primarily occur during the vegetative stage, for which pathways like β -oxidation and glyoxylate metabolism are coordinated to supply energy during sexual development (Guenther et al., 2009). Furthermore, lipids can act as signaling molecules. For instance, fatty acids can be converted into oxylipins, such as jasmonates (JA) in plants, which regulate defense mechanisms (Sugimoto et al., 2022). In fungi, oxylipins derived from oleic acid and linoleic acid influence sporulation and cellular differentiation, including hyphae branching (Niu et al., 2020; Oliw, 2021). Lipid signaling molecules, like lipo-chitooligosaccharides (LCOs), produced by fungi, have been shown to affect spore germination, hyphae branching, pseudohyphal growth, and transcription (Rush et al., 2020).

Analyzing lipids in the context of myco-hormone research is important to understand the different mechanisms in cell signaling. Techniques like lipidomics and mass spectrometry-based lipid analysis provide valuable insights into the lipid profiles of fungi, aiding in the understanding of lipid metabolism, possible myco-hormone signaling, and fungal growth and development.

S. macrospora is a microscopic model fungus known for its homothallic nature, short life cycle of 7 days, and the availability of its genome sequence. The life cycle of *S. macrospora* can be divided into two distinct phases: vegetative growth and sexual reproduction. Under optimal conditions, sexual reproduction initiates on the second day with the formation of ascogonium (asc). By the fourth day, the ascogonium develops into protoperithecium (pro), followed by the formation of perithecium (per) on the sixth day.

Finally, on the eighth day, the perithecium matures into fruiting bodies containing mature ascospores ready for release.

In this study, I investigated the metabolomes of *S. macrospora's* life cycle using different mutant strains that alter specific stages of development, including *spt3-asc*, *smatg4-asc*, *pro1*, *pro11*, *per5*, *smgp1*, and the wild-type (WT) strain. The approach involved a combination of targeted, semi-targeted, and untargeted metabolomics techniques. I quantified endogenous cytokinins (CKs), analyzed energetic metabolites, and explored lipid classes throughout the life cycle of *S. macrospora*.

The stages analyzed for the WT and mutant strains included ascogonium (day 2), protoperithecium (day 4), unmaturing perithecium (day 6), mature perithecium (day 8), and the accumulation of fruiting bodies (day 12). Through comprehensive profiling of 30 naturally occurring phytohormones, I identified the presence of CKs, such as cZ, iP, and IAA, in *S. macrospora*. Changes in those hormones suggest that CKs are involved in fruiting bodies, particularly during the ascosporeogenesis stage. Additionally, upregulation of IAA and several metabolites involved in energetic pathways was observed, particularly during the protoperithecium stage, which marks the beginning of fruiting body formation. Moreover, special attention should be given to lipids, specifically sterols, as they demonstrated enrichment throughout the fungal life cycle. Together, these findings provide valuable insights into the metabolic dynamics of *S. macrospora* and shed light on the potential roles of CKs, energetic pathways, and lipids, in the intricate process of fungal growth and fruiting body development.

2.2 MATERIALS AND METHODS

Chemicals

Chemicals were purchased from Sigma-Aldrich (St. Louis, Missouri, USA) and Fisher Scientific (Hampton, New Hampshire, USA).

Fungal Material

The *Sordaria macrospora* WT and mutant strains (listed in Table 3) were gifted by Dr. Nowrousian (Ruhr University) and Dr. Pöggeler (Universität Göttingen). The strains were initially received in corn agar media. For recovery, the strains were transferred to fresh corn agar media (CAM) and cultured for 7 days at 26°C under a 16/8 photoperiod (light/dark). To eliminate corn residues, the strains were transferred to *Sordaria macrospora* minimal media (SMM) as described by Westergard and Mitchell (1947). The SMM composition consisted of 2% glucose (w/v), 0.1% arginine (w/v) and 0.1% biotin (v/v), (0.1% (w/v) KNO₃, 0.1% (w/v) KH₂PO₄, 0.05% (w/v) MgSO₄ heptahydrate, 0.01% (w/v) NaCl, 0.01% (w/v) CaCl₂, 0.01% (v/v) trace-element stock solution [5% (w/v) citric acid (C₆H₈O₇ monohydrate), 5% (w/v) ZnSO₄ heptahydrate, 1% (w/v) Fe(NH₄)₂(SO₄)₂ hexahydrate, 0.25% (w/v) CuSO₄ pentahydrate, 0.05% (w/v) MnSO₄ monohydrate, 0.05% (w/v) H₃BO₃, 0.05% (w/v) NaMoO₄ dihydrate], pH 6.5; 1.5% (w/v) agar-agar for solid medium).

Fungal growth and harvesting

To ensure the absence of CAM residues in the *S. macrospora* fungal strains, the strains were transferred to SMM every 7 days for three consecutive weeks, maintaining the same growth conditions. During the final week prior to harvesting, the incubation period was extended to 2 weeks and large agar Petri dishes 150 mm x 50 mm were used (Fisher Scientific, Canada).

To maintain consistent fungal diameter, aseptic fungal discs were obtained using a Pasteur pipette from the large Petri dish. To collect enough tissue for the LC-MS analysis, 4 to 17 petri dishes were used for each replicate, depending on the fungal strain, and the developmental stage, the replicates were transferred from the same source (large Petri dishes). The *S. macrospora* fungal discs were inoculated into a Petri dish containing SMM media supplemented with 2% agar; after agar solidification 3.5 ml of liquid SMM was added to the Petri dishes. The number of fungal discs inoculated varied depending on the collection stage, as specified in Table 2. After 2 to 12 days post-inoculation (dpi) the stages were confirmed under a microscope, the fungal tissue was carefully collected with cell spreaders hockey sticks and filtered in a 2 mL tube with Whatman paper (#2) for one minute in the centrifuge at 10,000 rpm. Immediately after the filtration, 0.1 g of tissue was weighed, flash-frozen in liquid nitrogen, and stored at -80°C for further analysis. For media blanks, 3 replicates were collected on different days (1-12), and the liquid was chunked with a hockey stick and filtered through Whatman paper, identically as the actual experiment.

Table 2. Strains used in this study. The table describes the phenotype, developmental stage, and genotype of the *S. macrospora* strains used in this study. Also the number of inoculated discs per petri dish according to the harvesting stage. The grey cells represent the final developmental stage of the strain.

<i>S. macrospora</i> strains used in this study				Number of fungal discs inoculated/ petri dish				
Strain	Phenotype -stage	Genotype	Reference	stage 1	stage2	stage 3	stage 4	ex
<i>Spt3</i>	sterile; stage 1	Spt3 deletion, unit of the SAGA complex	DMCB	<u>4</u>	3			
<i>Smagt4</i>	sterile; stage 1	atg4 deletion, autophagy protein	DGEM	<u>4</u>	3			
Pro1	sterile; stage 2	C-6 zinc finger transcription factor	DMCB	4	<u>3</u>	2		
Pro11	sterile; stage 2	Stripak ortholog deletion	DMCB	4	<u>3</u>	2		
Per5	sterile; stage 3	homology Acl deletion, lipid metabolism	DMCB	4	3	<u>2</u>	1	
<i>Smgpi1</i>	FB overproduction; stage 4	gpi1 deletion; glycosylphosphatidylinositol	DGEM	4	3	2	<u>1</u>	
WT	Wild- type; stage 4		DMCB	4	3	2	<u>1</u>	

DGEM. Dept. Genetics of Eukaryotic Microorganisms- Ruhr University

DMCB. Department of Molecular and Cellular Botany- Universität Göttingen

FB- fruiting body

Microscopy

To confirm the stage of each strain, pictures of the fungal strains in Petri dishes were analyzed using an inverted microscope (Nikon, Eclipse Ts2), and pictures of three biological replicates were taken at 5 different time points (2-12 days) (To see the images Supplementary material Figures S1 to S21).

Extraction Method

Metabolites, lipids, and phytohormone samples were randomized and extracted using the Folch method (Wang et al., 2022) with some modifications. Frozen fungal

samples and 9 extraction blanks were reconstituted with 0.8 mL of cold (-20°C) methanol under cold conditions. Labeled deuterated internal standards (refer to Table 3) were added to each sample, followed by homogenization in a ball milling machine with zirconium oxide grinding beads for 3 minutes at 25 Hz (Comeau Technique Ltd., Vaudreuil-Dorion, Canada). The homogenized samples were further processed using a cold ultrasonic bath for 30 minutes. Subsequently, 0.75 ml of chloroform was added to each sample, which was then vortexed for 30s. To induce phase separation, 0.3 ml of B-pure water was added, vortexed for 30 seconds, and centrifuged for 10 minutes at 10,000 rpm. The upper polar phase was collected and divided into two portions for phytohormone and energetic metabolite (EnM) analysis. The lower (non-polar phase) fraction was collected by adding 0.3 ml of methanol, vortexing for 30 seconds, and centrifuging for 10 minutes at 10,000 rpm for protein precipitation. The resulting non-polar supernatant was transferred to glass vials for lipid analysis. All the samples were then dried using a speed vacuum (Savant SPD111V, UVS400, Thermo Fisher Scientific, Waltham, MA, USA) at room temperature. For the phytohormone fraction, a previously described derivatization method was employed (Kojima et al., 2009) the dried samples were resuspended in 0.75 µl of 1-propanol and vortexed for 45 minutes. Subsequently, 20 µl of B-pure water, 5 µl of 500 mM bromocholine, and 1 µl of Triethylamine were added to each sample. The samples were incubated for 2 hours at 80°C, cooled down on ice, and dried in a speed vacuum. The three sets of samples, including lipids, phytohormones, and EnM, were stored at -80°C before LC-MS analysis.

Liquid Chromatography -Mass Spectrometry (LC-MS)

Each sample fraction was reconstituted as depicted in Table 3. Quality control (QC) samples were prepared using a master mix that included pooled samples from all experimental groups. The randomized samples were analyzed using ultra-high-performance liquid chromatography (Thermo Ultimate 3000 HPLC) coupled to a mass spectrometer (Thermo Q-ExactiveTM, Orbitrap) equipped with a heated electrospray ionization (HESI) source (Thermo Scientific, San Jose, CA, USA). Quality management was ensured by including systemic blanks, system suitability (CK and amino acid standards), Quality Control (QC) samples (at the beginning and every 20 samples), and extraction blanks following the guidelines described by Broadhurst et al. (2018). Only, mixes made of pooled samples of each strain (WT and mutants) were used to run into Liquid Chromatography - tandem Mass Spectrometry (LC-MS/MS) for phytohormones and EnM (as shown in Table 4), while all lipid samples were analyzed using LC-MS/MS for all samples. LC-MS method changes slightly for each sample type, the parameters are shown in Tables 3 and 4. For lipidomics, the WT was analyzed from stages two to five, skipping stage 1 due to the loss of the samples therefore strain *per5* (E) was analyzed for lipid comparison in stage 3 with WT stage 3.

Table 3. Liquid chromatography parameters for phytohormones, Energetic metabolites (EnM), and lipid analysis

Fraction	Resuspended	Internal standards	Gradients	Flow	HPLC settings
Phytohormones	0.5ml of 0.08 % Acetic acid 5% aqueous ACN	CKs: 10 ng of each ([2H7]BA, [2H7]BAR, [2H5]ZOG, [2H7]DHZOG, [2H5]ZROG, [2H7]DHZROG, [2H5]Z7G, [2H5]Z9G, [2H6]iP7G [2H5]2MeSZ, [2H6]2MeSiP, [2H5]2MeSZR, [2H6]2MeSiPR, [2H6]iPR, [2H5]ZR, [2H3]DHZR, [2H6]iP, [2H3]DHZ, [2H5]Z, (OChemIm Ltd., Olomouc, Czech Republic). 5,8',8',8'-, [13C6] IAA (Cambridge Isotopes (Andover, Massachusetts, U.S.A.) 68ng of [2H4] -ABA (NRC-PBI, Saskatoon, Saskatchewan, CA)	A:0.08% AcA in water	95% (B), changing linearly to 55% (B) in 4 minutes and then changing to 25% (B) in 5 minutes. At 5.1 minutes, conditions change to 5% (B) for 1 minute and then returned to initial conditions at 6.2 minutes for a 2 minute re-equilibration period for a total run time of 8.2 minutes.	Column: Kinetex C18 column (2.1 x 100 mm, 1.9 µm solid core, 0.35 µm porous shell; Phenomenex, Torrance, CA, U.S.A.)
			B: 0.08% in ACN	Flow rate: 0.5 ml/min Sample injection: 25 uL	Track temperature 4°C Column Temperature 25 °C
EnM	0.5 ml of 90% ACN in water	0.5 µM concentration of [13] and N[15] labeled amino acids (Glycine , Alanine , Serine , Proline , Valine , Threonine , Asparagine , Aspartate , Isoleucine , Leucine , Glutamine , Glutamate , Lysine , Methionine , Histidine , Phenylalanine , Arginine , Tyrosine , Tryptophan , Cystine) (Cambridge Isotope Laboratories, Tewksbury, MA, USA)	A:0.08% AcA in water	95% (B), changing linearly to 55% (B) in 4 minutes and then changing to 25% (B) in 5 minutes. At 5.1 minutes, conditions change to 5% (B) for 1 minute and then returned to initial conditions at 6.2 minutes for a 3.8 minute re-equilibration period for a total run time of 10 minutes.	Column: Halo 2.7 µm C18 column (50 mm × 2.1 mm; Canadian Life Science, Peterborough, Canada)
			B: 0.08% in ACN	Flow rate: 0.25 ml/min Sample injection: 25 uL	Track temperature 4°C Column Temperature 25 °C
Lipids	IPA:CAN:H ₂ O (2:1:1 v/v)	N/A	A:60% ACN, 10 mM AmFm and 0.1% FmA in water	B (20–100% from 0.5 to 8.5 min, keep 100% from 8.5 to 12.5, and 20% from 12.5 to 15 min, initial conditions are run for 3 for a total run of time of 18 min	Column: Halo 2.7 µm C18 column (50 mm × 2.1 mm; Canadian Life Science, Peterborough, Canada)
			B: 90% IPA, 10 mM AmFm and 0.1% FmA in water	Flow: 0.3 ml/min Sample injection: 25 uL	Track temperature 10°C Column temperature 40°C

Table 4. Mass spectrometry parameters for phytohormones, Energetic metabolites (EnM), and lipids.

Mass spectrometry settings	Phytohormones and EnM		Lipids	
	MS1 Full scan dual mode	MS2 For both polarities	MS1 Full scan for both modes	MS2 For both polarities
Resolution	140,000	17,500	70,000	17,500
AGC target	3.00E+06	5.00E+05	5.00E+05	5.00E+04
Max IT (ms)	524	64	100	10
Scan range (m/z)	150-500		100-1300	200-2000
CE/Steeped CE	40 kV			25, 30
Min AGC target	1.00E+04			5.00E+02
Intensity threshold	1.60E+05			1.00E+04
Dynamic exclusion	10s			15s

AcA, Acetic acid; AmFm, Ammonium Formate; FmA, Formic Acid; ACN, Acetonitrile; IPA,

Data Analysis

For **phytohormones and EnM**, Data analysis was performed using Thermo Xcalibur (v 3.0.63) software (Thermo Scientific, San Jose, CA, USA), to calculate peak areas. Quantification of phytohormones and relative quantification of energetic metabolites was achieved through isotope dilution analysis based on the recovery of [^2H], [^{13}C], or [^{15}N]- labeled internal standards.

To determine the relative EnM quantification, the peak areas were normalized based on the average recovery of labeled amino acid standards, including Histidine, Asparagine, Glutamine, Serine, Threonine, Proline, Valine, Isoleucine, and Tyrosine. These specific standards were chosen as they were the only ones that could be reliably recovered due to potential amino acid damage or matrix effects.

For **lipids** analysis the raw data files were converted to an. mzXML format in centroid mode using MSconvert from the ProteoWizard package (Kessner et al., 2008). The mzXML files were then processed using MZmine software (Version 3.3.0) (Schmid et al., 2023). A signal threshold of 1.8×10^5 was applied for MS1 mass detection within the mzXML files. The detected masses were used to build extracted ion chromatograms (EIC) using the ADAP module, with a minimum intensity, threshold of $1.8E^5$, a minimum highest intensity of 1×10^6 (AU) and a 5 ppm relative mass tolerance. Smoothing of the EIC was performed using the Savitzky-Golay algorithm. Chromatographic deconvolution was carried out with the "Local minimum feature resolver" algorithm, utilizing various parameters such as minimum absolute peak height (1×10^6 AU), chromatographic threshold (of 70%), the minimum retention time for peak scoring (0.5 min), and height to side peak ratio of 1.4. Following deconvolution, isotope peak grouping and alignment of EICs were performed with specific mass and retention time tolerances, 5 ppm and 0.1 min respectively. Only aligned EICs containing a minimum of two isotope peaks and occurring in at least two samples were included. Missing values in the EICs were filled using a window of tolerance for mass 5 ppm and retention time 0.1 min. Duplicate peaks were removed within a window of mass of 5 ppm and retention time of 0.4 min. Finally, lipid annotation was performed with a 5 ppm error tolerance using MZmine 3.

The functional and statistical analysis of the lipidomics data was performed using MetaboAnalyst 5.0 (<https://www.metaboanalyst.ca/>). MetaboAnalyst is a comprehensive web-based tool designed for metabolomics data analysis, visualization, and interpretation.

Functional analysis was conducted to identify the underlying biological pathways and processes that are significantly associated with the lipidomics data. The pathway

enrichment analysis utilizes an over-representation analysis (ORA) approach, which compares the observed metabolite sets with a predefined pathway database. The statistically significant pathways were identified based on the Mummichog version 2.0 algorithm with a 0.1 p-value cut-off. The pathway database used for analysis was “Lipids -Main Chemical Class” and “Lipid -Sub Chemical Class”.

Statistical analysis was performed to identify differential metabolites and to assess the significance of the observed changes between different experimental groups.

Statistical methods such as t-tests, volcano plots, and analysis of variance (ANOVA) were performed with nonparametric tests with unequal variances and p-values adjusted for false-discovery rate. The significant changes were considered for $P < 0.1$.

Multivariate analysis was performed to capture the overall patterns and variation in the metabolomics data. Principal component analysis (PCA) and partial least squares-discriminant analysis (PLS-DA) were employed to visualize and discriminate different sample groups based on their metabolic profiles.

To visualize the patterns of metabolite abundance across different experimental conditions, Heatmaps were used to provide a graphical representation of the data, allowing for the identification of clusters or groups of metabolites with similar abundance patterns.

Finally, volcano plots were generated to visualize the fold-change and statistical significance of differentially expressed metabolites. Data were plotted with log₂ fold change on the x-axis and the negative log₁₀ of the p-value on the y-axis. The significance threshold was set based on $P < 0.1$.

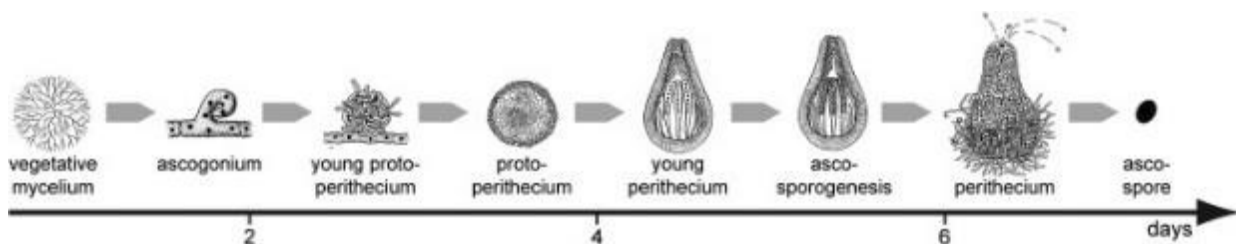
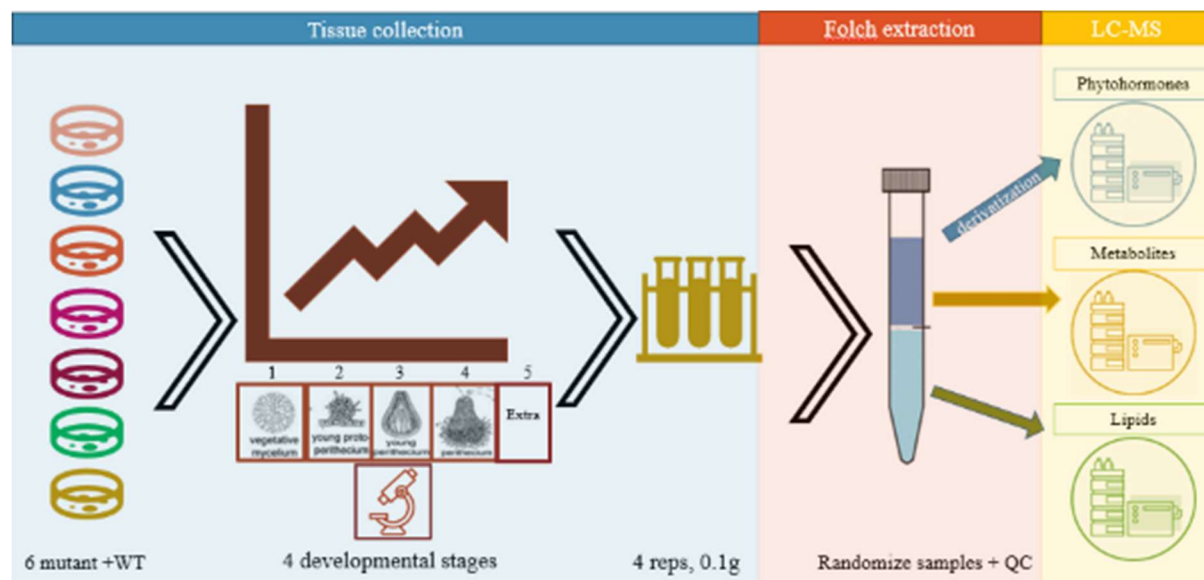


Figure 4. A) Schematic representation of the methodology for the analysis of phytohormones, metabolites, and lipids in the *S. macrospora* strains, B) Schematic representation of the life cycle of *S. macrospora* (image obtained from Teichert et al. (2020)), in this study day 2, 4, 6, and 8 corresponded to stages 1, 2, 3, and 4, respectively.

2.3 RESULTS

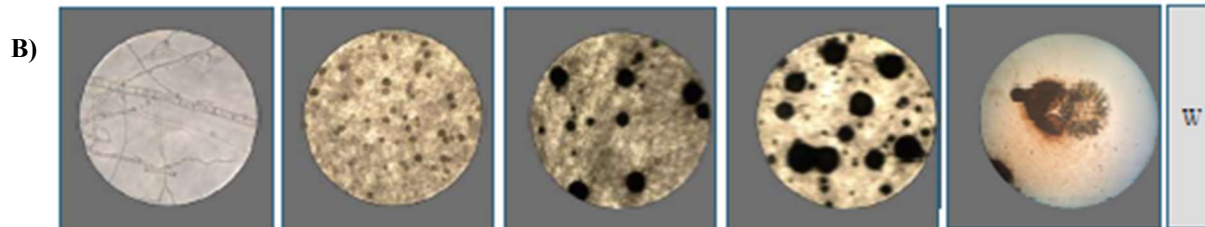
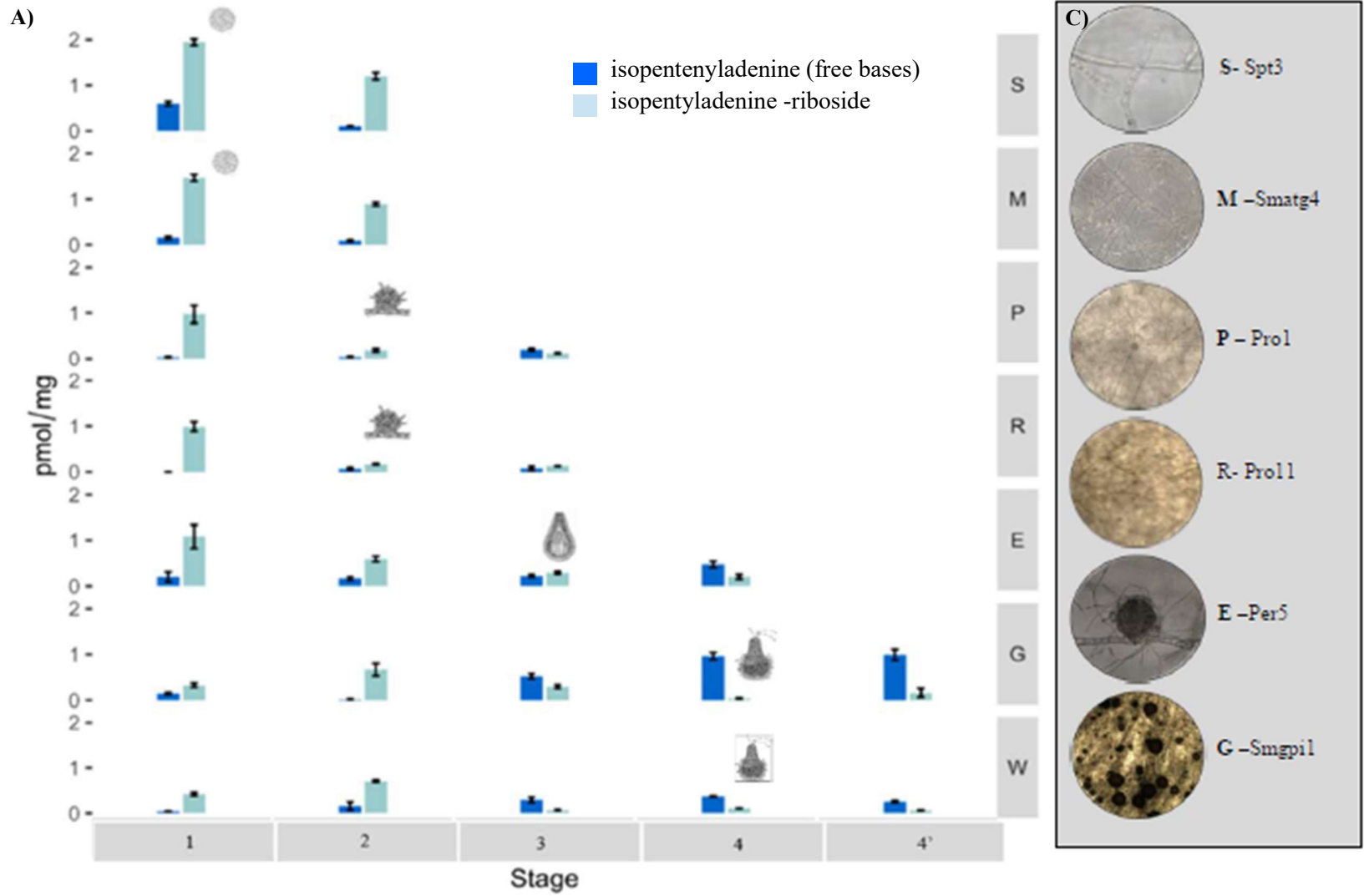
2.3.1 Endogenous Phytohormones in *Sordaria macrospora*

To investigate whether the production and regulation of endogenous phytohormones might play a role in the development of *Sordaria macrospora* life cycle, thirty phytohormones were analyzed via LC-MS/MS at the different developmental stages (Table 4). No phytohormones were detected in the control media or extraction blanks.

Cytokinins (CKs)– S. macrospora produces more free base CKs in the last stages of sexual reproduction.

In *S. macrospora*, both iP and cZ were produced at different concentrations during the fungus life cycle, and their conversion from ribosides to freebases occurred during the development of the fruiting body. Previous studies have demonstrated fungi produce CKs, such as iP and cZ, are more biologically active than their riboside fractions (iPR and cZR) (Nguyen et al., 2021). Interestingly, the ratio of free base: riboside forms of both iP and cZ types showed an increase from ~1:4 to 4:1 during stage 3 (Figure 5), which is the transition from young perithecium to ascosporeogenesis (Figure 1A). Furthermore, the production of the cZ types (cZ and cZR) was 4 times greater than the iP type (iP and iPR), ranging from 1.05 to 4.3 and 0.3 to 0.8 pmol/g, respectively. These findings suggest that there is a shift towards more active CK types, that may play a crucial role as a signaling molecule during the fruiting body development of *S. macrospora*. This occurred in the WT and any mutants that completed the transition to the final stage. However, the mutant strains that could not progress to the final stage did not show a shift to the more active CK free bases. The strains that arrested at the first developmental stage and produced only mycelium, *spt3* (S) and *smatg4* (M), demonstrated a greater production of ribosides than free bases, with no variation in the production of CKs at the different time points (Figure 5). Likewise, the strains which develop until the 2nd stage accumulating protoperithecium tissue, *pro1* (P) and *pro11* (R), decreased the R production but the FB remained steady. The strain *per5* (E), which stops development at stage 3 when perithecium begins to form, demonstrated a decrease in the production of iPR and cZR, while cZ remained steady, and iP increased

during the initial stages of the perithecium (Figure 5). Finally, strain *smgpil* (G), which completes all the developmental stages (and in fact produced more fruiting bodies than the wild type) also displayed a switch from ribosides to free bases. However, G produced up to 3 and 5 times more iP and cZ, respectively, compared to the wild type. This suggests that CKs may play a role as signaling molecules in the development of this fungus, specifically in spore formation, further studies are needed to fully understand their exact mechanisms and function.



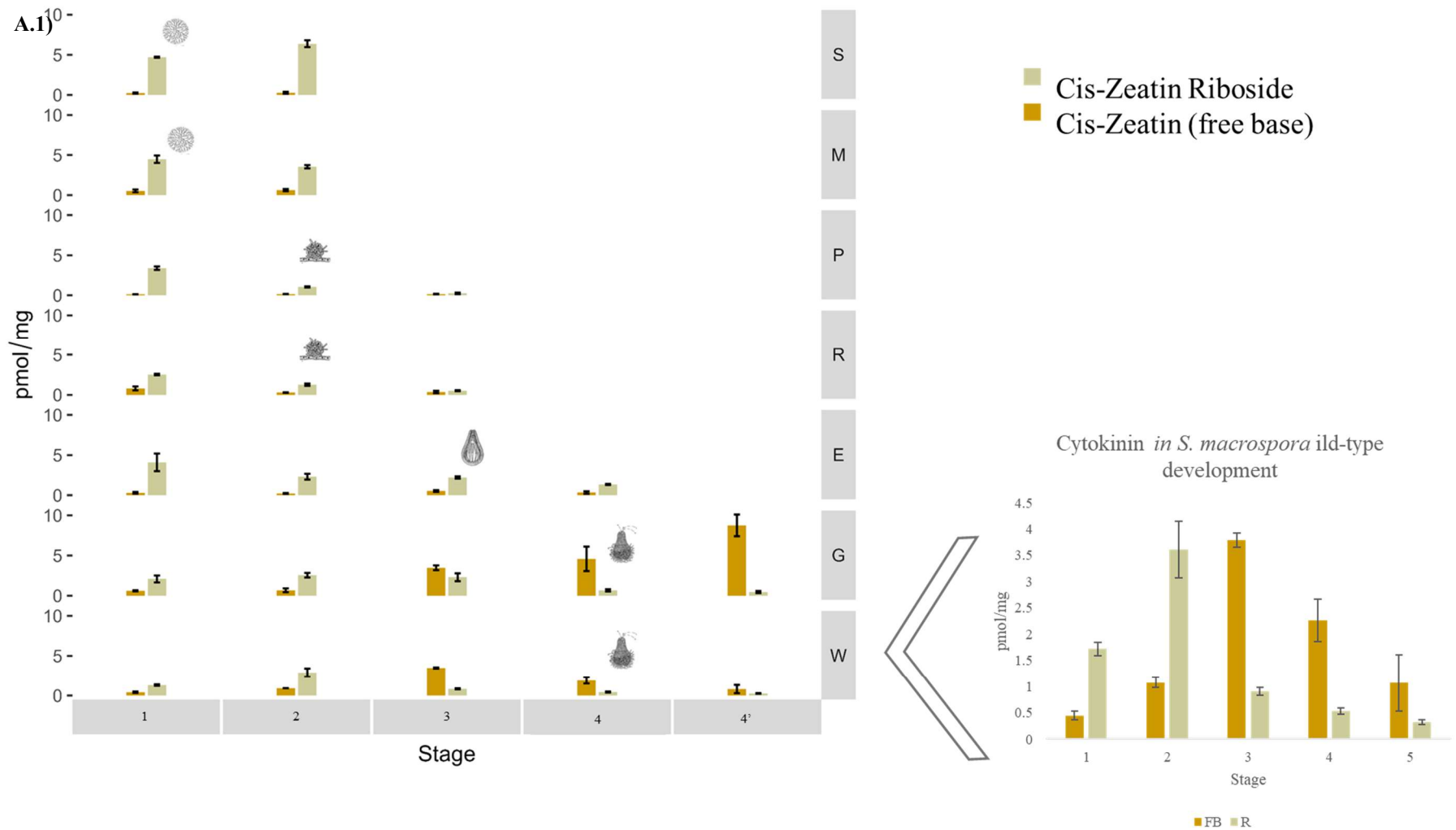


Figure 5. Production of cytokinins in different stages of *S. macrospora*. The strains were cultured in *Sordaria macrospora* minimum media and harvested at each stage until their developmental last developmental stage, with an additional stage included (2 more days). The strains *Spt3* (S)

and *Smagt4* (*M*) exhibit stagnation in the first stage; *Pro1* (*P*) and *Pro11* (*R*) in the second stage; *Per5* (*E*) in the third stage; and *Smgpi1* (*G*) is characterized by excessive fruiting body production. **A)** In vitro production of the *iP* type and **A.1)** *cis*-Zeatin type by *S. macrospora* wildtype and mutants at different developmental stages. The x-axis represents the developmental stages: 1 vegetative mycelium, 2 protoperithecium, 3 young perithecium, 4 mature perithecium, and 5 tissue collected 12dpi. The y-axis represents the concentration in pmol/mg. The error bars represent the standard deviation ($SD\pm$) for 4 biological replicates ($n=4$). The small tissue icons in the graphs represent the developmental stagnation of each strain. The stages of the strains were confirmed using an inverted microscope. **B)** Microscope images showing the different developmental stages (1 to 4) of *S. macrospora* wildtype. **C)** Microscope images showing the last developmental stage of *S. macrospora* mutants.

Auxin in S. macrospora increases in the transition from vegetative to sexual reproduction.

S. macrospora strains exhibited the capacity to biosynthesize the auxin indoleacetic acid (IAA). Moreover, there was an increase in IAA accumulation in the second and third stages in any strains that were able to produce mature fruiting bodies, such as WT and G (Figure 6). In *S. macrospora*, the transition from vegetative to sexual reproduction occurs in stage 2, which corresponds to day 4 of the life cycle (Nowrousian et al., 1999a). This transition demands high quantities of energy (Kück et al., 2009). The WT showed an increase from 0.89 to 7.75 pmol/g in the second stage and then remained steady until the final stage, where it dropped to 3.75 pmol/g. Similar to the WT, *per5* reached the highest concentrations of IAA at stages 1 and 2, with 98.8 and 105.73 pmol/g FW, respectively. However, *per5* produced up to 60 times more IAA than the wild type at the second stage (Figure 6).

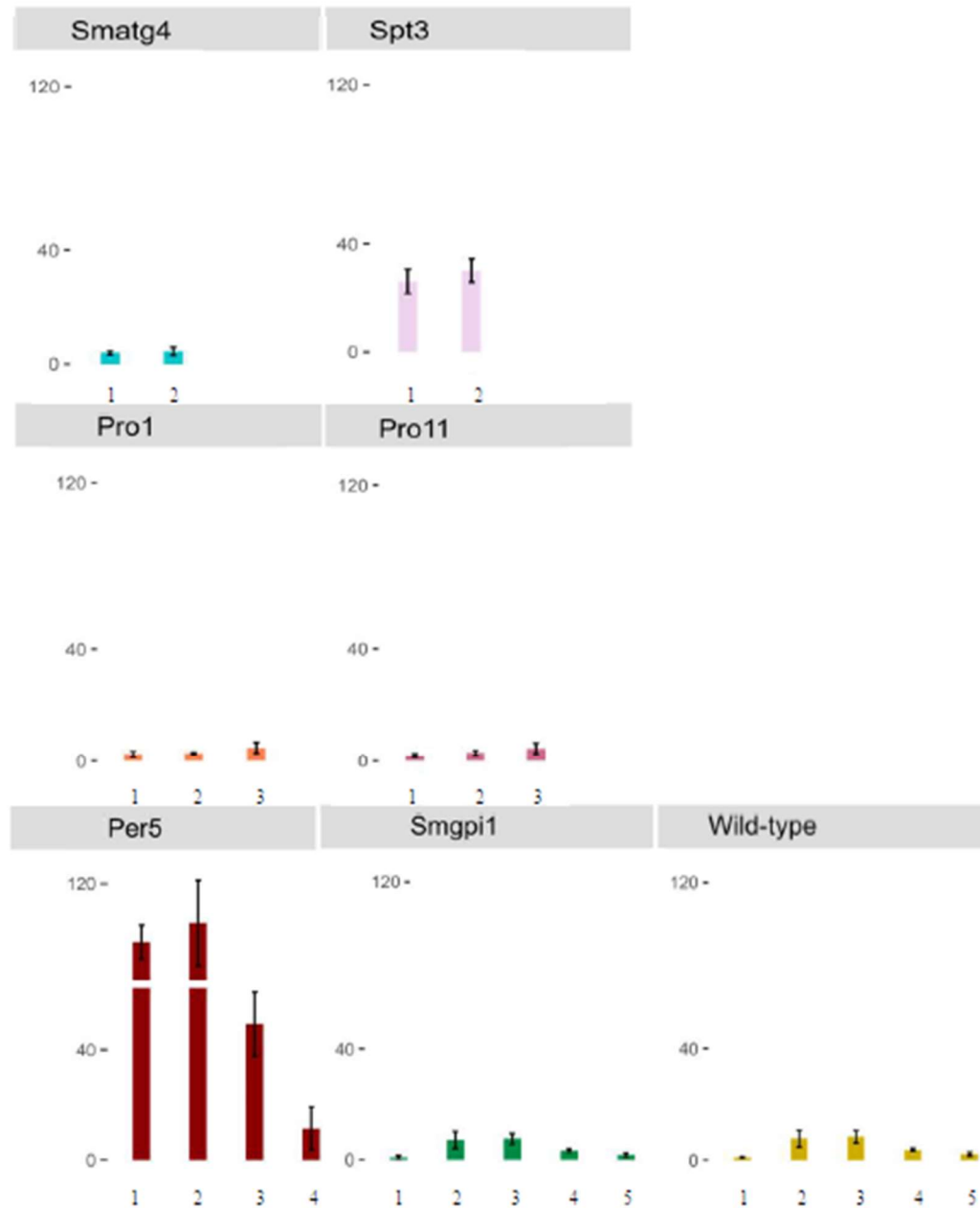


Figure 6. Production of the auxin indole acetic acid (IAA) in the *S. macrospora* strains at the different developmental stages. The strains were cultured in *Sordaria macrospora* minimum media and harvested at each stage until their developmental last developmental stage, with an additional stage included (2 more days). The strains *Spt3* (S) and *Smagt4* (M) exhibit stagnation in the first stage; *Pro1* (P) and *Pro11* (R) in the second stage; *Per5* (E) in the third stage; and *Smgpi1* (G) is characterized by excessive fruiting body production. The x-axis represents the developmental stages: 1 vegetative mycelium, 2 protoperithecium, 3 young perithecium, 4 mature perithecium, and 5 tissue collected 12dpi. The y-axis represents the concentration in pmol/mg. The error bars represent the standard deviation (SD±) for 4 biological replicates (n=4).

2.3.2 Semi-targeted analysis of the Energy metabolome (EnM) in *S. macrospora* wild type

The purpose of conducting LC-MS semi-targeted analysis was to investigate the metabolic processes occurring during the stages of phytohormone changes, aiming to gain a better understanding of the potential mechanisms underlying phytohormone actions in the fungi, while also exploring the possibility of detecting other metabolites that could serve as potential myco-hormones for fungal growth and development. A semi-targeted approach allowed for the identification and relative quantification of a wide range of metabolites. This approach relies on the use of known metabolites, often with similar chemical properties to the metabolite group of interest, for relative quantification (Billet et al., 2020; Reisz et al., 2019).

In this study, labelled amino acids (Table 3) were used for the analysis of energy metabolome (EnM) that consisted of metabolites involved in energy pathways that are essential for meeting cellular needs and maintaining proper functioning. A total of 150 metabolites were initially targeted, approximately 60 metabolites were successfully manually scored and matched with their MS/MS spectra. From the list of 150 metabolites, only arginine and glucose were found in the control media, but not in the extraction blanks.

Organic Acids are regulated during the Transition to Sexual Reproduction of S. macrospora wild type.

The metabolic profile of *S. macrospora* WT strain revealed regulation of organic acids throughout the fungus life cycle. The most upregulated organic acids were L-Ketoisovalerat, 2-Hydroxyglutarate, citrate/isocitrate, cis-Aconitate, Shikimate, Glycolate,

Lactate, Glyceric acid, Fumarate, succinate, gluconic acid, and uric acid (Figure 7) and the amino acids Alanine, Leucine, GABA, Methionine, Proline, Histidine, Amino adipate, Phenylalanine, and Tryptophan (Figure 8)

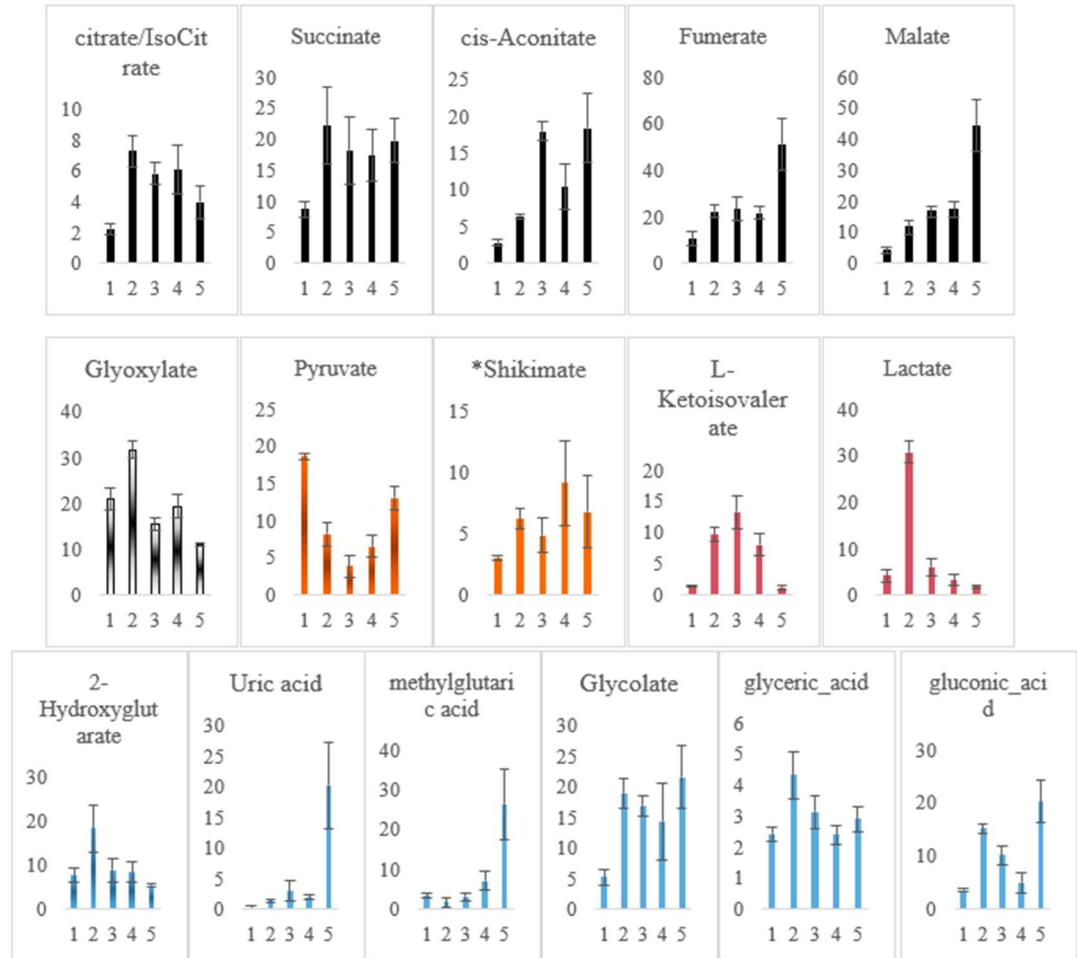


Figure 7. Organic acids (OAs) detected with LC-MS/MS in *S. macrospora*. The fungus was grown in *Sordaria Minimal Media* (SMM) for 12 days. The x-axis represents the developmental stages: 1 vegetative mycelium, 2 protoperithecium, 3 young perithecium, 4 mature perithecium, and 5 tissue collected 12dpi. The y-axis represents the relative abundance according to the recovery of the labeled internal standards ($[^{15}\text{N}]$ or $[^{13}\text{C}]$ labelled aminoacids). The error bars represent Standard Error (SE \pm) for 4 biological replicates. The graphs are color-coded, with black bars representing OAs associated with the tricarboxylic acid (TCA) cycle and glycolysis, white (glyoxylate) a variation of the TCA cycle, the orange precursor is phosphoenolpyruvate, the pink precursor is pyruvate and blue other metabolites. *Shikimate was confirmed only with MS¹.

TCA cycle Organic acids

The analysis of organic acids associated with the tricarboxylic acid cycle (TCA) revealed noteworthy alterations throughout the developmental stages of *S. macrospora* wild type. Among those organic acids detected through LC-MS/MS, citrate/isocitrate, succinate, cis-Aconitate, fumarate, and malate, showed an increase, particularly during the second developmental stage. Subsequently, these compounds did not exhibit notable changes throughout the remaining life cycle stages, except for fumarate and malate, which demonstrated an increase during the last stage (stage 5). These findings highlight the distinct regulation of organic acids within the TCA cycle, reflecting their essential roles in energy metabolism and developmental transitions in *S. macrospora* wild type.

Non-TCA cycle Organic acids

Pyruvate decreased in concentration, reaching its lowest point by the third stage of development. The decrease in pyruvate levels may indicate its utilization or conversion to other metabolites during this stage. Similar to the TCA cycle organic acids, the levels of glyoxylate, shikimate, and lactate also increased during the second stage of development in *S. macrospora*. This observation may be attributed to the transition from vegetative mycelium to sexual growth, as previously described. However, these organic acids subsequently showed a decrease in concentration during stage 3 of development. This decline could be indicative of a shift in metabolic priorities or the utilization of alternative pathways as the fungus progresses through its developmental stages (Ene et al. 2014).

L-ketosiovalerate (KIV), methylglutyric acid, and 2-Hydroxylglutaraic acid (2-HG) are important intermediates in the breakdown of valine, leucine, and lysine,

respectively (Engqvist et al., 2014; Jones et al., 2020; Takpho et al., 2018). In *S. macrospora*, the levels of methylglutyric acid decrease by stage 2 of the life cycle, however, by stage 5, the levels of methylglutyric acid showed a remarkable increase, reaching a level that was approximately ten times higher than those observed in stage 2. KIV is a key intermediate derived from pyruvate and can be further metabolized to generate energy or other biosynthetic compounds. Interestingly, KIV shows a peak concentration at the third stage, contrasting with pyruvate, which declined. 2-Hydroxyglutarate, apart from its role in amino acid digestion, enters the mitochondria and participates in various metabolic pathways for energy generation (Engqvist et al., 2014). It peaked at stage 2, suggesting it was used as an energy source early in development, and decreased over time. This indicates it has a potential a regulatory role throughout the life cycle of *S. macrospora*.

Amino acids

The amino acid profile of the *S. macrospora* WT (Figure 8, the graphs are divided by colors based on the organic acid precursor of the glycolysis pathway) reveals there was an overall increase in amino acid levels during the transition from vegetative mycelium to the protoperithecium stage. This may indicate there was heightened amino acid metabolism during the onset of sexual reproduction. However, arginine, glutamic acid, and ornithine showed notable decreases during this same transition, suggesting distinct roles in the metabolic pathways associated with sexual development. Glutamic acid recovered to its initial concentration by the end of the life cycle, indicating a potential regulatory mechanism, while arginine and ornithine were completely depleted, indicating other metabolic processes were higher priority. Threonine, valine, and glycine remained

relatively stable across the life cycle, suggesting they are consistently needed in essential cellular functions and metabolic processes.

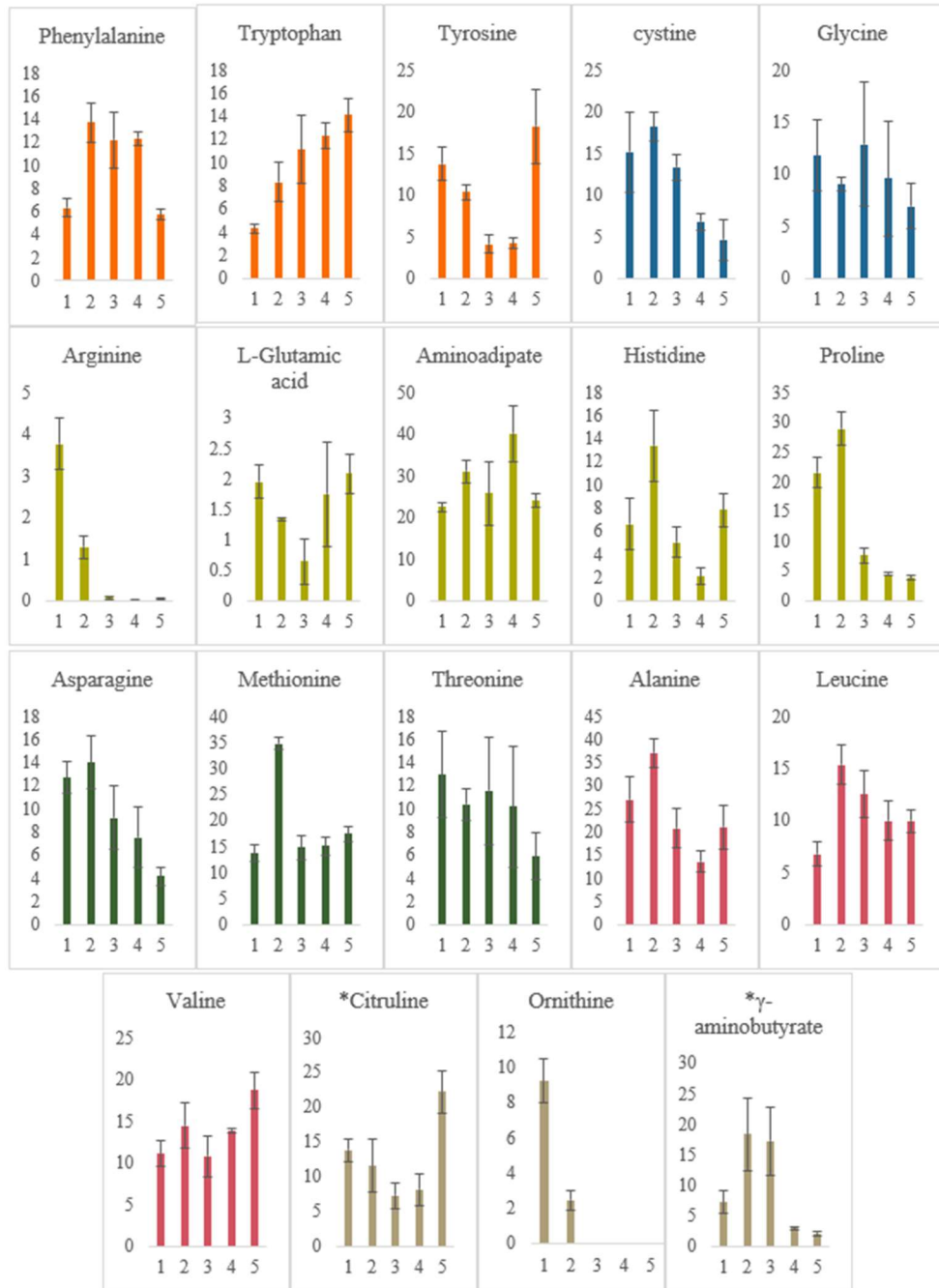


Figure 8. Amino acids detected with LC-MS/MS in *S. macrospora* across different developmental stages. The fungus was grown in Sordaria Minimal Media (SMM) for 12 days. The x-axis of the graphs represents the developmental stages: 1 vegetative mycelium, 2 protoperithecium, 3 young perithecium, 4 mature perithecium, and 5 tissue collected 12dpi. The y-axis represents the relative abundance according to the recovery of the labeled internal

standards ($[^{15}\text{N}]$ or $[^{13}\text{C}]$ labelled aminoacids). The error bars represent Standard Error (SE \pm) for 4 biological replicates. The graphs are color-coded based on the organic acid precursors derived from *Saccharomyces cerevisiae* glycolysis metabolism (Ljungdahl & Daignan-Fornier, 2012; Takpho et al., 2018; Yang et al., 2020). The orange bars represent amino acids originating from phosphoenolpyruvate, blue bars represent amino acids derived from 3-phosphoglycerate, yellow bars represent amino acids derived from α -ketoglutarate, green bars represent amino acids derived from oxaloacetate, pink bars represent amino acids derived from pyruvate and grey bars represent proteinogenic amino acids. * means data confirmed only with MS¹ analysis.

Nucleosides, nucleotides, and nucleobases in S. macrospora wild type

The study of nucleosides, nucleotides, and nucleobases (NNNs) provides insight into DNA and RNA metabolism, as well as cell signaling and communication (Phan et al., 2018). In the *S. macrospora* life cycle, guanine was the only detected nucleobase, and it showed an increase in the second stage. Nucleosides detected in *S. macrospora* grown in SMM media included: uridine, thymidine, inosine, guanosine, and cordycepin. Nucleoside levels generally increased in the second stage, except for thymidine and cordycepin. By the third stage, most nucleosides decreased to their lowest levels but recovered by the fifth stage, except for inosine which remained elevated. Cordycepin and thymine showed different patterns, with no increase in the second stage and a sharp decrease to stages 3 and 4.; followed by a rebounding increase by the fifth stage. Cyclic AMP (cAMP) increased during the second and fourth stages, corresponding to sexual development and sporulation. Uridine monophosphate reached its lowest point in the third stage, while 5'-methylthioadenosine (MTA) peaked in the same stage.

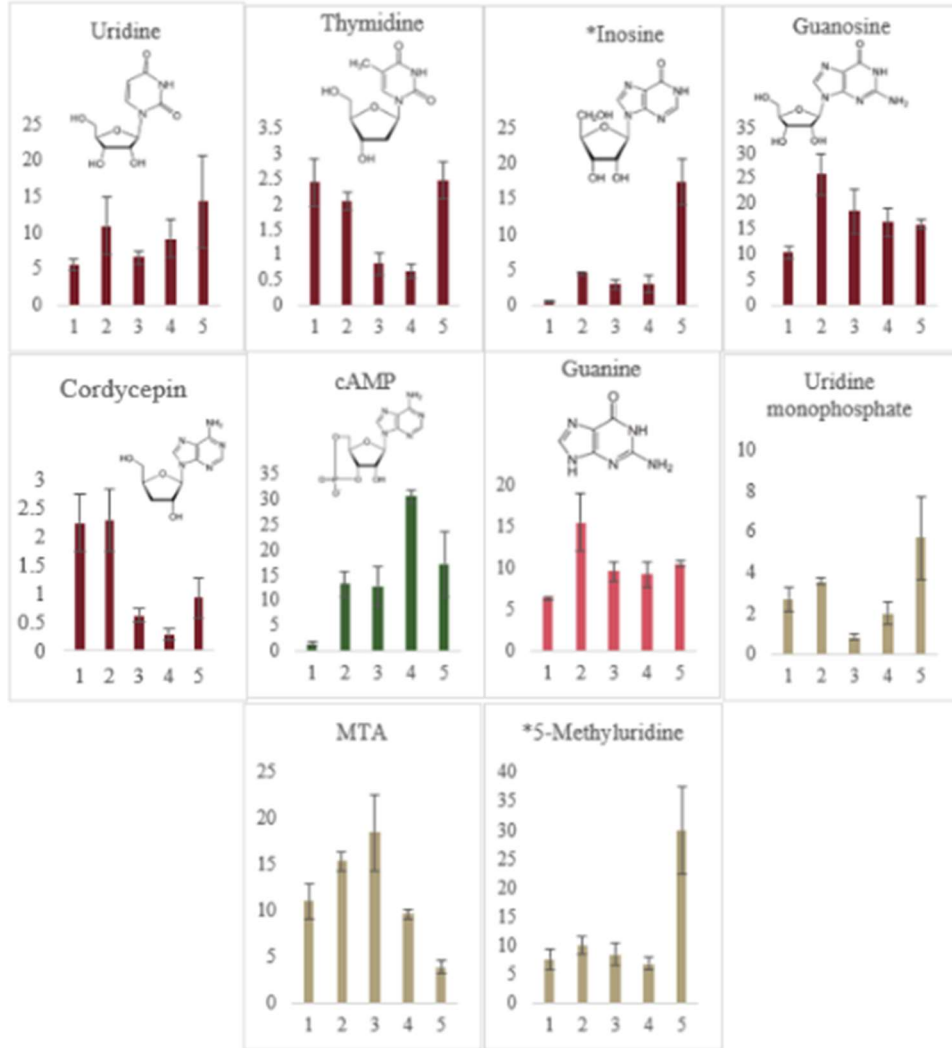


Figure 9. Nucleosides, nucleotides, and nucleobases (NNNs) detected with LC-MS/MS in *S. macrospora* across different developmental stages. The fungus was grown in Sordaria Minimal Media (SMM) for 12 days. The x-axis of the graphs represents the developmental stages: 1 vegetative mycelium, 2 protoperithecium, 3 young perithecium, 4 mature perithecium, and 5 tissue collected 12dpi. The y-axis represents the relative abundance according to the recovery of the labeled internal standards ($[^{15}\text{N}]$ or $[^{13}\text{C}]$ labelled aminoacids). The error bars represent Standard Error ($\text{SE} \pm$) for 4 biological replicates. The graphs are color-coded based on the molecule, red represents the nucleosides, pink the nucleotides, and grey and green the nucleobases. cyclic adenosine monophosphate (cAMP), and 5'-Deoxy-5'-Methylthioadenosine (MTA). *MTA was confirmed only with MS^1 .

Other semi-targeted metabolites

I analyzed other small metabolites that play important regulatory roles in fungal processes. Among these metabolites are monosaccharides, which can be hydrolyzed to pyruvate. Pyruvate serves as an energy source and biosynthesis of essential metabolites involved in various cellular processes in fungi (Vetter, 2023). Furthermore, metabolites such as choline and mevalonate, are known to have significant implications for fungal growth. Choline is essential for the biosynthesis of phospholipids, key components of cell membranes that contribute to structural integrity and cellular functions (Markham et al., 1993). Mevalonate, on the other hand, is crucial for the biosynthesis of sterols, including important sterols like ergosterol, which are vital for fungal membrane stability and function (Yasmin et al., 2012).

Throughout the *S. macrospora* life cycle, various monosaccharides were identified including riboside, fructose, sucrose, mannitol, ribose-5-phosphate, fructose/glucose-6-phosphate, and uridine diphosphate glucose (Figure 10). As well as the small molecules choline, mevalonate, indole-3-carboxylic acid, quinic acid, pyrogallol, and hydroxybenzotriazole (Figure 11). Sugar levels generally decrease over time, with ribose showing a drop in the fourth stage but recovering in the fifth stage. Mannitol is used for rapid energy acquisition and adjustment of osmotic potential, pH, and is a co-factor for regulation of morphogenesis and sporulation in filamentous fungi (Meena et al., 2015; Vetter, 2023). Initially had low levels but increased by the second stage; and subsequently it decreased throughout the life cycle. Isomeric forms of sucrose and fructose 6-phosphate were observed, but no specific trend in their levels was detected. These findings enhance our understanding of sugar metabolism dynamics and the presence of other small

molecules during the *S. macrospora* life cycle, shedding light on their potential roles in different developmental stages.

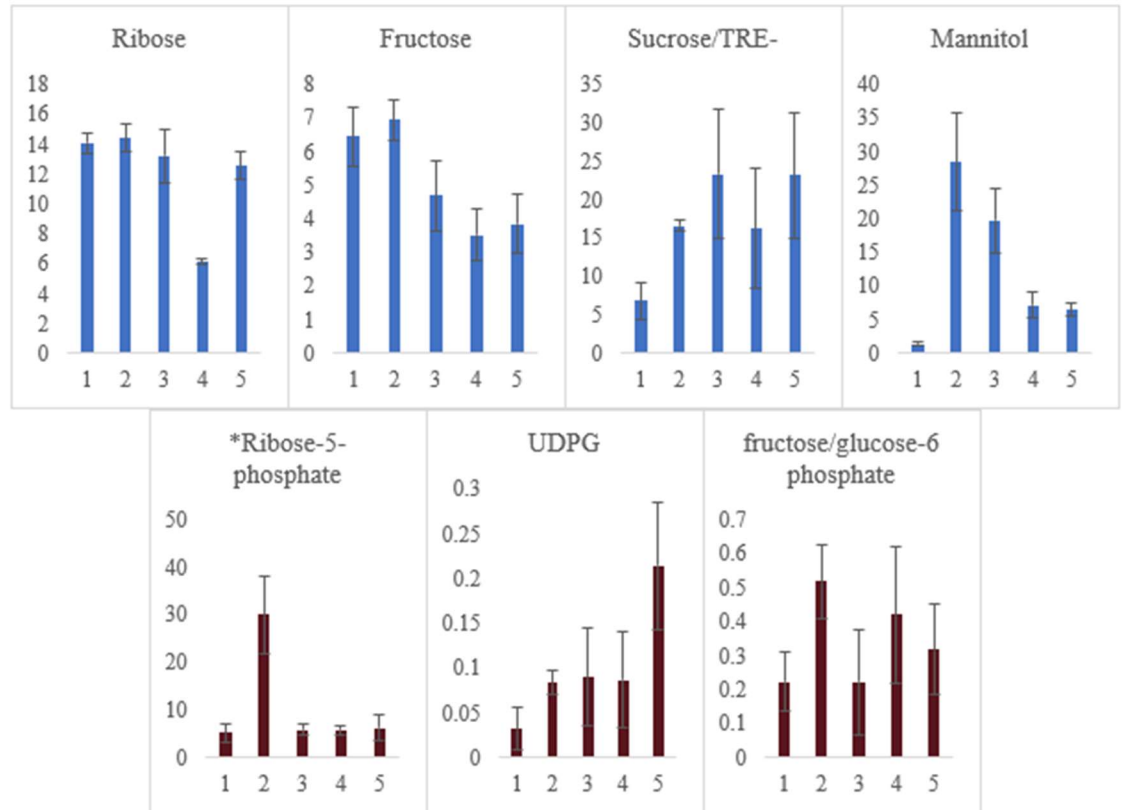


Figure 10. Sugars detected with LC-MS/MS in *S. macrospora* across different developmental stages. The y-axis represents the normalized peak areas. The x-axis of the graphs represents the developmental stages: 1 vegetative mycelium, 2 protoperithecium, 3 young perithecium, 4 mature perithecium, and 5 tissue collected 12dpi. The y-axis represents the relative abundance according to the recovery of the labeled internal standards ($[^{15}\text{N}]$ or $[^{13}\text{C}]$ labelled aminoacids). The error bars represent Standard Error (SE \pm) for 4 biological replicates. The sugar trehalose (TRE) and sucrose are isomers, as well as fructose and glucose. The isomers were scored together. * Ribose-5-phosphate was confirmed only with MS¹

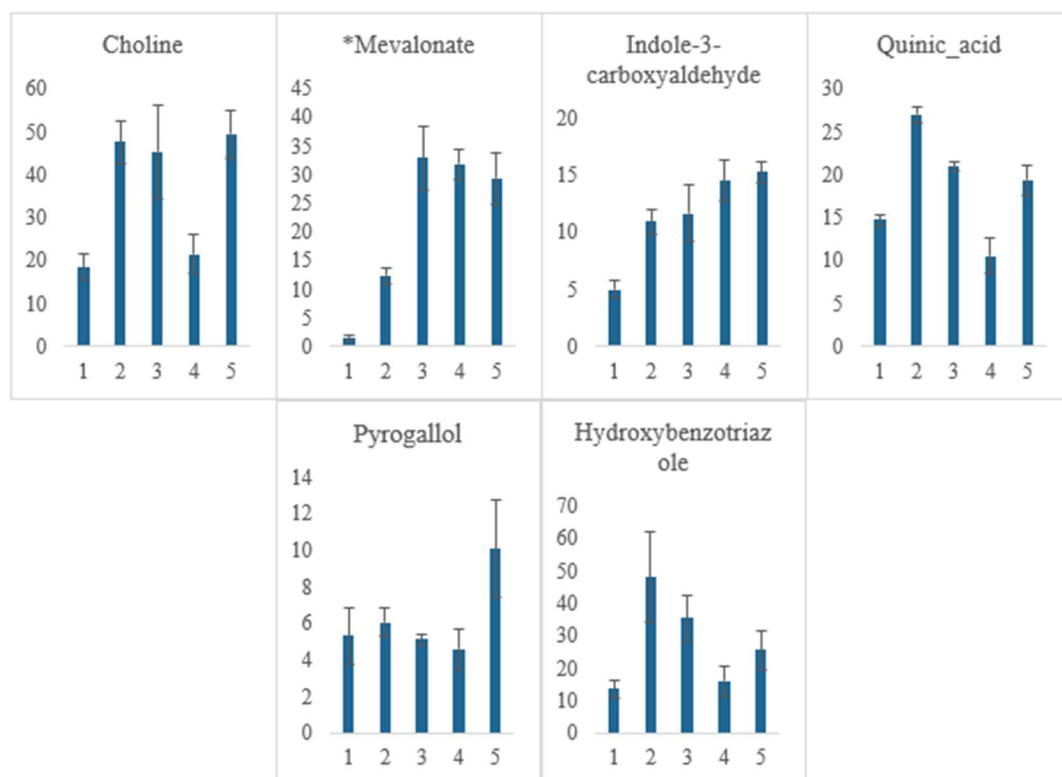


Figure 11. Other small molecules analyzed with LC-MS/MS in *S. macrospora* across different developmental stages. The x-axis of the graphs represents the developmental stages: 1 vegetative mycelium, 2 protoperithecium, 3 young perithecium, 4 mature perithecium, and 5 tissue collected 12dpi. The y-axis represents the relative abundance according to the recovery of the labeled internal standards ($[^{15}\text{N}]$ or $[^{13}\text{C}]$ labelled aminoacids). The error bars represent Standard Error (SE \pm) for 4 biological replicates. *Mevalonate was confirmed only with MS¹.

2.3.3 Lipidomics of *S. macrospora*

LC-MS lipidomic analysis was performed in *S. macrospora* wild type at stages 2, 3, 4, and 5, and the mutant *per5* at stage 3. The *S. macrospora per5* mutant (E) was chosen for the comparative analysis due to the lack of *acl* gene which regulates fatty acid and sterol pathways, interestingly *per5* produces fruiting bodies but is unable to produce spores.

LC-MS lipidomic analysis of *S. macrospora* wild type and the *per5* mutant at different stages revealed 7380 detected features. LC-MS analysis using Mzmine identified a total of 1333 lipids, with 362 lipids positively identified by MS/MS confirmation and an

additional 971 lipids putatively identified through mass-match analysis (m/z error ≤ 5 ppm, using MZmine). The relative abundance of lipid classes was determined across stages 2 to 5 in the WT and in strain E at stage 3' (last developmental stage, perithecium in the mutant strain E).

Table 5 shows the relative abundance of lipid classes. In stage 2, the most abundant lipids within their respective classes were Monoglycerides (MG), Phosphatidylserines (PS), Glycosylmonoacylglycerols-MG (SQMG), oxidized Lyso-Phosphatidylinositol (LPIO), Phosphatidylglycerol-O (PGO), Phosphatidylserine-O (PSO), Phosphatidylinositol (PI), and Phosphatidylethanolamine-O (PEO). Stage 3 exhibited a higher abundance of Glycosylmonoacylglycerols-Diglycerides (SQDG), Lyso-Phosphatidylethanolamine-O (LPEO), Lyso-Phosphatidylserine-O (LPSO), and Phosphatidylcholines (PC). Finally, at stage 4, Triacylglycerols (TG), Diacylglyceryl-N,N,N-trimethylhomoserine (DGTS), Lyso-Diacylglyceryl-N,N,N-trimethylhomoserine (lyso-DGTS), Phosphatidic Acids (PAO), Lyso-Phosphatidic Acids (LPAO), Phosphatidylglycerols (PG), Phosphatidic Acids (PA), Phosphatidylserines (PS) showed increased relative abundance compared to other lipid classes.

The *per5* strain had a distinct lipidomic profile compared to the wild type whereby it showed higher relative abundance in: Phosphatidylserines (DG), Triacylglycerols-O (TGO), Phosphatidylinositol-O (PIO), Phosphatidylcholine-O (PCO), Monoglycerides (MGO), and Monoglycerides of Monoglycerides (MGMG).

Table 5. Relative abundance within each class of lipids (mass tolerance of 10 ppm) across the life cycle of *S. macrospora* wild type (Stages 2 to 5) and *per5* strain (Stage 3'). In this representation, red indicates a higher abundance, while blue signifies a lower abundance within the lipid class.

Main class	lipid class	Stage				
		Wt-2	Wt-3	Wt-4	Wt-5	per5-3'
GP	LPGO	0.99	0.97	0.80	1.00	0.66
GL	DGDG	0.64	0.72	0.76	1.00	0.49
GP	CL	0.85	0.90	0.95	1.00	0.71
GL	LDGTS	0.68	0.81	1.00	0.60	0.56
GL	DGTS	0.50	0.73	1.00	0.67	0.66
GL	TG	0.87	0.93	1.00	0.70	0.88
GP	PAO	0.58	0.34	1.00	0.26	0.26
GP	LPAO	0.72	0.44	1.00	0.41	0.45
GP	PG	0.06	0.54	1.00	0.58	0.05
GP	PA		0.32	1.00	0.38	
GP	PE	0.88	1.00	0.97	0.86	0.77
GP	LPSO	0.81	1.00	0.85	0.83	0.57
GP	LPEO	0.95	1.00	0.92	0.97	0.94
GL	SQDG	0.80	1.00	0.96	0.94	0.85
GP	PC	0.23	1.00			0.43
GL	MG	1.00	0.97	0.87	0.95	0.88
GP	PS	1.00	0.98	0.24	0.93	0.78
GL	SQMG	1.00	0.96	0.78	0.83	0.86
GP	LPIO	1.00	0.97	0.89	0.80	0.59
GP	PGO	1.00	0.58	0.19	0.52	0.83
GP	PSO	1.00	0.45	0.44	0.33	0.29
GP	PI	1.00	0.52	0.16	0.48	0.64
GP	PEO	1.00	0.42	0.45	0.43	0.31
GL	DG	0.46	0.52	0.66	0.40	1.00
GL	TGO	0.93	0.94	0.96	0.70	1.00
GP	PIO	0.86	0.72	0.75	0.55	1.00
GP	PCO	0.95	0.98	0.77	0.85	1.00
GL	MGO	0.36	0.21	0.28	0.36	1.00
GL	MGDG	0.75	0.95	0.97	0.93	1.00

GL: glycerolipids

GP: Glycerophospholipids

SQ:Glycosylmonoacylglycerols

L: one FA chain

O : alkyl ether substitute

DG:Glycosyldiacylglycerols

MG: Glycosylmonoacylglycerols

O: alkyl ether substitute

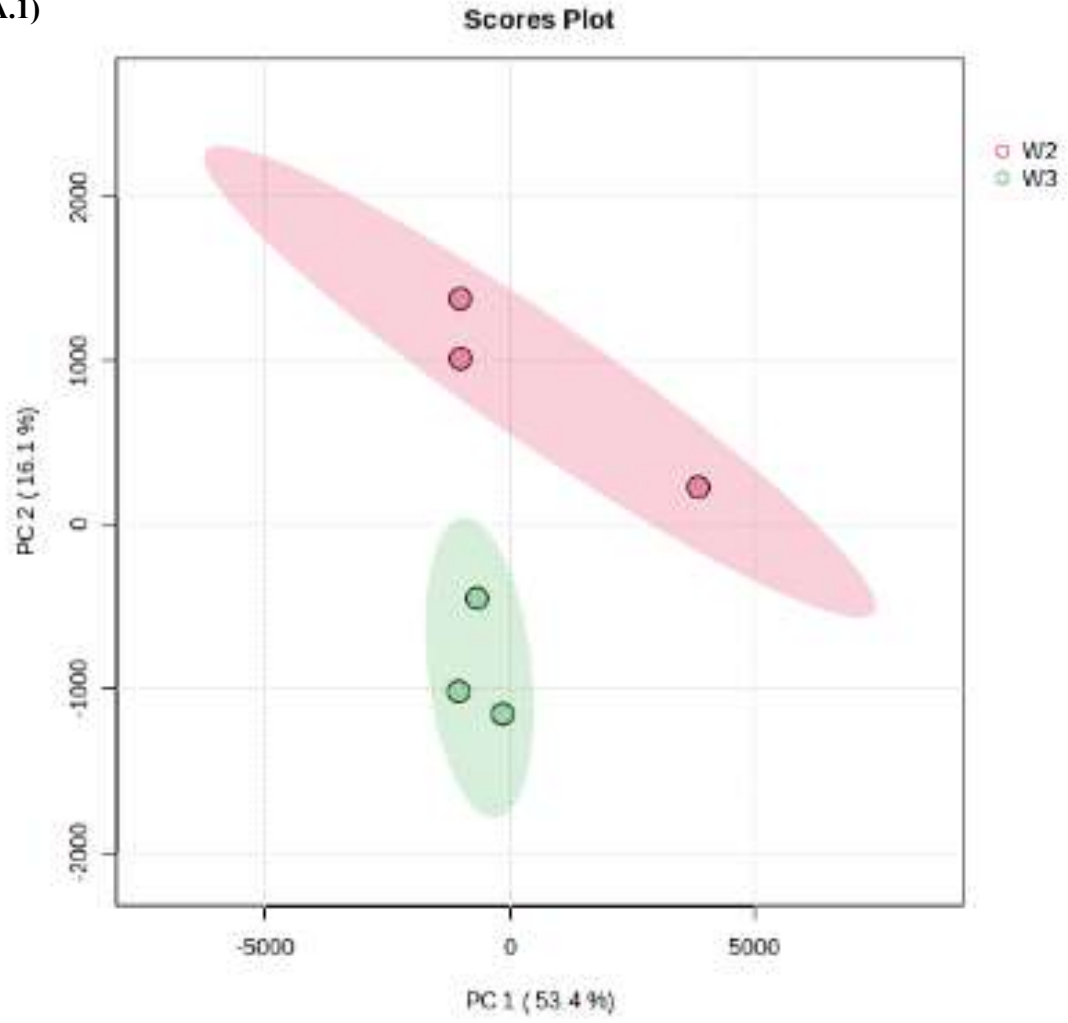
Statistical methods, including t-tests and analysis of variance (ANOVA), showed that the changes in lipid concentrations during the developmental stages of *S. macrospora* were significant during the different developmental stages of the fungus. Nonparametric tests with unequal variances and p-values adjusted for false discovery rate were employed, considering changes with $P < 0.1$ as significant. Comparisons were made between consecutive stages of the wild type and between the *per5* mutant and wild type stage 3.

The PCA score plot clearly demonstrated group separation based on lipid profiles, particularly the W2/W3 and W3/E3 groups (Figure 12). The PCAs for W3/W4 and W4/W5 overlapped due to the complexity of the data and the advanced stage of sexual reproduction in the fungus (Supplementary data Figure S22 and Figure S23).

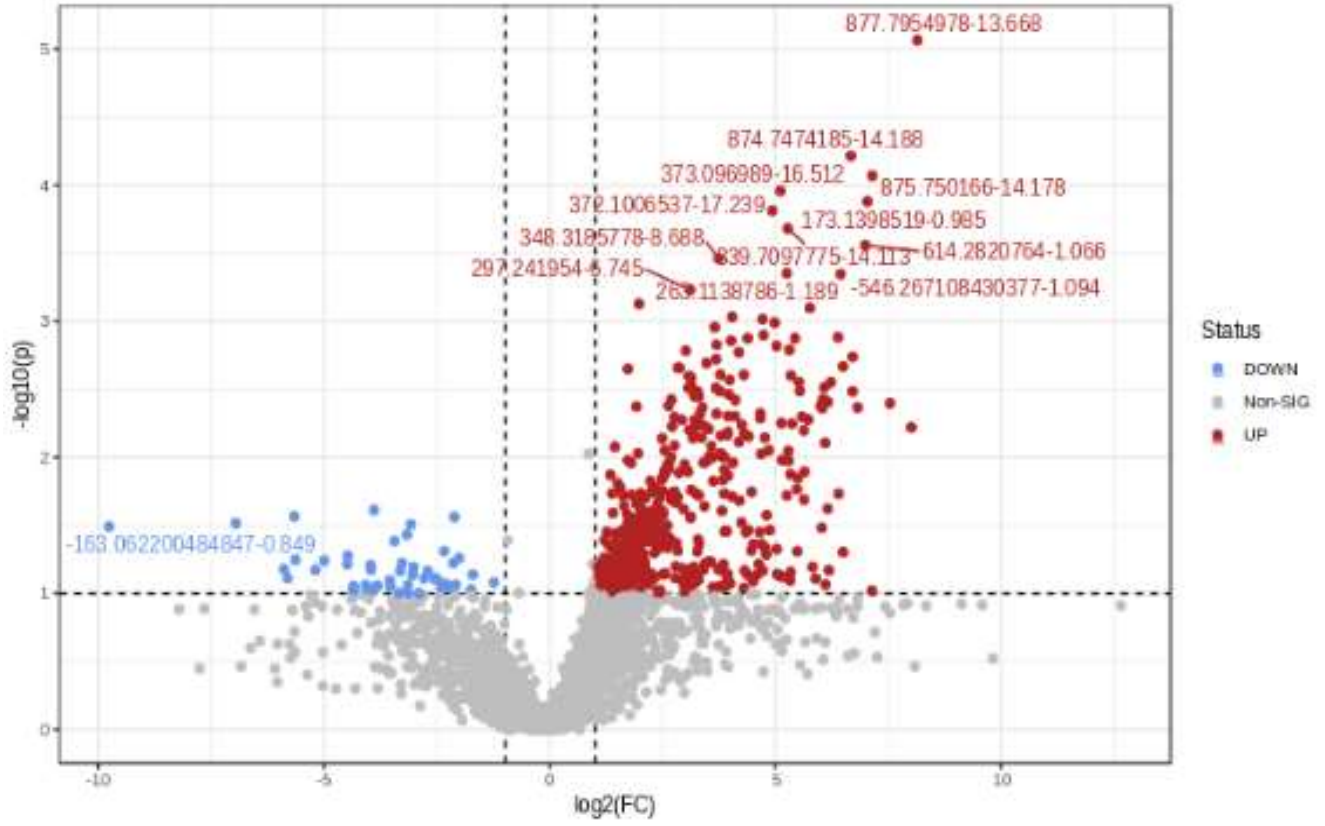
Clustering analysis showed good grouping within sample groups for metabolites with similar abundance, especially notable in the W3/E3 comparison due to the *per5* mutant's inability to produce cytosolic lipids. The volcano plot analysis, considering fold change (FC) of ± 2 and $P < 0.1$, highlighted significant alterations in lipid composition between the *S. macrospora* wild type and *per5* mutant (Figure 12).

Overall, a large number of metabolites, around 600, exhibited up- and down-regulation across the *S. macrospora* life cycle, except for the W2/W3 stage comparison, which predominantly showed upregulation in lipid intensities. These findings align with the relative abundance analysis of the major lipids (Table 5).

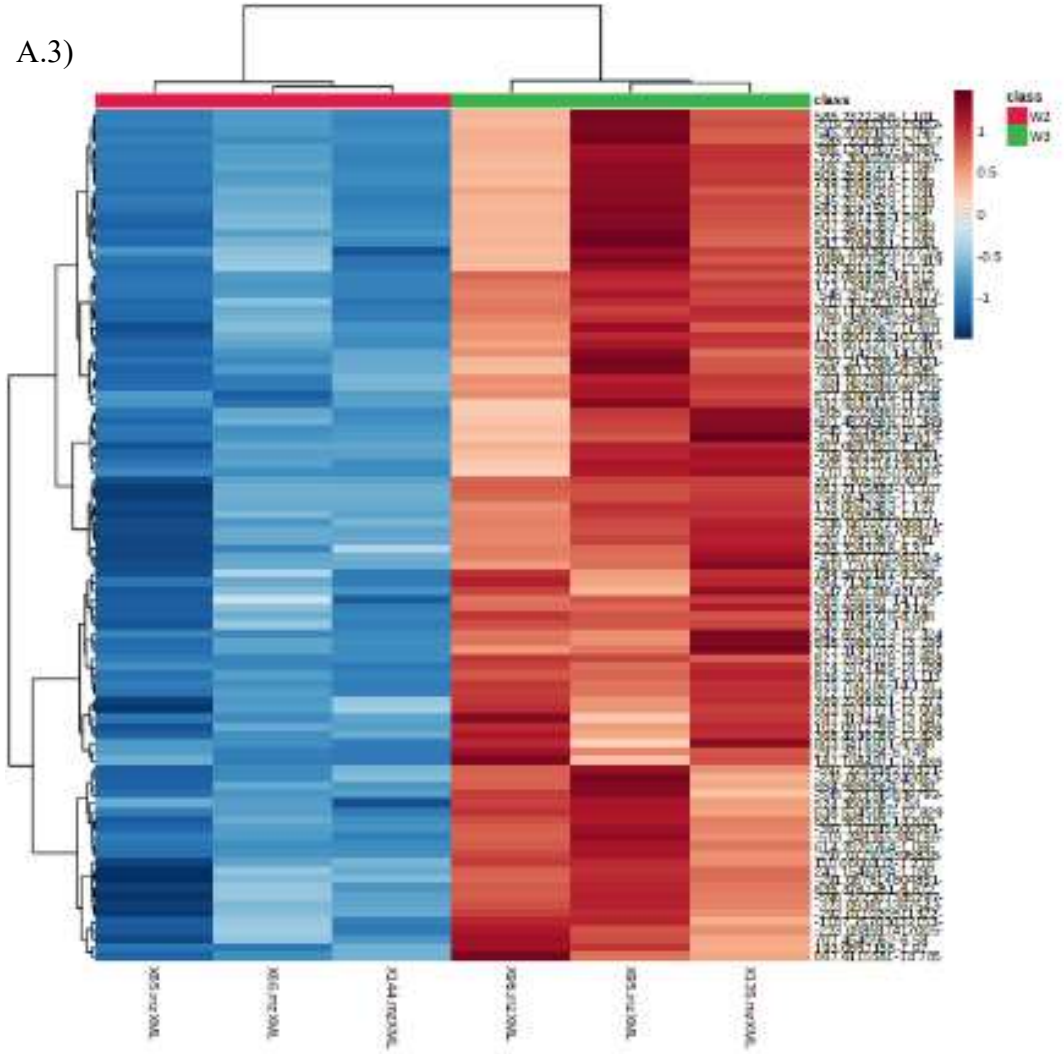
A.1)



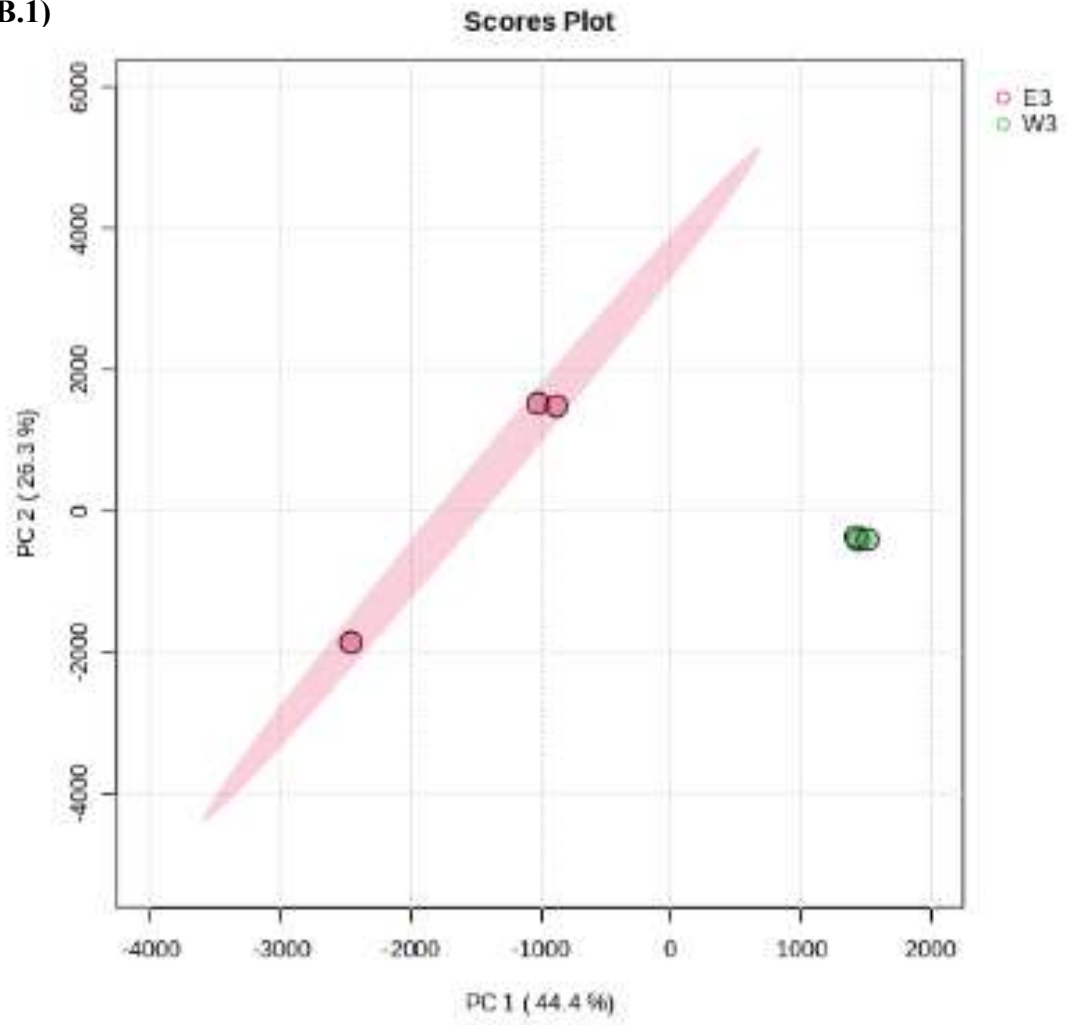
A.2)



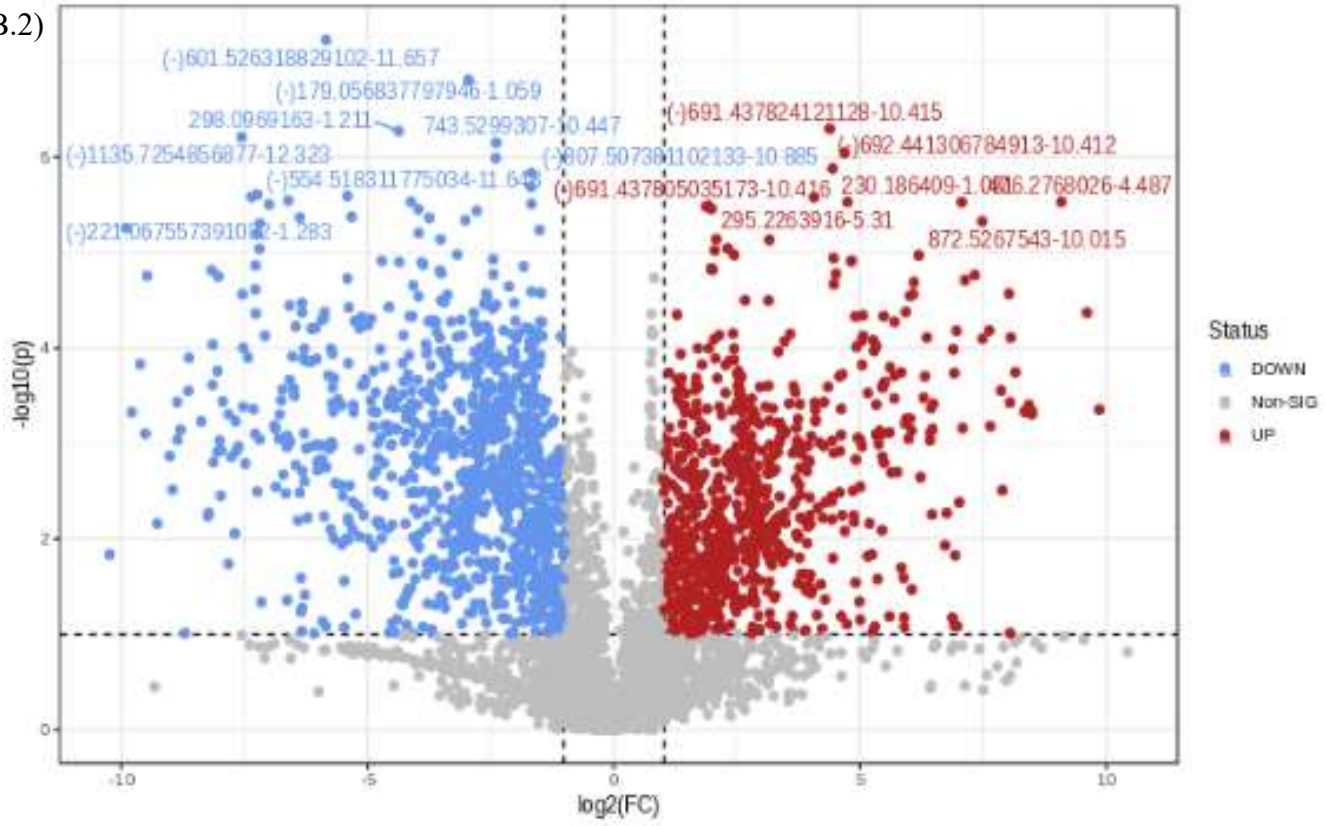
A.3)



B.1)



B.2)



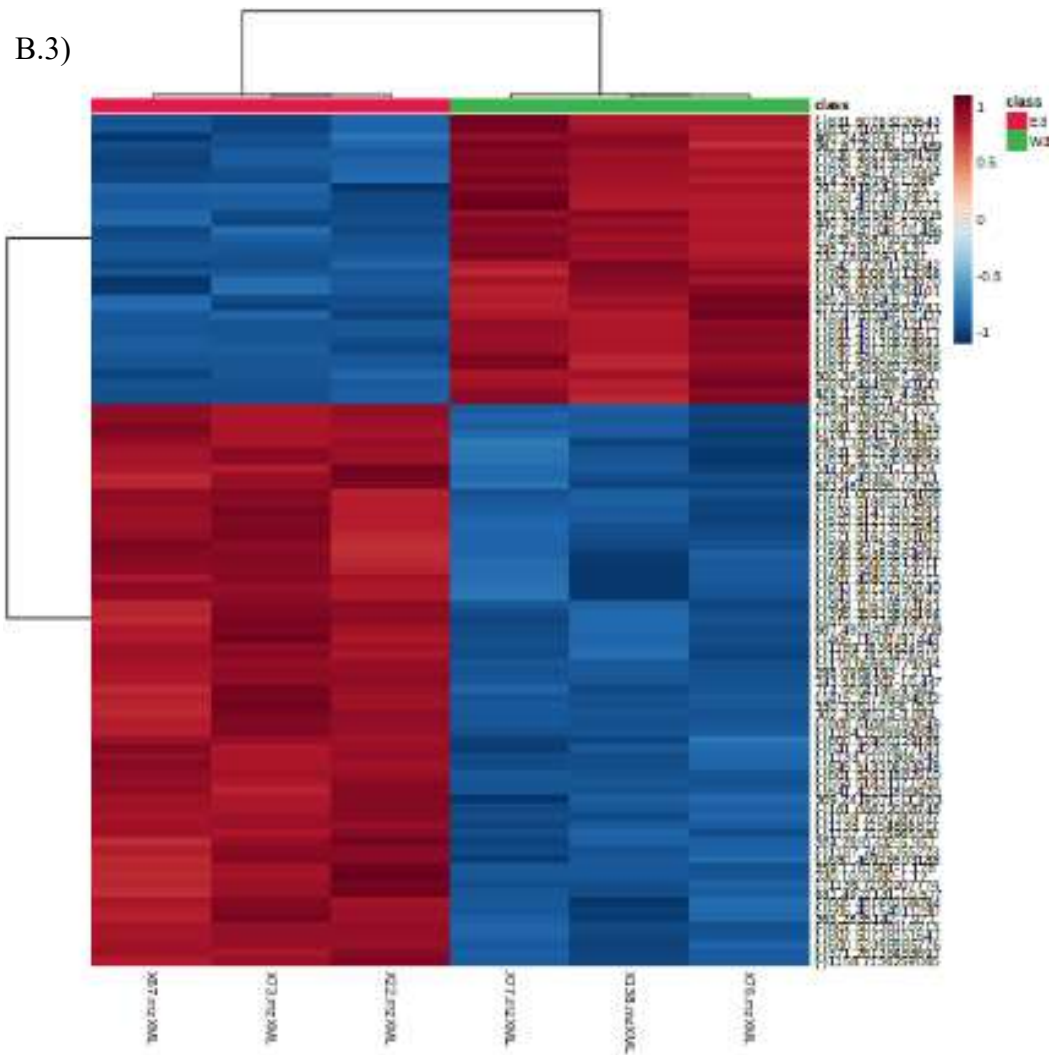


Figure 12. Analysis for lipidomic of *S. macrospora*, comparison in A) stage 2 and stage 3 wildtype and B) stage 3 for wild type and the strain per5. 1) PCA score plot, 2) Volcano plot ($p < 0.1$ and $FC > 2$ or < -2), and 3) Heatmap (t-Test) for the top 150 top feature.

Functional analysis was performed to investigate the biological pathways and processes associated with the lipidomics data of *S. macrospora*. Pathway enrichment analysis was conducted for the main lipid chemical classes, focusing on pathways with a $P \leq 0.05$ in at least one of the comparisons. A total of 15 pathways exhibited significant changes across the *S. macrospora* WT and *per5* mutant (Table 6).

Notably, the flavonoid and phenylpropanoid pathways were significantly changing during the early stage of sexual development (W2/W3). Glycerophosphocholines and cinnamic acids showed the most pronounced alterations between W3/W4, but also in the *per5* mutant.

Furthermore, cinnamic acids, glycerophosphoethanolamines, glycerophosphoinositol, glycerophosphoerines, phosphosphingolipids, and secosterol pathways displayed significant changes during the WT fruiting body development. These pathways were also found to be enriched in the *per5* mutant and WT (W3/E3), suggesting their potential involvement in the ascopogenesis (stage 3) in *S. macrospora*.

Table 6. Pathways that were significantly changing (Enrichment $p < 0.05$) across the life cycle of *S. macrospora*. The comparison was done with the next stage (W2, W3, W4, and W5, representing wild-type strain in the different stages, E3 represents the strain per 5 after 6 days post-inoculation). Data analyzed with MetaboAnalysis

Pathway	p value				Matched compound (Mass diff < 0.002)
	W2/W3	W3/W4	W4/W5	W3/E3	
Bile acids	0.00482	N/A	0.26848	0.04437	3alpha,7alpha,12alpha,24-Tetrahydroxy-24-methyl-5beta-cholestan-26-oic acid ; 12-Ketodeoxycholic acid
Ceramides	0.01895	0.00140	0.21685	0.63127	Cer(d14:0/26:0) ; Cer(d14:0/22:1) ; CerP(d14:1/30:0)* ; Cer(d14:1/21:0) ; Cer(d14:2/13:0) ; Cer(d14:2/26:2) ; Cer(d15:0/22:4) ; Cer(d15:2/22:1(OH)) ; Cer(d18:1/20:2(OH)) ; Cer(d20:1/22:6)* ; CerP(d14:0/10:0) ; CerP(d14:2/30:0) ; CerP(d15:0/24:4)* ; CerP(d18:0/26:0(OH))* ; CerP(d19:2/26:2) ; CerP(d20:2/26:2)* ; Cer(t14:0/22:0(OH)) ; Cer(t14:0/22:1(OH)) ; Cer(t14:0/23:0(OH)) ; Cer(t15:0/22:1(OH)) ; Cer(t20:0/22:6)
Cinnamic acids	0.02089	0.02079	NA	0.06148	(E)-3-(4-Hydroxyphenyl)-2-propenal ; 3-(2-hydroxyphenyl)prop-2-enoic acid ; (E)-3-(4-Hydroxyphenyl)-2-propenal ; Methyl cinnamate ; 4-Methoxycinnamic acid ; 3,4,5-Trimethoxycinnamic acid ; cis-Sinapic acid
Fatty acids	0.69904	0.04801	0.71324	0.78348	11-Octadecyenoic acid ; 3-Methyl-octadecanoic acid ; 5-Amino-2-oxopentanoic acid ; 2-Aminoisobutyric acid ; (S)-5-Amino-3-oxohexanoate ; 18-Oxonadecanoic acid ; 3-Amino-octanoic acid ; 4-Methoxycinnamic acid ; Hexacosapentaenoic acid ; Hydroxyheneicosadienoic acid ; Hydroxyheneicosatrienoic acid ; Hydroxyheptacosenoic acid ; Hydroxynonacosatetraenoic acid ; (22E,24E)-1alpha,25-Dihydroxy-22,23,24,24a-tetrahydro-24a-homovitamin D3 ; Isoglutamic acid ; Gamma-Tocotrienol ; Octacosaoctanoic acid ; Catechin ; Dicumarol ; 10-Hydroxy-8E-Decene-2,4,6-triynoic acid ; Afroomsin ; 7-O-Methyluteone ; Betagarin ; Daphnoretin ; Karanjin ; Kievitone ; 2-Phenylpropionate ; Fraxetin ; Phaseollidin ; Sophoracoumestan A
Flavonoids	0.00000	0.08896	0.49984	0.10309	PA(10:0 22:0)* ; LysoPA(18:1(9Z):0:0) ; LysoPA(16:0:0:0) ; DG(40:11) ; PA(14:1 29:0)* ; PA(14:1 31:0)* ; PA(17:2 24:4) ; PA(18:3 27:0)* ; PA(O-22:0/24:4) ; PA(10:0 26:2)* ; PA(13:0 20:3)* ; PA(14:0 22:6)* ; PA(11:0 22:4)* ; PA(11:0 24:4)* ; PA(13:0 22:5)* ; PA(18:4 20:5)* ; PA(20:3 24:4) ; PA(15:0 20:3)* ; DG(38:11) ; PA(14:0 22:5)* ; PA(22:5 24:4)
Glycerophosphates	0.99777	0.09192	0.00856	0.80805	CerP(d14:2/12:0(OH)) ; PC(10:0 18:2) ; PC(11:0 22:2) ; PC(11:0 24:4) ; PC(13:0 22:5) ; LPC(15:1) ; CerP(d14:0/10:0) ; PC(10:0 16:0) ; PC(10:0 17:0) ; PC(10:0 18:3) ; PC(11:0 22:1) ; PC(P-32:9)/PC(O-32:10) ; PC(10:0 18:0) ; PC(10:0 22:4)* ; PC(15:0 20:3)* ; PC(22:5 22:6) ; PC(14:0 20:3)* ; PC(O-16:2/22:5)* ; PC(P-18:0/22:6)/PC(O-18:1/22:6)* ; LPC(14:1(9Z)) ; PC(O-16:0/22:6)* ; LPC(14:2) ; LPC(15:1)* ; PC(11:0 22:6)* ; PC(O-20:0/22:6)* ; PC(P-37:6)/PC(O-37:7)* ; PC(P-39:6)/PC(O-39:7)* ; PC(P-40:11)/PC(O-40:12)* ; PC(P-41:5)/PC(O-41:6)* ; PC(P-42:11)/PC(O-42:12)* ; PE(O-14:0/22:6)* ; LPC(15:1) ; PC(10:0 16:0) ; PC(10:0 17:0) ; PC(11:0 22:1) ; PC(11:0 22:2) ; PC(10:0 18:2) ; PC(10:0 18:3) ; PC(11:0 24:4) ; PC(13:0 22:5) ; PC(11:0 22:6)* ; PE(P-16:0/22:6)/PE(O-16:1/22:6)* ; PC(P-37:6)/PC(O-37:7)* ; LPC(15:1)* ; CerP(d14:1/15:0(OH)) ; LPC(14:1(9Z)) ; LPC(14:2) ; LPS(P-16:0)/LPS(O-16:1) ; PC(P-41:5)/PC(O-41:6)* ; PC(P-39:6)/PC(O-39:7)* ; PC(O-16:0/22:6)*
Glycerophosphocholines	0.34115	0.19581	0.01490	0.00179	PC(15:0 20:3)* ; PC(22:5 22:6) ; PC(14:0 20:3)* ; PC(O-16:2/22:5)* ; PC(P-18:0/22:6)/PC(O-18:1/22:6)* ; LPC(14:1(9Z)) ; PC(O-16:0/22:6)* ; LPC(14:2) ; LPC(15:1)* ; PC(11:0 22:6)* ; PC(O-20:0/22:6)* ; PC(P-37:6)/PC(O-37:7)* ; PC(P-39:6)/PC(O-39:7)* ; PC(P-40:11)/PC(O-40:12)* ; PC(P-41:5)/PC(O-41:6)* ; PC(P-42:11)/PC(O-42:12)* ; PE(O-14:0/22:6)* ; LPC(15:1) ; PC(10:0 16:0) ; PC(10:0 17:0) ; PC(11:0 22:1) ; PC(11:0 22:2) ; PC(10:0 18:2) ; PC(10:0 18:3) ; PC(11:0 24:4) ; PC(13:0 22:5) ; PC(11:0 22:6)* ; PE(P-16:0/22:6)/PE(O-16:1/22:6)* ; PC(P-37:6)/PC(O-37:7)* ; LPC(15:1)* ; CerP(d14:1/15:0(OH)) ; LPC(14:1(9Z)) ; LPC(14:2) ; LPS(P-16:0)/LPS(O-16:1) ; PC(P-41:5)/PC(O-41:6)* ; PC(P-39:6)/PC(O-39:7)* ; PC(O-16:0/22:6)*
Glycerophosphoethanolamines	0.04230	0.55833	0.05446	0.05324	PE(O-14:0/22:6)* ; LPC(15:1) ; PC(10:0 16:0) ; PC(10:0 17:0) ; PC(11:0 22:1) ; PC(11:0 22:2) ; PC(10:0 18:2) ; PC(10:0 18:3) ; PC(11:0 24:4) ; PC(13:0 22:5) ; PC(11:0 22:6)* ; PE(P-16:0/22:6)/PE(O-16:1/22:6)* ; PC(P-37:6)/PC(O-37:7)* ; LPC(15:1)* ; CerP(d14:1/15:0(OH)) ; LPC(14:1(9Z)) ; LPC(14:2) ; LPS(P-16:0)/LPS(O-16:1) ; PC(P-41:5)/PC(O-41:6)* ; PC(P-39:6)/PC(O-39:7)* ; PC(O-16:0/22:6)*
Glycerophosphoglycerols	N/A	N/A	0.01721	0.61617	LPGP(36:0) ; PG(13:0 26:1)* ; PG(14:1 22:6) ; PG(O-14:0/18:4)* ; PG(O-16:0/17:2)* ; PG(P-14:0/14:1)/PG(O-14:1/14:1)* ; PG(P-14:0/16:1)/PG(O-14:1/16:1)* ; PG(P-14:0/18:4)/PG(O-14:1/18:4)* ; PG(P-16:1/14:1)/PG(O-16:2/14:1)*
Glycerophosphoinositols	0.64244	0.91950	0.25536	0.06731	PI(10:0 22:2) ; PI(10:0 22:0)* ; LPIP(26:1) ; LPIP(26:2) ; PI(11:0 22:2) ; PS(10:0 22:0) ; PS(10:0 26:0) ; PS(11:0 22:2) ; PS(16:1 22:2)* ; PS(O-14:0/16:1) ; PS(P-14:0/16:1)/PS(O-14:1/16:1) ; PS(P-20:0 17:2) ; PS(P-20:1/17:2)/PS(O-20:2/17:2) ; PS(13:0 22:2)* ; PS(18:2 22:6)* ; PS(13:0 24:4)* ; PS(16:1 24:4)* ; LPS(21:0)* ; LPS(O-16:0) ; LPS(P-16:0)/LPS(O-16:1) ; PS(15:1 22:2)* ; PS(15:1 24:4)* ; PS(17:0 26:2)* ; PS(17:1 22:2)* ; PS(O-14:0/20:3)* ; PS(P-16:0/17:2)/PS(O-16:1/17:2)* ; PS(P-20:1/17:2)/PS(O-20:2/17:2)*
Glycerophosphoserines	0.82529	0.99995	0.04231	0.02987	PS(13:0 22:2)* ; PS(18:2 22:6)* ; PS(13:0 24:4)* ; PS(16:1 24:4)* ; LPS(21:0)* ; LPS(O-16:0) ; LPS(P-16:0)/LPS(O-16:1) ; PS(15:1 22:2)* ; PS(15:1 24:4)* ; PS(17:0 26:2)* ; PS(17:1 22:2)* ; PS(O-14:0/20:3)* ; PS(P-16:0/17:2)/PS(O-16:1/17:2)* ; PS(P-20:1/17:2)/PS(O-20:2/17:2)*
Phenylpropanoids	0.00452	0.06166	0.65784	0.20628	Metyrosine ; 2-Phenylpropionate ; 10-Hydroxy-2E,8E-decadiene-4,6-diynoic acid ; Hydroferulic acid
Phosphosphingolipids	0.02528	0.97583	0.95857	0.09416	PE-Cer(d14:0/15:0) ; PE-Cer(d14:1/23:0(OH)) ; PE-Cer(d14:2/23:0) ; PE-Cer(d17:1/24:4)* ; PE-Cer(d22:1/22:6)* ; PI-Cer(d14:0/25:0)* ; PI-Cer(d14:1/21:0)* ; PI-Cer(d14:1/22:2)* ; PI-Cer(d14:1/23:0)* ; PI-Cer(d14:1/24:4)* ; PI-Cer(d14:2/24:4)* ; PI-Cer(d15:2/24:4)* ; PI-Cer(d17:1/22:6)* ; PI-Cer(d18:1/24:4)* ; PI-Cer(d18:2/22:6)* ; PI-Cer(d19:2/22:6)*
Secosterols	N/A	0.02626	0.47380	N/A	1-a,24R,25-Trihydroxyvitamin D2 ; 1alpha,25-Dihydroxy-2beta-(4-hydroxybutoxy)vitamin D3 ; 1alpha,25-Dihydroxy-3-deoxy-3-thiavitamin D3 ; (22E,24E)-1alpha,25-Dihydroxy-22,23,24,24a-tetrahydro-24a-homovitamin D3 ; 1-a,24R,25-Trihydroxyvitamin D2 ; 1alpha,25-Dihydroxy-2beta-(4-hydroxybutoxy)vitamin D3 ; 1alpha,25-Dihydroxy-3-deoxy-3-thiavitamin D3 ; (22E,24E)-1alpha,25-Dihydroxy-22,23,24,24a-tetrahydro-24a-homovitamin D3
Sterols	0.01596	0.19700	0.34691	0.67719	3alpha,7alpha,12alpha,24-Tetrahydroxy-24-methyl-5beta-cholestan-26-oic acid ; Dolicholide

* 0.005 < Mass diff > 0.002

2.4 DISCUSSION

2.4.1 An overview of the metabolome of *S. macrospora*

The understanding of the metabolite chemistry of fungal growth and development and associated signaling controls is currently quite limited. To address this knowledge gap, I conducted a metabolomic analysis of *S. macrospora* across different developmental stages using LC-MS. I employed targeted, semi-targeted, and untargeted approaches to investigate phytohormones, energetic metabolites (EnM), and lipids, respectively. Each approach provided valuable insights into fungal metabolism during fruiting body development.

The targeted approach focused on phytohormones, as they have the potential to regulate fungal cell processes. Despite being typically associated with plant interactions, phytohormones have been found to be produced by various fungal species, independent of their interaction with living plants. Earlier research has demonstrated potential for some phytohormones including CKs and IAA, to control mycelial growth and spore germination (Barker & Tagu, 2000; Lee, 1961; Nakamura et al., 1978; Tomita et al., 1984). Thus, I screened 30 phytohormones and identified cZ, iP, cZR, iPR, and IAA at different concentrations throughout the life cycle of a *S. macrospora* WT and 6 related mutant strains. The CKs results showed a clear switch between CKs ribosides and CKs free bases. While iPR and cZR levels decreased, cZ and iP, increased during the stage 3 of *S. macrospora* WT life cycle, known as ascosporegenesis. This pattern was also observed in the *S. macrospora* mutant strain smgp11, which produced more fruiting bodies and CK free bases (iP and cZ) compared to the wild type. On the other hand, IAA increased in the 2nd

stage of *S. macrospora* WT and mutants, the transition to sexual development. Interestingly the enzyme *acl* (for fatty acid biosynthesis) was found to increase the enzyme activity in this same stage (Nowrousian et al., 1999a). The deletion in this gene (which refers to the mutant strain *per5*) resulted in a substantial increase, up to 100-fold, of IAA production compared to the WT. Thus, the timing and different patterns seen between the mutant and WT of *S. macrospora* suggests the involvement of CKs and auxins in fungal growth and development.

In the case of EnM and lipids, the goal of the thesis was to understand the immediate energy requirements, metabolite biosynthesis and cell communications in the fungus life cycle. Therefore, a semi-targeted approach was used and 60 metabolites of the 160 semi-targeted EnM were successfully confirmed with a high confidence of level 2 (Reisdorph et al., 2020), through MS/MS analysis in *S. macrospora* WT.

In terms of the lipidome, the untargeted analysis of lipids, in *S. macrospora* WT at stages 2, 3, and 5 and the mutant strain *per5* at stage 3, resulted in 7380 detected features, where 1333 lipids were identified using MS, and 365 were confirmed through MS/MS. Furthermore, metabolic pathway enrichment of different main lipid classes was performed with a mass difference of 0.002 for lipid identification.

By integrating the results from these different approaches, we can gain insight into the biology of phytohormones and metabolites across the life cycle of *S. macrospora*. Furthermore, we can explore sterols and secosterols as potential myco-hormones for fungal development. However, the challenges of untargeted metabolomics in identifying potential myco-hormones necessitate further investigation, and the candidates identified thus far are represented within metabolite classes for future research.

In this study, the mutant strain *per5*, which lacks the *acl* gene responsible for lipid production via the cytosol, exhibited significantly higher levels of IAA compared to the WT. This suggests a correlation between lipid metabolism and IAA production. Furthermore, semi-targeted and untargeted approaches revealed an upregulation of metabolites associated with the TCA cycle, organic acids, amino acids, and an enrichment of lipids, such as fatty acids, during the transition to sexual development in *S. macrospora*, particularly in stage 2. This suggests that IAA may act as an energetic or lipid regulator during the transition to sexual development, a stage known for its high energy demands.

Additionally, a notable switch from CK ribosides to CK free bases was observed during stage 3 (ascospore development) in *S. macrospora*. The mutant strain *smgpi1*, which produces more mature fruiting bodies than the WT, also exhibited higher levels of CKs free bases. Conversely, the mutant strains unable to produce spores did not show this CK switch. Finally, the increase in mevalonate, and the enrichment of the pathways in sterols and secosterols in the 3rd stage suggests a potential relationship with CKs, particularly during the third stage of ascospore development.

Overall, the different approaches to metabolomic analysis provided valuable insights into the roles of phytohormones and other metabolites in fungal growth and development, illuminating the intricate processes underlying fungal physiology. These findings contribute to our broader understanding of fungal biology and open possibilities for the identification of novel myco-hormones involved in fungal growth regulation.

2.4.1 Production of cytokinins by *S. macrospora*

Cytokinins (CKs) are well-known phytohormones that have been reported to be produced by fungi (Table 1). However, their specific roles in fungal growth and development remain unknown, as most of the research on fungal endogenous CKs has focused on their interactions with plants. Studies on CKs and fungi have primarily been conducted in the context of pathogenic or beneficial fungi, where CKs have been shown to play a crucial role in successful fungal colonization or interactions with host plants (Chanclud et al., 2016; Chanclud & Morel, 2016; Hinsch et al., 2015; Morrison et al., 2017; Trdá et al., 2017).

To our knowledge, this study represents the first investigation of phytohormones at different developmental stages of fungi, using a model genetic fungus, *S. macrospora*. In addition to a wildtype, phytohormones were analyzed in six *S. macrospora* mutant strains characterized by blocked development at specific stages (asc, pro, per, and pile).

Results of this thesis show that *S. macrospora* biosynthesizes cytokinin through a tRNA degradation pathway. *S. macrospora* wild type and mutant strains produced different concentration of cZ and iP type during the fungus life cycle. Earlier studies have shown that other fungi produce mainly cZ and iP type regardless of the nutrition mode, suggesting the predominance or unique presence of a tRNA pathway proposed by Morrison et al. (2015). Furthermore, fungi have a CK-degradation enzyme, cytokinin oxidase/dehydrogenase (CKX) (Trdá et al., 2017). These findings raise the question of whether CKs act as regulators of fungal physiology or metabolism.

A consistent finding of this study was that during the vegetative (asexual) reproduction of *S. macrospora*, CK ribosides were found to be predominant until stage 3.

Interestingly, the asc mutants, which cannot progress past the vegetative stage (stage 1), did not exhibit any such changes in CK riboside concentrations. This observation is in line with a study on the arbuscular mycorrhizal fungus *Rhizophagus irregularis*, where iPR, IAA, and ethylene were detected in the spore exudates during the early stages of fungal growth (Pons et al., 2020). The production of these hormones at such early stages suggests that CK ribosides (iPR and cZR) may be involved in early stages of fungal development.

Along with a switch away from CK ribosides, there was an accumulation of free base CKs which suggests they have a role in the sexual development of fungi. This was the case for the WT and a mutant *smgpi1* which produced unusually high amounts of fruiting structures. Thus, in the case of *S. macrospora* WT and *Smgpi1*, a switch from CK riboside to free base production was observed during the third stage of sexual reproduction, corresponding to the formation of ascospores in the mature perithecium (Figure 2). Interestingly, *Smgpi1*, that produces more mature fruiting bodies than the WT, also showed greater production of CKs free bases compared to the WT.

Previous studies on CKs in fungi primarily focused on their interactions with host plants, such as the fungal plant pathogen *Magnaporthe oryzae*, where deletion of the CK production gene (*cks1*) abolished CK production but did not show significant changes *in vitro* fungal growth compared to the wild type (Chanclud et al., 2016). However, it is important to note that *Magnaporthe oryzae* is a heterothallic fungus, requiring a mating partner to initiate sexual reproduction (J. Wang et al., 2021). Therefore, the *in vitro* growth tested by Chanclud et al. (2016) mainly represents vegetative growth, which might explain the lack of significant changes in fungal growth observed in the impaired CK mutant strain.

A study conducted by Lee (1961) demonstrated restored fertility in crosses of mutant strains of the heterothallic fungus *N. crassa*.

Furthermore, the inability to colonize may be attributed to disruptions in other metabolic pathways that may not be phenotypically apparent during asexual growth. For example, recent research by Gautam et al. (2022) demonstrated that CKs regulate energy utilization in the fungus *Botrytis cinerea*, whereby exogenous CK application significantly enriched glycolysis, sucrose metabolism, and oxidative phosphorylation pathways.

2.4.2 Cytokinin and metabolites

Nucleosides, nucleotides, and nucleobases (NNNs) have been investigated in fungi for their bioactive roles in diverse human physiological processes (Phan et al., 2018). However, the exact role of NNNs in fungal growth and developments remains unclear. Purine metabolism, which encompasses the breakdown and synthesis of purines, has been implicated in cytokinin metabolism and transport (Schoor et al., 2011; X. Zhang et al., 2013). For example, adenosine kinase, primarily known for its role in phosphorylating adenosine to adenosine monophosphate, has also been implicated in the interconversion of cytokinin ribosides to their nucleotide forms (Schoor et al., 2011). For a better understating of CKs and NNNs, I screened the levels of different NNNs at different developmental stages of *S. macrospora*.

The NNNs detected in *S. macrospora*, (including uridine, thymidine, inosine, guanosine, and cordycepin, Cyclic AMP (cAMP), MTA (5'-methylthioadenosine)), exhibited distinct patterns throughout the life cycle (Figure 9). Generally, the levels of nucleosides increased during the second stage, indicating their potential involvement in

critical processes associated with fungal development. However, two nucleosides, thymidine, and cordycepin, showed different trends.

Thymidine and cordycepin did not exhibit an increase during the second stage, with their levels remaining relatively constant until the third stage. Interestingly, in the third stage, both nucleosides experienced a noticeable decrease, reaching their lowest levels. The observed trends in thymidine and cordycepin parallel the patterns seen with iPR and cZR, suggesting a potential relationship in the regulatory mechanisms in the fungus development. Further investigations are necessary to unravel the precise mechanisms and interactions between nucleosides, cytokinins, and other molecules during the third stage of *S. macrospora* life cycle.

On the other hand, mevalonate is a crucial precursor in the biosynthesis of isoprenoids, including sterols, which are essential for various cellular processes including cell growth and proliferation (Gong et al., 2019; Kasahara et al., 2004). In this study, a positive correlation between mevalonate levels and the free base CKs in the third stage, ascospore formation, of *S. macrospora* was observed. The enrichment of sterols and secosterols observed through untargeted lipid analysis further supports the potential interplay between free base cytokinins and the mevalonate pathway. It is plausible that the increase in free base cytokinins stimulates the expression or activity of enzymes involved in the mevalonate pathway, leading to elevated mevalonate levels. This, in turn, could promote the biosynthesis of sterols and other isoprenoid compounds that might be essential for ascospore formation in the sexual reproduction of *S. macrospora*. However, further studies are required to investigate the functional significance of this correlation and elucidate the underlying molecular mechanisms.

2.4.3 Auxins

Auxins, known for their roles in plant growth and development, are produced via tryptophan or indole-3-pyruvate pathways in different fungi, such as *Fusarium sp* (Tsavkelova et al., 2012) and *Ustilago* and *Leptosphaeria maculans* (Leontovyčová et al., 2020; REINEKE et al., 2008), respectively.

In the case of *S. macrospora*, both the wild type and mutant strains exhibited a similar pattern in indole-3-acetic acid (IAA), production across different life cycle stages (Figure 6). Notably, there was an increase in the IAA during the transition to sexual reproduction, stage 2, in various strains (Figure 6). Likewise, a study conducted on the fungus *N. crassa* demonstrated that exogenous treatment of IAA promotes spore germination and hyphae elongation (Nakamura et al., 1978; Tomita et al., 1984). Together these observations suggest that auxins are involved in early stages of fungal growth and development.

Lipids serve as energy storage molecules in organisms (Ahmed et al., 2023), the ACL enzyme is responsible for the conversion of citrate to Acetyl-CoA in the cytosol, a precursor for the biosynthesis of fatty acids and sterols (Rangasamy & Ratledge, 2000; Verschueren et al., 2019) vy. Transcriptome analysis in *S. macrospora* revealed that *acl* expression was more active during stage 2, which corresponds to the transition to sexual development (Nowrousian et al., 1999b). The current study also supports the hypothesis that auxins are involved in *S. macrospora* during its transition to sexual development. Accordingly, the mutant strain per5 (E), for which *acl* gene was deleted, exhibited a higher auxin production compared to the wild type (Figure 6). Given that the transition to sexual

development might require substantial energy (Chinnici et al., 2014; Hamann et al., 2022; Voigt & Pöggeler, 2013), it is reasonable to hypothesize that auxins are involved in the energy supply mechanism in *S. macrospora*.

2.4.4 Auxins and lipids

Auxins are known to regulate lipids in algae, and palmitic acid in safflower plants (Krzemińska et al., 2023; Mousavi Basir Seyed and Sayfzadeh, 2022; Sivaramakrishnan & Incharoensakdi, 2020). Similarly, lysophospholipids are indicators or second messengers for stress caused by high auxin concentrations (Holk & Scherer, 1998). Additionally, a direct correlation of auxin biosynthesis and β -oxidation of fatty acids facilitated by peroxisomal enzymes, has been described (Spiess & Zolman, 2013).

With these possible effects of IAA in mind, relationships with auxin and the lipidome were investigated. Some interesting patterns arose. In the *S. macrospora* wild type Phosphatidic acid (PA) was not detected at stage 2 and showed a higher concentration at stage 4 (Table 5). PA is known to serve as a lipid messenger in plants, modulating growth, development, and stress responses by binding to target proteins and regulating signaling pathways, including auxin signaling (Du et al., 2022; P. Wang et al., 2019). For instance, PA in *Arabidopsis thaliana* responds to phosphorous (P) deficiency by regulating auxin activity and root hair development (Lin et al., 2020). Interestingly, in this study, the accumulation of PA showed a negative correlation with auxin production. Moreover, the *per5* mutant, which exhibited significantly higher auxin abundance, did not produce detectable levels of PA. These findings suggest a potential relationship between PA and auxin signaling in *S. macrospora*.

In this study, fatty acids, were significantly enriched between the stages W3/W4 in the WT. And interestingly fatty acids have been implicated as second messengers in several auxin functions (Holk & Scherer, 1998; Roudier et al., 2010). This includes auxin biosynthesis through lipid metabolism such as β - oxidation (Spiess & Zolman, 2013). Furthermore, it was already known that exogenous application of auxin in algae could upregulate the biosynthesis of lipids, especially unsaturated fatty acids (Krzemińska et al., 2023; Sivaramakrishnan & Incharoensakdi, 2020). Thus, the enrichment of these fatty acids, especially in the W3/W4 developmental stage of *S. macrospora*, suggests their potential involvement in auxin-related processes.

In summary, the increase on auxin production in the transition to sexual development in both WT and mutant strains of *S. macrospora*, along with the overproduction of IAA in the mutant strain *per5*, and the enrichment of fatty acid pathways, provide evidence for the connection between auxins and lipids in the development process of *S. macrospora*.

2.4.5 Auxins and the energy metabolome

The TCA cycle, plays a crucial role in the production of energy and the generation of metabolites essential for cellular function (Tao et al., 2017), and might be associated with IAA production. Studies on *Escherichia coli* using microarray analysis demonstrated upregulation of genes involved in the tricarboxylic acid (TCA) cycle and glyoxylate pathways in response to IAA. Furthermore, malic acid, a key component in the production of pyruvate dehydrogenase, which aids in the conversion of pyruvate to acetyl-CoA, was

also upregulated. The increase in acetyl-CoA and decrease in the NADH/NAD⁺ ratio were observed in *E. coli* during the IAA response (Bianco et al., 2006).

S. macrospora, exhibits a diverse range of mechanisms to obtain energy, which can vary depending on its energy demands and environmental conditions. Our observed upregulation of IAA and organic acids within and outside the TCA cycle, (with the exception of pyruvate; Figure 7), during the second *S. macrospora* life cycle stage suggests a potential involvement of energy metabolism. This finding aligns with previous observations of higher organic acid production in early fruiting bodies of edible mushrooms (Nagy et al., 2022), and further emphasizes the significance of organic acids in fungal energy metabolism.

Interestingly, during the second stage of the WT, pyruvate levels showed a decrease and reached their lowest point by the third stage, before levels eventually recovered in the final stage (Figure 7). This temporal pattern of pyruvate levels, a precursor for Acetyl-CoA, supports the hypothesis that lipid breakdown may be occurring to provide the necessary energy for the transition to sexual development. Lipids, as energy-rich molecules, can be catabolized to generate acetyl-CoA, a key intermediate in the TCA cycle (Ahmed et al., 2023). This suggests that the breakdown of lipids supplies energy required for fruiting body formation.

Furthermore, in the bacteria *E. coli* the observed increase in the biosynthesis of amino acids, including leucine, isoleucine, valine, and proline, in response to exogenous treatment with IAA (Bianco et al., 2006). Similarly, the corresponding increase in these amino acids during the second stage of *S. macrospora* (Figure 5), suggests a potential regulatory role of IAA in amino acid metabolism. This correlation implies that IAA may

contribute to the enhanced production of these specific amino acids during fungal development.

In the case of the amino acid arginine, it is well known that its addition to the Sordaria Minimal Media (SMM) is necessary for the fruiting body formation and hyphae branching in *S. macrospora* (Hock et al., 1978). In this study arginine decreased during the life cycle of *S. macrospora*, and several factors could potentially explain this phenomenon. One possible explanation is that arginine is being utilized or metabolized for other cellular processes or pathways during the specific stages of fungal development. For example, arginine can serve as a precursor for the biosynthesis of other metabolites, such as polyamines, which are involved in various physiological processes, including cell growth and differentiation (Maeda et al., 2006).

Alternatively, the decrease in arginine levels, the solely amino acid added to the growing media, could be attributed to its utilization as a nitrogen source by the fungus. Fungi have the ability to scavenge and utilize different nitrogen sources depending on their availability in the environment. It is possible that arginine, being an important nitrogen-rich amino acid, is actively taken up and utilized by *S. macrospora* as a nitrogen source during specific developmental stages, leading to its depletion in the cellular pool (Hock et al., 1978).

Finally, auxins were found to boost energy generation for different processes in plants, such as pollen maturation through the regulation of the central carbon metabolism (Amanda et al., 2022). In fungi, mannitol a sugar alcohol synthesised from fructose, is thought to be necessary for for rapid energy acquisition, osmotic potential, pH, and cofactor regulation of fruiting body formation and sporulation (Vetter, 2023; Meena et al., 2015).

In this study, mannitol, was found to be upregulated, in a manner that is similar to IAA, during the second stage of the *S. macrospora* life cycle.

In summary, the findings of this study suggest that IAA may play a role in regulating energy-related metabolic pathways in *S. macrospora* during different stages of its life cycle. The interplay between organic acids, including those involved in the TCA cycle, and lipid metabolism in *S. macrospora* underscores the intricate relationship between energy production, nutrient utilization, and fungal development. The metabolic priorities and requirements of the fungus may vary during different stages of development, leading to fluctuations in the levels of specific amino acids, including arginine. Further investigations are required to elucidate the precise molecular mechanisms by which IAA influences energy metabolism and lipid utilization during the developmental stages of *S. macrospora*.

2.4.6 Lipidomics in *S. macrospora*

Lipids are known to be involved in cell signaling in various organisms, such as yeast and plants. For instance, lipid rafts, specialized membrane domains rich in sphingolipids and cholesterol/ergosterol, can modulate cell movement and cytokinesis in yeast (Mollinedo, 2012; Peraza Reyes & Berteaux-Lecellier, 2013). Additionally, phosphatidic acid and glycerophospholipids regulate phytohormones in plants, such as auxins and ABA (Janda et al., 2013; P. Wang et al., 2019).

In fungi, the understanding of lipids in development is still limited, and to the best of our knowledge, this study represents the first attempt to investigate lipidomics in fungi at different developmental stages. The results of this study shed light on the potential involvement of specific lipid classes in *S. macrospora* development.

Lipid rafts, characterized by their high content of sphingolipids and cholesterol/ergosterol, play a crucial role in concentrating lipid-binding proteins and organizing specific regions of the plasma membrane (Bieberich, 2018; Mollinedo, 2012). The enrichment of sterol pathways in the comparison of stages W2/W3 suggests their potential importance in the transition to sexual development in *S. macrospora*. Ergosterol, cholesterol, 24-methyl cholesterol, 24-ethyl cholesterol, and brassicasterol have been identified as the primary sterols in ascomycetes fungi (Weete et al., 2010), contributing to hyphae septa formation and morphogenesis (Alvarez et al., 2007). However, their specific roles in lipid, for fungal growth and development, are still poorly understood. Further investigation into the functions of sterols in fungal development could provide valuable insights.

Secosteroles, also known as vitamin D, are human hormones involved in various physiological processes. Interestingly, secosteroles have been reported in both edible mushrooms and yeast (Cardwell et al., 2018; Kessi-Pérez et al., 2022; Savidov et al., 2018). In this study, the significant enrichment of the secosteroles pathway between stages W3/W4, when the fruiting bodies become mature and ready to release spores, raises possibilities that secosteroles are myco-hormones in fungal development. Future research should focus on elucidating the functions of sterols, secosteroles, in the context of developmental processes in fungi.

Flavonoids are well-known signaling molecules in plant-fungi symbioses, where they play crucial roles. For instance, studies have shown that flavonoids enhance spore germination in the arbuscular mycorrhizal fungus *Rhizophagus irregularis* in both in vitro and in vivo conditions (Lidoy et al., 2023). The Folch method was used in this study, and is a widely used extraction technique, that efficiently extracts flavonoids (Saini et al., 2021). In the current study, flavonoids were significantly enriched at an early stage of vegetative growth in the life cycle of *S. macrospora* (Table 7). While some metabolic pathways have been reported in the synthesis of fungal flavonoids (Mohanta, 2020; W. Zhang et al., 2023), the screening for flavonoids in edible mushrooms, (unlike the present study), did not showed detectable flavonoids (Gil-Ramírez et al., 2016). These finding together with the results in this study suggests that flavonoids may primarily participate in the early stages of fungal growth and development. Therefore, further investigations are necessary to elucidate the specific roles and mechanisms of flavonoids in *S. macrospora* and other fungi, particularly regarding their potential involvement in fungal vegetative developmental processes and interactions with their environment.

2.5 CONCLUSIONS

In conclusion, this study provides an extensive overview of the metabolome of *S. macrospora*, adding critical new insights into the potential roles of phytohormones, metabolites, and lipids in fungal growth and development. The targeted analysis of phytohormones revealed the presence of cytokinins (CKs) and auxins at different concentrations throughout the life cycle of *S. macrospora*, suggesting their involvement in

fungal development, specifically in ascospore formation and the transition to sexual reproduction, respectively. The semi-targeted and untargeted approaches allowed for the identification of energetic metabolites and lipids, respectively, revealing aspects into the energy requirements, metabolite biosynthesis, and cell communication during different stages of the fungus's life cycle.

The analysis of nucleotides, nucleosides, and nucleobases revealed distinct patterns throughout the life cycle, with an increase in nucleoside levels during the second stage, indicating their potential involvement in critical processes associated with fungal development. Thymidine and cordycepin showed different trends, suggesting a potential interplay and shared regulatory mechanisms with CKs during the third growth stage, W3. The correlation between mevalonate levels and free base CKs suggests their potential involvement in sterol and isoprenoid biosynthesis during ascospore formation.

The presence of auxins in *S. macrospora* was demonstrated through the analysis of indole-3-acetic acid (IAA). The increase in IAA during the transition to sexual development suggests it has a role as an energetic regulator. The correlation between IAA and organic acids, amino acids, and lipids implies it has a potential regulatory role in energy metabolism and lipid utilization during fungal development. Furthermore, the upregulation of mannitol, similar to IAA, during the second stage suggests that they could have a biological relationship in processes for fruiting body formation.

The lipidomics analysis gains novel insights into the lipid composition and potential roles of specific lipid classes during *S. macrospora* development. The enrichment

of sterol and secosterol pathways suggests their involvement in the transition to sexual development and spore release. The potential roles of flavonoids, phosphatidic acid (PA), and fatty acids together with auxin-related processes were also highlighted in fungal development.

Overall, this study contributes to our understanding of fungal biology by uncovering the connections between phytohormones, metabolites, and lipids in the growth and development of *S. macrospora*. The findings suggest the presence of intricate regulatory mechanisms and provide a basis for further investigations into the molecular mechanisms underlying fungal development and the identification of myco-hormones involved in growth regulation.

CHAPTER 3 – The effects of cytokinins on *S. macrospora* growth and development

3.1 INTRODUCTION

Cytokinins (CKs) are a group of phytohormones known for their crucial roles in plant growth and development (Pal et al., 2023). They are involved in various aspects of the plant life cycle, including cell differentiation, seed development, shoot formation, and the maintenance of meristematic cells (J. Wang et al., 2020; Wu et al., 2021). CKs were

traditionally believed to be exclusive to plants, but recent research has revealed that fungi also produce CKs, particularly isopentyladenine (iP) and *cis*-Zeatin (cZ) which are a part of a tRNA-degradation pathway (Table 1). This pathway was proposed after screening CK profiles in 20 temperate forest fungi (Morrison et al., 2015).

The biosynthesis of CKs in plants involves two main pathways. The *de novo* pathway leads to the production of *trans*-Zeatin (tZ) and dihydrozeatin (DZ), while the tRNA degradation pathway generates iP, cZ, and 2-methylthiolated CKs (2MeS) (Sakakibara, 2006). The presence of iP and cZ in fungi suggests that they utilize a similar tRNA degradation pathway for CK biosynthesis. However, the precise roles of CKs in fungal growth and development remains largely uninvestigated.

Early studies showed that physiological effects in fungi caused by exogenously applied CKs were dose-dependent. For instance, in *Neurospora crassa* strains, concentrations ranging from 10 to 20 μM of Kinetin, a synthetic CKs, had positive effects on fertility, peritheciium formation, and ascospore production (Lee, 1961). Conversely, 500 μM of iP showed inhibitory effects, while 50 μM resulted in an increased growth diameter in the fungus *Pleurotus ostreatus* (Grich, 2021). Similarly, in *Botrytis cinerea*, *Fusarium oxysporum*, and *Sclerotium rolfsii*, the addition of 100 μM of the non-endogenous CK, 6-BAP, exhibited inhibitory effects, while 1 μM did not affect fungal growth (Rupali et al., 2021).

However, it is important to note that the concentrations used in those applications often did not align with the typical levels found in biological systems. For example, in *Ustilago maydis*-*Zea mays* infected cob tissue, CK concentrations range from ~ 1 to 1000 pmol/g FW (Morrison et al., 2017), while *Magnaporthe oryzae*-infected rice produces CKs

ranging from 0.1 to 300 pmol/g FW (Jiang et al., 2013). A survey of the literature reveals that fungi naturally produce CKs within the pmol range (0.1 to 200 pmol/g FW) (Table 1).

S. macrospora, with its short life cycle of 7 days and well-studied characteristics, serves as an excellent model organism for investigating the impact of exogenous CKs on fungal growth and development. This fungus undergoes both vegetative growth and sexual reproduction, encompassing various stages of tissue formation, such as ascogonium (asc), protoperithecium (pro), immature perithecium (per), and mature perithecium (fruiting bodies) (Lord & Read, 2011).

This study focuses on the application of CKs at lower, more physiologically relevant concentrations, ranging from 0.01 μM to 100 μM , and 2 different time points (0 and 5 days post inoculation) to investigate their biological effects in *S. macrospora* growth and development. The results revealed that the positive effects of CKs are highly dependent on the specific type of CK, the concentration utilized, and the developmental stage of *S. macrospora* at the time of application. Optimal concentrations ranging from 0.01 μM to 10 μM were observed in the increase of tissue mass of *S. macrospora* when the CKs were applied on day 5 of the fungus development. As expected from previous studies, concentrations of 100 μM exhibited inhibitory effects irrespective of the type of CK applied. These findings provide valuable insights into the intricate relationship between CKs, fungal physiology, and developmental stages.

3.2 METHODS

Exogenous application of cytokinin on *S. macrospora*

The study aimed to investigate the effects of exogenously applied CKs on *S. macrospora*. Two experiments were conducted, with control groups included for comparison. In experiment one the hormones were added at the beginning of the experiment. In experiment two, the exogenous CKs were added after 5 days post inoculation (dpi). This timing was chosen based on the targeted metabolomics results (see Chapter 2 - Metabolome of *S. macrospora*- Figure 5), which coincide with a switch from ribosides to free bases produced by *S. macrospora* wild type.

Experiment 1 CKs exogenous application at the beginning of *S. macrospora* life cycle

For fungal preparation, *S. macrospora* wild type was cultivated in Sordaria Minimal Media (described in Chapter 2- Metabolome of *S. macrospora*, fungal growth methods section) agar media (SMM), by transferring to fresh media performed every 7th day to maintain optimal growth conditions for three consecutive weeks. Fungal discs were obtained using glass Pasteur pipettes, ensuring a consistent diameter. These fungal discs were then inoculated onto Petri dishes containing 20 mL of SM agar media (2% agar), following the procedures outlined in the chapter 2- Metabolome of *S. macrospora*, fungal growth method section. Subsequently, 3.5 mL of liquid SM media, supplemented with either 0.1 μ M of cZ or Kinetin riboside (KR), were added to the Petri dishes containing the fungal discs. The CKs were initially dissolved in MeOH and then further diluted in MeOH to achieve a total volume of 100 μ L of MeOH added to the media. This serial dilution process was performed to ensure accurate measurement and delivery of the desired concentration of CKs in the experimental setup.

After 5 days post inoculation (dpi), specifically between stages 2 and 3 of the *S. macrospora* life cycle (see Chapter 2 - Metabolome of *S. macrospora*- results section), 3.5 mL of liquid SM media supplemented with 100 μ L of MeOH was added to the Petri dish, similar to experiment 2 to facilitate data comparisons.

Experiment 2- CK exogenous application in the protoperithecium stage in *S. macrospora*

The fungal preparation was carried out as described in experiment 1. After fungal disc inoculation in the petri dish with SM agar (2%), 3.5 mL of liquid SM media supplemented with 100 μ L of MeOH were added to the Petri dishes. After 5 dpi, 3.5 mL of liquid SM with one of 5 different concentrations, (0.01, 0.1, 1, 10 and 100 μ M) and one of 4 different hormones (iP, iPR, cZ, or KR) was added to the fungal strains. The CK treatments were prepared as described in experiment 1, using MeOH.

Controls

For the 2 experiments, the control group was performed at the same time points of the experiment 1 and 2 (0 and 5 dpi) but with the addition of MeOH without CKs, whereby 3.5 mL of liquid SMM supplemented with 100 μ L of MeOH were added to the petri dish after at the beginning of the fungus life cycle and on the protoperithecium stage, 0 and 5 dpi, respectively.

A total of 4 replicates for each treatment and 8 replicates for the control groups were analyzed. The fresh fungal tissue was weighed, and fruiting bodies were counted through microscopy photos after 8 dpi (Figure 14).

Microscopy

The number of fruiting bodies was assessed using an inverted microscope (Nikon, Eclipse Ts2). To ensure consistency, two random triangular pieces were selected from the petri dish, maintaining a constant area across the samples ($\frac{1}{2} 5 \text{ cm} * 3 \text{ cm} = 7.5 \text{ cm}^2$). The triangles were carefully cut and placed upside-down on a cleaned platform, which was positioned on the inverted microscope for image acquisition. To capture a representative sample, three different distances starting from the inoculated fungal disc were chosen for image acquisition. As a result, a total of six images per replicate were generated (Supplementary material for the images).

Data analysis

The acquired images were analyzed using CellProfiler 4.2.5, a software tool designed for quantitative image analysis. A custom pipeline named "Tissue Neighbors" was used as a template and modified to count and measure *S. macrospora* fruiting bodies.

Prior to the analysis, the images were preprocessed to prepare them for further analysis steps. The preprocessing steps included converting the images from color to grayscale using the "ColortoGray" module. Subsequently, the grayscale intensities were inverted using the "ImageMath" module. A noise reduction step using the "reduceNoise" module was applied, particularly to address mature fruiting bodies.

To identify the fruiting bodies, three "IdentifyPrimaryObjects" modules were added to the pipeline. Each module used different diameter units to target different stages of the fruiting bodies: small (50-150 pixels), medium (151-400 pixels), and large (401-9999

pixels) for proto-perithecium, young perithecium, and mature perithecium, respectively. The thresholding strategy employed was global, with the minimum Cross-Entropy method and a threshold correction factor of 2.3.

To handle clumped objects, intensity-based distinction was used, while shape-based division was employed to separate objects. For the identification of mature perithecium, two additional modules were added: "RemoveHoles" and "IdentifySecondaryObjects" using a global threshold strategy with the "Robustbackground" method.

The resulting measurements from CellProfiler included the area and shape of each identified fruiting body. To filter the data, objects with intensities lower than 0.4 or 0.6 (for proto-perithecium and perithecium, respectively) were excluded from further analysis.

The number of fruiting bodies per image and per replicate, along with their corresponding area and shape measurements, were recorded for subsequent analysis (Figure 13).

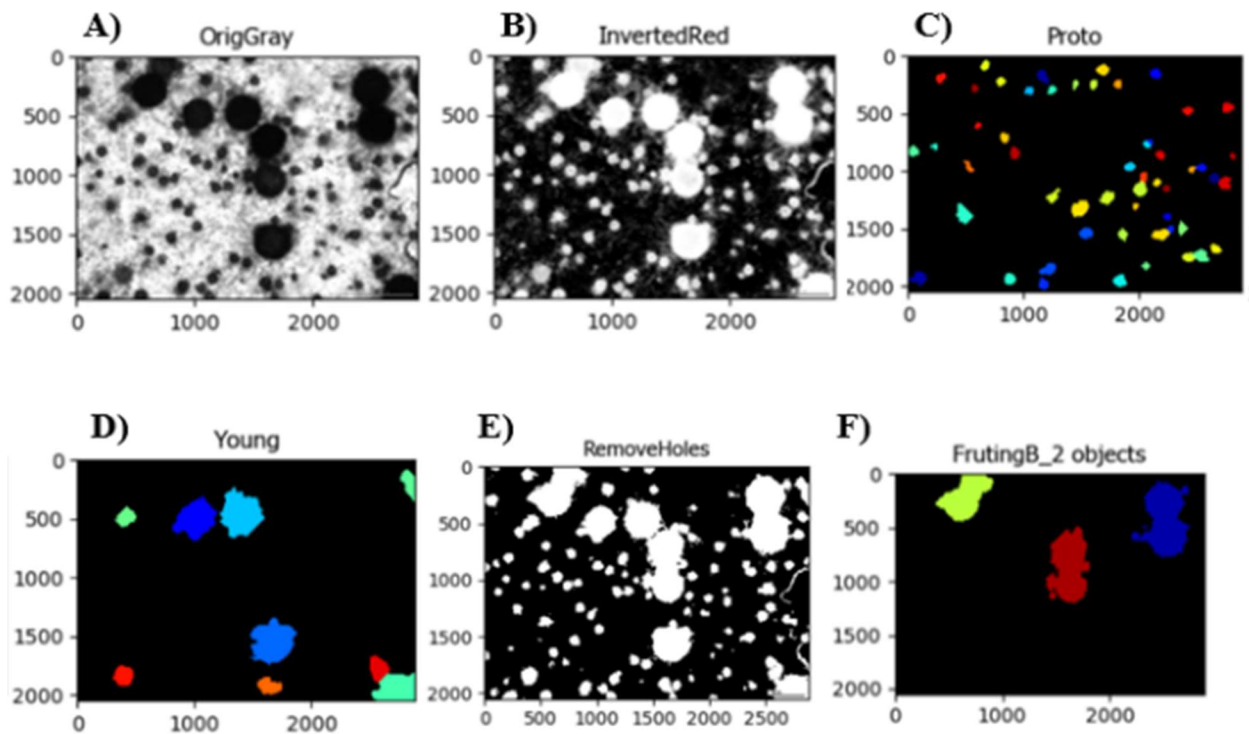


Figure 13. An example for CellProfiler analysis workflow using exogenous Kinetin Riboside $0.1\mu\text{M}$ treatment added at 0 day post-inoculation (dpi) in *S. macrospora*. The image was obtained with an inverted microscope (magnitude (4X) after 8 dpi. A) ColorioGray module, the original image was converted to gray scales, B) ImageMath module, to invert the gray intensities, C) Identification of protoperithecium, D) identification of young perithecium, E) removing holes of mature perithecium and F) Identification of mature perithecium.

3.3 RESULTS

To assess the effects of exogenously applied phytohormones on *S. macrospora* physiology CKs were applied at two developmental stages. Two experiments were conducted at the same time, with control groups included for comparison. In experiment one, the hormones cis-Zeatin (cZ) and kinetin riboside (KR) were added at $0.1\mu\text{M}$ at the

beginning of the experiment. While in experiment two, the exogenous application of the phytohormones cZ, KR, isopentenyl-adenine (iP), and iP riboside (iPR) was carried out at concentrations ranging from 0.01 to 100 μM and these were added after 5 days post inoculation (dpi). This timing was chosen based on the CK profiling results, described in Chapter 2- *Metabolome of S. macrospora*- which refer to a clear switch from CK-ribosides to CK-free bases that were naturally produced by *S. macrospora* wild type. After 8 days post inoculation, the tissue mass and fruiting body counts were taken for both experiments (Figure 14).

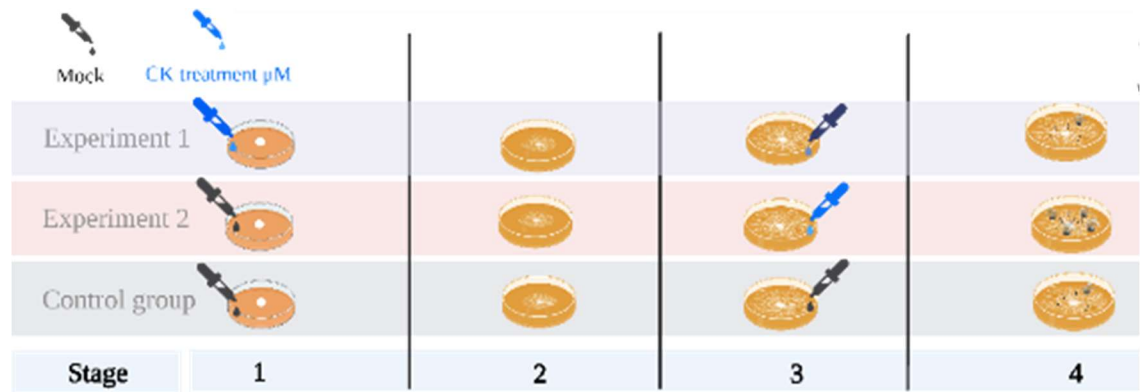


Figure 14. Schematic representation of the methodology employed for exogenous cytokinin treatments. In experiment 1, the growing media consisting of liquid Sordaria Minimal Media (SMM) was supplemented with either 0.1 μM cis-Zeatin (cZ) or Kinetin Riboside (KR) at 0 days post inoculation (dpi), and after 5 dpi (stage 3), liquid SMM without hormones was added to the media. In experiment 2, liquid SMM was added at 0 dpi, and after 5 dpi, liquid SMM supplemented with different concentrations ranging from 0.01 to 100 μM of cytokinins (cZ, KR, isopentenyl-adenine (iP), and iP-riboside (iPR)) was introduced. The control group received liquid SMM without any cytokinin supplementation at both 0 and 5 dpi. Tissue weight and fruiting body counts were recorded after 8 dpi to evaluate the effects of the treatments.

The effects of cytokinins in the early S. macrospora life cycle is cytokinin-type dependant.

The control group exhibited a tissue mass of 1.0973 g/petri dish (SE \pm 0.083), representing the baseline growth of *S. macrospora* in the absence of exogenous phytohormone treatment. The supplementation of 0.1 μM cZ to the growing media did not

have an effect on the tissue weight (Figure 15.A); however, it resulted in a 25% reduction in the production of fruiting bodies compared to the control group (Figure 15.B). Conversely, the supplementation of 0.1 μM KR led to a 22% increase in tissue weight, while the formation of fruiting bodies remained similar to that of the control group (Figure 15.B). These results suggest that KR at 0.1 μM concentration at the beginning of the fungal life cycle may have a potential influence on the vegetative growth of *S. macrospora*.

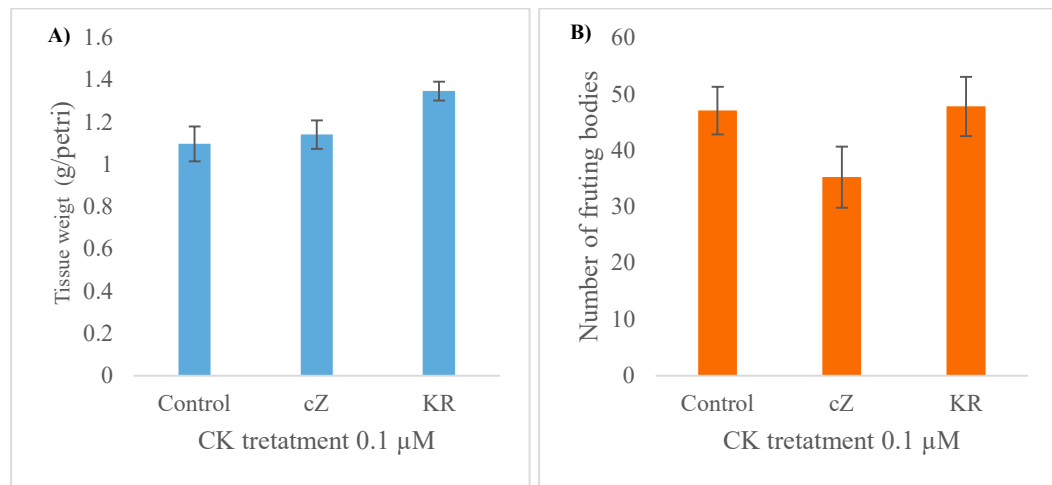


Figure 15. Effects of cis-Zeatin (cZ) or kinetin riboside (KR) on the growth of *S. macrospora* growth. The fungus was grown in Sordaria Minimal Media (SMM) for 8 days, the media was supplemented, with cZ or KR at 0.1 μM . A) Tissue weight in grams per petri dish, with SE (\pm) for 4 replicates. B) Relative number of fruiting bodies, including those ranging from protoperithecium to mature perithecium, with SE (\pm) for 6 images per 4 replicates

Cytokinin effects in S. macrospora are dose and time dependant

Overall, the addition of phytohormones at day 5 of *S. macrospora* life cycle resulted in higher biomass accumulation and fruiting body formation. The application of free bases CKs, iP and cZ, within the range of 0.01 – 10 μM , showed a slight increase in the tissue weight and an enhancement in fruiting body formation (Figure 16.B). In contrast, the

ribosides CKs, KR and iPR, treatments in the same concentration range as free bases, were observed to improve the tissue weight, but only iPR demonstrated higher formation of fruiting bodies compared to the control. The concentration of 100 μM showed inhibitory effects, resulting in a decrease in both the tissue weight and the formation of fruiting bodies (Figure 16).

More precisely, among the different concentrations of isopentenyl-adenine (iP), the highest tissue weight was observed at 10 μM iP, suggesting a stimulatory effect on biomass accumulation (Figure 16.B). While, 0.01 μM KR was sufficient to demonstrate a slight improvement in *S. macrospora* growth. These findings highlight the dose-dependent effects of phytohormones on the biomass accumulation of *S. macrospora*, underscoring the importance of the specific type and concentration of phytohormones in influencing fungal growth and development.

Regarding fruiting body formation, the application of 1 μM cis-Zeatin (cZ) resulted in the highest fruiting body formation count, indicating its potential to enhance reproductive development (Figure 16.B). In contrast, the lowest fruiting body count was observed at 100 μM of cZ and KR, suggesting a negative effect on fruiting body formation at this concentration. These findings highlight the importance of optimizing the concentration of cZ, and KR for maximizing fruiting body production in *S. macrospora*.

In summary, the exogenous application of phytohormones, particularly iP and cZ, exerted effects on the fruiting body formation in *S. macrospora*. The concentration-dependent responses observed in tissue weight and fruiting body count emphasize the

importance of the appropriate concentrations of phytohormones for regulating fungal development.

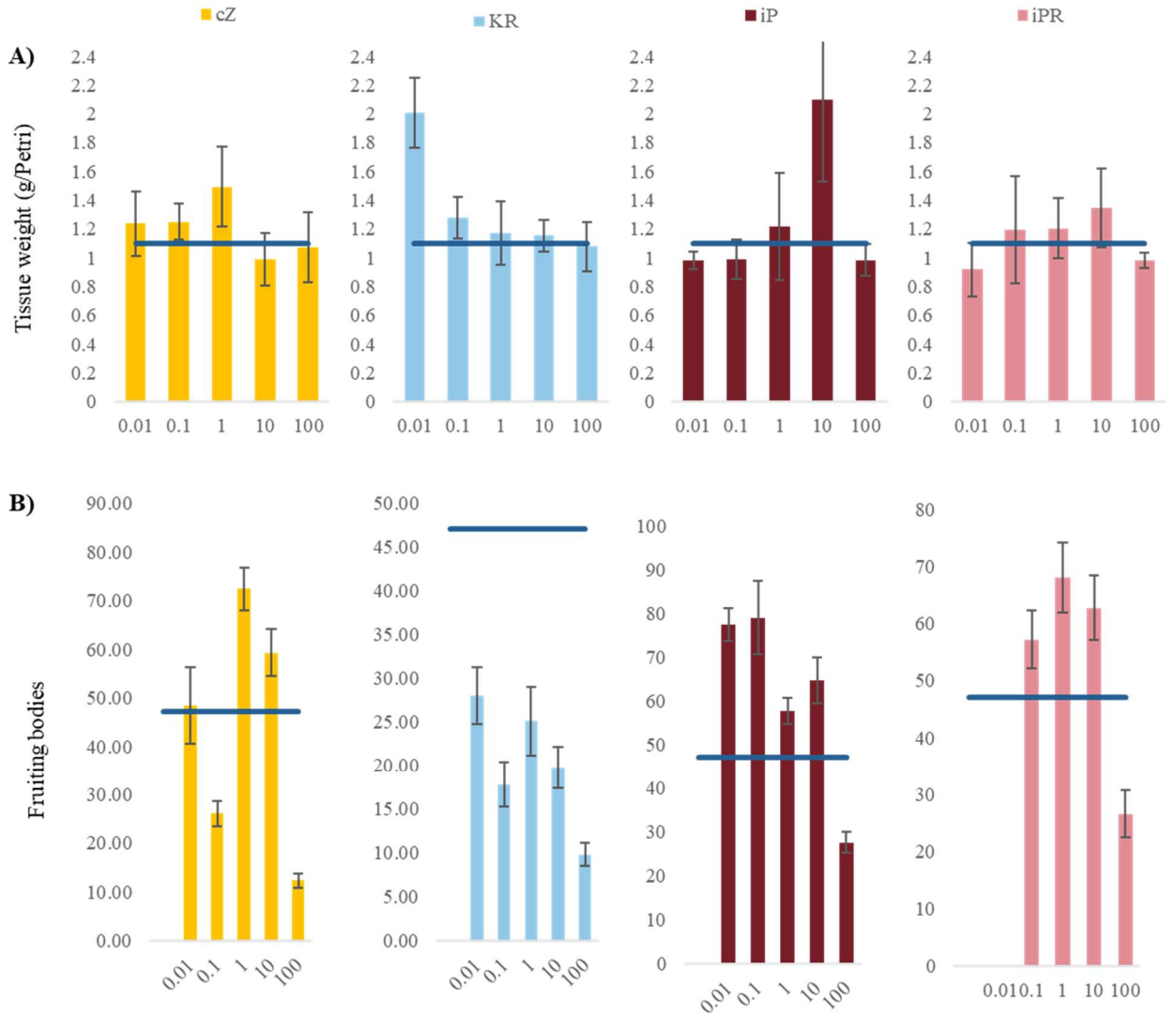


Figure 16. Effect of cytokinins in *Sordaria macrospora* growth. The fungus was grown in *Sordaria* Minimal Media (SMM) for 8 days, the media was supplemented, after 5 days of growth, with *cis*-Zeatin (cZ)- Kinetin Riboside (KR), isopentenyladenine (iP), and isopentenyl adenine riboside (iPR) at different concentrations ranging from 0.01 to 100 μ M. **A)** Tissue weight in grams per petri dish, with SD (\pm) of 4 replicates., **B)** Relative number of fruiting bodies including from protoperithecium to mature perithecium, with SE (\pm) for 6 images per 4 replicates. The blue line represents the average of the control in all the graphs.

The results from both experiments indicate that the exogenous application of phytohormones, including cZ, KR, iP, and iPR, at stage 3 (day 5) of the development of *S. macrospora*, can influence the growth and reproductive development of *S. macrospora*.

3.4 DISCUSSION

Fungi are known to produce CKs, regardless of their interaction with living plants (Table 1). However, the effects on CKs on fungal growth and development remains unclear. The fungus *S. macrospora*, a model organism in biology, demonstrated to produce different concentrations of the CKs such as iP, cZ, cZR, and iPR, through its life cycle (see Chapter 2- Metabolome of *S. macrospora*- Figure 5). The production of fungal CKs are in the range of pmol/g FW, for instance cZ in *S. macrospora* was around 4 pmol/g FW. Exogenous application of CKs in fungi has shown to be dose-dependent, with low doses (2 to 20 μ M) being beneficial, such as restore in fertility in mutant strains of *Neurospora crassa* (LEE, 1961), while higher doses (above 100 μ M) inhibiting growth (Table 7).

In this thesis (see Chapter 2- Metabolome of *S. macrospora*- Figure 5), it was observed that *S. macrospora* produces CK ribosides during the early stages of the fungus development (stage 1 and 2), and a switch to CK free bases in stage 3, the ascospore formation stage. To investigate the effect of low doses of CKs (from 0.01 to 100 μ M), the CK type, and the timing of CK exposure in the growth and development of *S. macrospora*, I performed 2 different experiments. In experiment 1, I added CK riboside and free bases at the beginning of the fungus life cycle. While, in experiment 2, I added CK ribosides and free bases at 5 dpi, the stage of ascosporegenesis, which coincides with the switch form

free bases to ribosides in *S. macrospora* (see Chapter 2- Metabolome of *S. macrospora*- Figure 5).

The results of the experiments demonstrate that cytokinins (CKs) have notable effects on the growth and development of *S. macrospora*. In the experiment one, the addition of 0.1 μM KR at the beginning of the cycle of *S. macrospora* resulted in increased tissue weight compared to the control. Additionally, in the experiment two, 0.01 to 10 μM of iPR and KR supplemented at day 5 (referencing the ascosporegenesis stage of the fungus), also resulted in a tissue weight increase. Since it was demonstrated that endogenous ribosides levels are higher in the vegetative growth stage (see Chapter 2- Metabolome of *S. macrospora*- results section). The findings suggest that CKs ribosides promote vegetative growth of *S. macrospora*. In the second experiment, four different cytokinins (cZ, KR, iP, and iPR) were tested at various concentrations and were added to the media at day 5. As expected (Gryndler et al., 1998; Kind et al., 2018; Rupali et al., 2021), a concentration of 100 μM of all the cytokinins inhibited tissue growth and led to a reduction in the formation of fruiting bodies. However, concentrations ranging from 0.1 to 10 μM of cZ and iP showed positive effects, with increased tissue weight and higher numbers of fruiting bodies compared to the control. These results highlight the concentration-dependent effects of cytokinins on fungal growth and development.

One possible explanation for the dose-dependent effects of exogenous cytokinin (CK) application in *S. macrospora* might be due to hormesis, a well studied phenomenon in endocrinology and recently gaining attention in agriculture (Godínez-Mendoza et al., 2023). Hormesis is a phenomenon where a substance (that can be harmful at high doses), in low doses, induces a beneficial response triggered by a mild stress. The response

typically follows a stimulatory curve, reaching an optimal dose where the effect is maximized, and then declining as the dose surpasses a certain threshold (Godínez-Mendoza et al., 2023). Similar hormetic effects have been observed in the response of animals to phytohormones (Kadlecová et al., 2019), plants to heavy metals (Małkowski et al., 2020), and fungi to fungicides (Zied et al., 2017). In the case of *S. macrospora* and phytohormones, iP at a concentration of 10 μ M stimulates biomass accumulation, reaching an optimal dose for maximum effect (Figure 16A).

These findings are in line with previous studies that have explored the effects of exogenous phytohormones applications in other fungal species. Liu et al. (2016) reported that the growth-promoting effects of indole-3-acetic acid (IAA) were observed only in *Saccharomyces* strains that naturally produced higher amounts of IAA while higher concentrations of IAA, as well as CKs, were found to have inhibitory effects in various fungi, including yeast (Y.-Y. Liu et al., 2016), *Fusarium delphinoides* (Kulkarni et al., 2013) and *Glomus mosseae* (Gryndler et al., 1998). Additionally, in a study conducted on *Alternaria alternata*, *Aspergillus niger*, and *Aspergillus oryzae*, it was observed that treatment with 45 mg/L of kinetin led to an increase in dry and fresh biomass, especially on *A. alternata*, compared to the control group. While, at a higher concentration of 60 mg/L, a reduction in fungal growth was observed compared to the 45 mg/L treatment in all the fungal strains (Nasmin & Rahman, 2009). These studies, combined with the present findings, suggest that the effects of phytohormones, specifically CKs, on fungal growth and development are species-specific and dependent on hormone concentration, in a pattern typical of hormesis.

Interestingly, the positive results obtained in the present study were achieved by treating the fungus with low concentrations of CKs free bases at day 5, just before the start of the third stage of the *S. macrospora* development, which involves neck and ascus formation. Furthermore, endogenous levels of freebases increased in this third stage (see Chapter 2- Metabolome of *S. macrospora*- results section). This is consistent with CKs play an active role during this critical stage of reproductive development. Similarly, in *N. crassa*, kinetin treatment has been shown to enhance perithecia and ascospore production, with optimal results observed at concentrations ranging from 5 to 20 μM (Lee, 1961).

Notably, the literature lacks studies investigating the addition of CKs at different stages of fungal development. Therefore, the current findings provide valuable insights into the potential of CKs as myco-hormones. Endogenously, a switch from cytokinin ribosides to free bases has been observed in the 3rd stage of the *S. macrospora* developmental stage, suggesting a dynamic regulation of cytokinin metabolism in *S. macrospora* (see Chapter 2- Metabolome of *S. macrospora*- results section). Additionally, this study demonstrates that an application of low concentrations of cytokinin (ranging from 1 to 10 μM) on day 5 (ascospore formation stage) in *S. macrospora* improves fruiting body formation and increases tissue weight. This observation, together with the physiological effects of different CKs concentrations reported in fungi (Braaksma et al., 2001; Gautam et al., 2022; Lee, 1961; Nasmin & Rahman, 2009), highlight the importance of considering the timing and concentration of CK application in *S. macrospora*.

In conclusion, CKs exhibit potential as regulators of fungal growth and development. The results of this study emphasize the importance of CKs in fungal biology, particularly in relation to the formation of reproductive structures. While previous research

has focused on high concentrations of exogenous CKs, the positive outcomes achieved in this study and in earlier studies from the 1980s and 1990s highlight the efficacy of low concentrations of CKs (Table 7). Further research in this area can explore effects and phytohormones, investigate the underlying molecular mechanisms behind the observed effects, and assess the potential applications of phytohormone manipulation in fungal biotechnology and other relevant fields. Such studies can lead to the development of innovative strategies to improve fungal production and contribute to advancements in agriculture, bioremediation, and other areas that rely on the beneficial properties of filamentous fungi.

Table 7. Effects of exogenous cytokinin treatment in fungi.

Fungus	Exogenous CKs	Concentration	Effects	Reference
<i>N. crassa</i>	KIN	0-50 μ M	Restore in fertility, and enhanced perithecium and ascospore formation in the crosses of <i>N. crassa</i> strains	Lee, 1961
<i>Glomus fistulosum</i>	ZR, KR, BAP, BA	0.1-100 μ M	Inhibitory effects above 10 μ M	Gryndler et al. 1998
<i>B. cinerea</i> , <i>F. oxysporum</i> , <i>S. rolfsii</i>	BAP	1-100 μ M	BAP does not irreversibly harm fungal development. The concentration of 1 μ M similar to the mock, while 100 μ M decrease in <i>B. cinerea</i> and <i>S. rolfsii</i> growth	Gupta et al. 2021
<i>P. ostreatus</i>	iP, tZ, BAP, KIN	50-500 μ M	50 μ M do not change the biomass compared to the control. However, 50 μ M iP showed an increase in the growth diameter. 500 μ M inhibits growth.	Grich, 2020
<i>B. cinerea</i>	BAP	100 μ M	The inhibitory effect of BAP against <i>B. cinerea</i> is based on nutrient availability. Glycolysis, sucrose metabolism, and oxidative phosphorylation pathways were significantly enriched upon BAP treatment. BAP was able to rescue the inhibition of glycolysis and ATP synthesis under glucose restriction in defined media	Anand et al. 2022
<i>C. purpurea</i>	iP	100 μ M-1mM	Above 10 μ M iP showed a decrease or inhibition of growth, 1 μ M of iP did not showed change in the transcriptome levels.	Kind et al. 2018

KIN Kinetin; ZR Zeatin Riboside; iP isopentenyl adenine; BAP 6-benzyl adenine; BA benzyl adenosine

CHAPTER 4- Conclusions and future work

Fungi, as a diverse kingdom of eukaryotic cells, play crucial roles in various ecological processes and have significant implications for human welfare. However, the mechanisms underlying fungal growth and development remain poorly understood. This thesis investigated the presence of myco-hormones during fungal growth and development of the model fungus *Sordaria macrospora*, known for its ability to produce mature fruiting bodies in just 7 days. Different metabolomic approaches were conducted via LC-MS/MS for the analysis of phytohormones, energetic metabolites, and lipids across four different developmental stages of the fungus and six different mutants. These mutants are characterized to blocked development at each stage. The objective was to shed light on the role of these metabolites during the fungus growth and development. To investigate the potential role of phytohormones, particularly CKs, as myco-hormones in fungal growth and development, I conducted experiments testing the effects of various CKs in terms of dose, time, and CK type on the biomass accumulation and fruiting body formation of *S. macrospora* WT (Figure 17).

Fungal endogenous phytohormones, such as cytokinins (CKs) and auxins, were found to be produced at different concentrations in the growth and development of *S. macrospora* throughout its life cycle. These findings indicate the potential role of CKs in the late stages of fruiting body formation in *S. macrospora* (Figure 17A). The free base class of CKs was observed to increase during the formation of ascospores. Interestingly,

mutant strains unable to form ascospores (asc, pro, and per mutants) did not show changes in free base CK levels, while a mutant, the strain smgpi1, that produces more fruiting bodies also showed elevated levels of free base CKs compared to the wild type. The increase in production of free bases only on the strains able to produce ascospores, WT and smgpi1, suggests a potential role of cytokinins in the last developmental stage of fruiting body formation in *S. macrospora*.

Furthermore, metabolites, including nucleosides and secosterols, exhibited changes during ascosporegenesis and may be closely associated with CKs, given that free base CKs are also upregulated during this stage. Moreover, CKs share a similar chemical structure with some nucleosides, and mevalonate has been described as a precursor for CKs and sterols in plants and fungi, respectively. Of particular interest are secosterols, such as vitamin D, which is known to increase in the presence of light in some fungal species. As light often triggers fruiting body formation in *S. macrospora* and other fungi, understanding the interplay between CKs and secosterols could provide valuable insights into fungal growth and development.

Furthermore, the effects of exogenous applications of different phytohormones were investigated at different times and concentrations in the fungus growth and development. Finally, the application of CKs to the growth media has a dose-time-dependent effect on tissue weight and the number of fruiting bodies in *S. macrospora* (Figure 17B). Optimal results were achieved when CKs were added at the beginning of ascsporegenesis, at concentrations below 10 μM . These findings pave the way for further exploration of CKs and their impact on fungal growth, particularly during the sexual development phase, the fruiting body formation.

On the other hand, the auxin IAA was found to increase in the early stages of *S. macrospora* fruiting body formation. The increase was noticed in the transition to sexual development, a transition known to require considerable amounts of energy. Furthermore, metabolites that participate in energy generation such as organic acids and amino acids were upregulated in this stage, while the fatty acid pathways were enriched in the transition, between stage W3/W4. These results suggest that IAA may upregulate energetic pathways to meet the high energy demands of transitioning to sexual reproduction in fungi. Interestingly, the mutant strain lacking the *acl*, gene responsible for fatty acid and sterol biosynthesis via the cytosol exhibited significantly higher concentrations of IAA (Figure 17A), further supporting the relationship between IAA and fungal energy levels and pathways. Therefore, special attention should be given to studying IAA and fungal energetics, including organic acids such as those in the TCA, amino acids, and lipids.

Working with *S. macrospora* offers several advantages for studying metabolomic and genetic changes throughout the fungal life cycle. The availability of a detailed gene deletion protocol via plasmid transformation (Nowrousian et al., 1999a; Pöggeler et al., 1997), the sequenced genome accessible online (<https://www.ncbi.nlm.nih.gov/datasets/taxonomy/771870/>), and the distinct tissue accumulation at each stage within a short 7-day cycle make it an ideal model organism to study myco-hormones for growth and development. Additionally, the implementation of CRISPR-Cas9, a gene editing technique reported in the filamentous fungi *Penicillium expansum* (Clemmensen et al., 2022), holds great potential for investigating the production of fungal phytohormones like CKs, since CKs are potentially derived from the tRNA degradation pathway in fungi.

By focusing on both vegetative and sexual growth after genetic modification, gene editing can provide valuable insights into the role of phytohormones in fungal development. Furthermore, metabolomics analysis can offer crucial information on the mode of action of CKs by examining metabolites such as mevalonate, mannitol, monosaccharides, nucleosides, sterols, and secosterols. Mevalonate is known to be a precursor of isoprene CKs in plants and sterols in fungi. The production of mevalonate in *S. macrospora* increased in coordination with free base CKs during ascospore formation. Mannitol and other sugars can provide insight into metabolic processes essential for the fungus's needs, as they participate in metabolic pathways, including energy generation. Finally, sterols are essential for various cellular processes, including cell growth and proliferation, as well as the biosynthesis of vitamin D in fungi. Sterol pathway demonstrated enrichment between the ascosporegenesis stage (stage 3) and the protoperithecium formation (stage 2). By studying this groups of metabolites can enrich our understanding of fungal growth and development.

Fungi, as a kingdom of eukaryotic cells, hold great potential for improving human economic and environmental health. This study offers new avenues for exploring the use of phytohormones as tools to enhance fungal systems. Future research should continue to investigate the intricate roles of phytohormones in fungal physiology, leading to advancements in harnessing the potential of fungi for various beneficial applications.

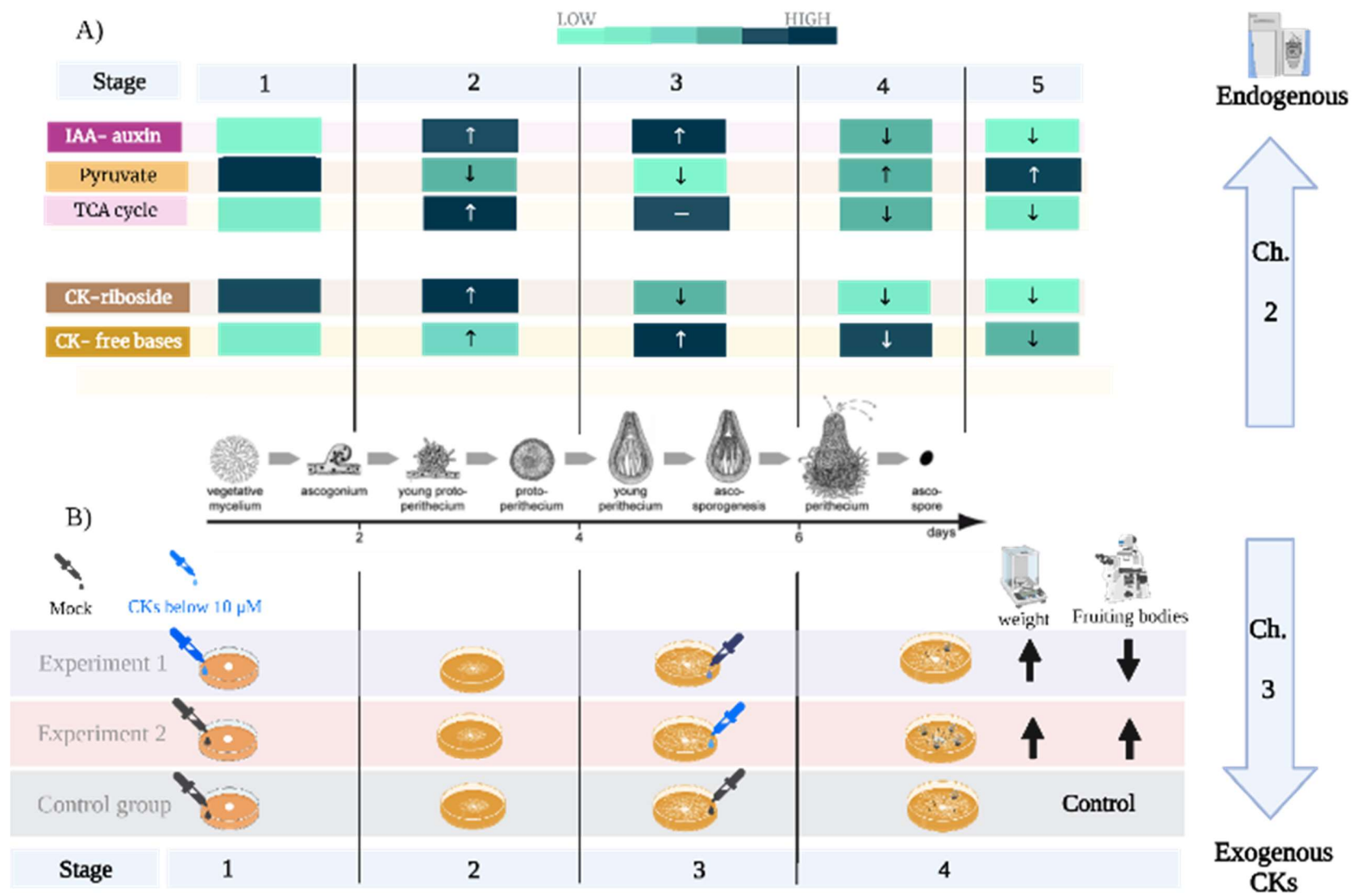


Figure 17. Schematic representation of the results in this thesis. A) The upper section depicts the findings described in Chapter 2, the metabolome analysis of *S. macrospora*. Liquid chromatography mass spectrometry was employed to analyze metabolites during the four stages of the fungus life cycle, with an additional fifth stage to study the accumulation of fruiting bodies. The blue squares in the figure represent the relative abundance of metabolites throughout the life cycle, with lighter blue squares indicating lower relative abundance and darker blue squares representing higher abundance. Key organic acids from the TCA cycle, such as citrate/isocitrate and malate, are the representative of TCA cycle in this figure. IAA- indoleacetic acid; CK riboside -cytokinin ribosides including cZR and iPR; CK free bases including cZ and iP.

B) The lower section of the figure represents the experimental procedure and results of Chapter 3, focusing on exogenous treatments of cytokinins. In Experiment 1, the growth media consisting of liquid *Sordaria* Minimal Media (SMM) was supplemented with either 0.1 μM cis-zeatin (cZ) or kinetin riboside (KR) at 0 days post-inoculation (dpi), and after 5 dpi (stage 3), liquid SMM without hormones was added to the media. In Experiment 2, liquid SMM was added at 0 dpi, and after 5 dpi, liquid SMM supplemented with different concentrations ranging from 0.01 to 100 μM of cytokinins (cZ, KR, isopentenyl-adenine (iP), and iP-riboside (iPR)) was introduced. The control group received liquid SMM without any cytokinin supplementation at both 0 and 5 dpi. Tissue weight and fruiting body counts were recorded after 8 dpi to evaluate the effects of the treatments. The results depicted in the figure are representative of the effects observed with the phytohormone concentrations ranging from 0.01 to 10 μM used in this thesis. The black arrows indicate changes in tissue weight and fruiting bodies compared to the control group.

REFERENCES

- Ahmed, S., Shah, P., & Ahmed, O. (2023). Biochemistry, Lipids. *StatPearls Publishing*.
- Alvarez, F. J., Douglas, L. M., & Konopka, J. B. (2007). Sterol-Rich Plasma Membrane Domains in Fungi. *Eukaryotic Cell*, 6(5), 755–763. <https://doi.org/10.1128/ec.00008-07>
- Amanda, D., Frey, F. P., Neumann, U., Przybyl, M., Šimura, J., Zhang, Y., Chen, Z., Gallavotti, A., Fernie, A. R., Ljung, K., & Acosta, I. F. (2022). Auxin boosts energy generation pathways to fuel pollen maturation in barley. *Current Biology*, 32(8), 1798-1811.e8. <https://doi.org/https://doi.org/10.1016/j.cub.2022.02.073>
- Aoki, M. M., Kisiala, A. B., Li, S., Stock, N. L., Brunetti, C. R., Huber, R. J., & Emery, R. J. N. (2019). Cytokinin Detection during the Dictyostelium discoideum Life Cycle: Profiles Are Dynamic and Affect Cell Growth and Spore Germination. *Biomolecules*, 9(11). <https://doi.org/10.3390/biom9110702>
- Aoki, M. M., Seegobin, M., Kisiala, A., Noble, A., Brunetti, C., & Emery, R. J. N. (2019). Phytohormone metabolism in human cells: Cytokinins are taken up and interconverted in HeLa cell culture. *FASEB BioAdvances*, 1(5), 320–331. <https://doi.org/https://doi.org/10.1096/fba.2018-00032>
- Ballweg, S., Sezgin, E., Doktorova, M., Covino, R., Reinhard, J., Wunnicke, D., Hänel, I., Levental, I., Hummer, G., & Ernst, R. (2020). Regulation of lipid saturation without sensing membrane fluidity. *Nature Communications*, 11(1), 756. <https://doi.org/10.1038/s41467-020-14528-1>

- Barker, S. J., & Tagu, D. (2000). The Roles of Auxins and Cytokinins in Mycorrhizal Symbioses. *Journal of Plant Growth Regulation*, 19(2), 144–154. <https://doi.org/10.1007/s003440000021>
- Bates, T. S., Cropsey, G. W., Gregory, C. J., Rob, K., & Noah, F. (2011). Bacterial Communities Associated with the Lichen Symbiosis. *Applied and Environmental Microbiology*, 77(4), 1309–1314. <https://doi.org/10.1128/AEM.02257-10>
- Bean, K. M., Kisiala, A. B., Morrison, E. N., & Emery, R. J. N. (2022). Trichoderma Synthesizes Cytokinins and Alters Cytokinin Dynamics of Inoculated Arabidopsis Seedlings. *Journal of Plant Growth Regulation*, 41(7), 2678–2694. <https://doi.org/10.1007/s00344-021-10466-4>
- Bérangère, P.-L., Axelle, B., & Corinne, C. (2005). Accelerated Cell Death in *Podospora* Autophagy Mutants. *Eukaryotic Cell*, 4(11), 1765–1774. <https://doi.org/10.1128/ec.4.11.1765-1774.2005>
- Bianco, C., Imperlini, E., Calogero, R., Senatore, B., Pucci, P., & Defez, R. (2006). Indole-3-acetic acid regulates the central metabolic pathways in *Escherichia coli*. *Microbiology*, 152(8), 2421–2431. <https://doi.org/https://doi.org/10.1099/mic.0.28765-0>
- Bieberich, E. (2018). Sphingolipids and lipid rafts: Novel concepts and methods of analysis. *Chemistry and Physics of Lipids*, 216, 114–131. <https://doi.org/https://doi.org/10.1016/j.chemphyslip.2018.08.003>
- Billet, K., Malinowska, M. A., Munsch, T., Unlubayir, M., Adler, S., Delanoue, G., & Lanoue, A. (2020). Semi-Targeted Metabolomics to Validate Biomarkers of Grape

- Downy Mildew Infection Under Field Conditions. *Plants*, 9(8).
<https://doi.org/10.3390/plants9081008>
- Bloemendal, S., Bernhards, Y., Bartho, K., Dettmann, A., Voigt, O., Teichert, I., Seiler, S., Wolters, D. A., Pöggeler, S., & Kück, U. (2012). A homologue of the human STRIPAK complex controls sexual development in fungi. *Molecular Microbiology*, 84(2), 310–323. <https://doi.org/https://doi.org/10.1111/j.1365-2958.2012.08024.x>
- Braaksma, A., Schaap, D. J., Donkers, J. W., & Schipper, C. M. A. (2001). Effect of cytokinin on cap opening in *Agaricus bisporus* during storage. *Postharvest Biology and Technology*, 23(2), 171–173. [https://doi.org/https://doi.org/10.1016/S0925-5214\(01\)00114-4](https://doi.org/https://doi.org/10.1016/S0925-5214(01)00114-4)
- Broadhurst, D., Goodacre, R., Reinke, S. N., Kuligowski, J., Wilson, I. D., Lewis, M. R., & Dunn, W. B. (2018). Guidelines and considerations for the use of system suitability and quality control samples in mass spectrometry assays applied in untargeted clinical metabolomic studies. *Metabolomics*, 14(6), 72. <https://doi.org/10.1007/s11306-018-1367-3>
- Bruce, S. A., Saville, B. J., & Neil Emery, R. J. (2011). *Ustilago maydis* Produces Cytokinins and Abscisic Acid for Potential Regulation of Tumor Formation in Maize. *Journal of Plant Growth Regulation*, 30(1), 51–63. <https://doi.org/10.1007/s00344-010-9166-8>
- Cardwell, G., Bornman, J. F., James, A. P., & Black, L. J. (2018). A Review of Mushrooms as a Potential Source of Dietary Vitamin D. *Nutrients*, 10(10).
<https://doi.org/10.3390/nu10101498>

- Chanclud, E., Kisiala, A., Emery, N. R. J., Chalvon, V., Ducasse, A., Romiti-Michel, C., Gravot, A., Kroj, T., & Morel, J.-B. (2016). Cytokinin Production by the Rice Blast Fungus Is a Pivotal Requirement for Full Virulence. *PLOS Pathogens*, *12*(2), e1005457-. <https://doi.org/10.1371/journal.ppat.1005457>
- Chanclud, E., & Morel, J.-B. (2016). Plant hormones: a fungal point of view. *Molecular Plant Pathology*, *17*(8), 1289–1297. <https://doi.org/https://doi.org/10.1111/mpp.12393>
- Chinnici, J. L., Fu, C., Caccamise, L. M., Arnold, J. W., & Free, S. J. (2014). Neurospora crassa Female Development Requires the PACC and Other Signal Transduction Pathways, Transcription Factors, Chromatin Remodeling, Cell-To-Cell Fusion, and Autophagy. *PLOS ONE*, *9*(10), e110603-. <https://doi.org/10.1371/journal.pone.0110603>
- Clemmensen, S. E., Kromphardt, K. J. K., & Frandsen, R. J. N. (2022). Marker-free CRISPR-Cas9 based genetic engineering of the phytopathogenic fungus, Penicillium expansum. *Fungal Genetics and Biology*, *160*, 103689. <https://doi.org/https://doi.org/10.1016/j.fgb.2022.103689>
- Combarrous, Y., & Nguyen, T. M. D. (2019). Comparative Overview of the Mechanisms of Action of Hormones and Endocrine Disruptor Compounds. *Toxics*, *7*(1). <https://doi.org/10.3390/toxics7010005>
- Devos, S., Laukens, K., Deckers, P., Van Der Straeten, D., Beeckman, T., Inzé, D., Van Onckelen, H., Witters, E., & Prinsen, E. (2006). A Hormone and Proteome Approach to Picturing the Initial Metabolic Events During Plasmodiophora brassicae Infection

- on *Arabidopsis*. *Molecular Plant-Microbe Interactions*®, 19(12), 1431–1443.
<https://doi.org/10.1094/MPMI-19-1431>
- Du, X.-Q., Yao, H.-Y., Luo, P., Tang, X.-C., & Xue, H.-W. (2022). Cytidinediphosphate diacylglycerol synthase—Mediated phosphatidic acid metabolism is crucial for early embryonic development of *Arabidopsis*. *PLOS Genetics*, 18(7), e1010320.
<https://doi.org/10.1371/journal.pgen.1010320>
- Engqvist, M. K. M., Eßer, C., Maier, A., Lercher, M. J., & Maurino, V. G. (2014). Mitochondrial 2-hydroxyglutarate metabolism. *Mitochondrion*, 19, 275–281.
<https://doi.org/https://doi.org/10.1016/j.mito.2014.02.009>
- Fahy, E., Subramaniam, S., Murphy, R. C., Nishijima, M., Raetz, C. R. H., Shimizu, T., Spener, F., van Meer, G., Wakelam, M. J. O., & Dennis, E. A. (2009). Update of the LIPID MAPS comprehensive classification system for lipids1. *Journal of Lipid Research*, 50, S9–S14. <https://doi.org/https://doi.org/10.1194/jlr.R800095-JLR200>
- Frey, S., Lahmann, Y., Hartmann, T., Seiler, S., & Pöggeler, S. (2015). Deletion of *Smgpi1* encoding a GPI-anchored protein suppresses sterility of the STRIPAK mutant Δ *Smmob3* in the filamentous ascomycete *Sordaria macrospora*. *Molecular Microbiology*, 97(4), 676–697. <https://doi.org/https://doi.org/10.1111/mmi.13054>
- Frey, S., Reschka, E. J., & Pöggeler, S. (2015). Germinal Center Kinases SmKIN3 and SmKIN24 Are Associated with the *Sordaria macrospora* Striatin-Interacting Phosphatase and Kinase (STRIPAK) Complex. *PLOS ONE*, 10(9), e0139163.
<https://doi.org/10.1371/journal.pone.0139163>
- Gao, J., Xu, X., Huang, K., & Liang, Z. (2021). Fungal G-Protein-Coupled Receptors: A Promising Mediator of the Impact of Extracellular Signals on Biosynthesis of

- Ochratoxin A. *Frontiers in Microbiology*, 12.
<https://doi.org/10.3389/fmicb.2021.631392>
- Gautam, A., Rupali, G., & Maya, B. (2022). Cytokinin Regulates Energy Utilization in *Botrytis cinerea*. *Microbiology Spectrum*, 10(4), e00280-22.
<https://doi.org/10.1128/spectrum.00280-22>
- Gil-Ramírez, A., Pavo-Caballero, C., Baeza, E., Baenas, N., Garcia-Viguera, C., Marín, F. R., & Soler-Rivas, C. (2016). Mushrooms do not contain flavonoids. *Journal of Functional Foods*, 25, 1–13. <https://doi.org/10.1016/j.jff.2016.05.005>
- Godínez-Mendoza, P. L., Rico-Chávez, A. K., Ferrusquía-Jimenez, N. I., Carbajal-Valenzuela, I. A., Villagómez-Aranda, A. L., Torres-Pacheco, I., & Guevara-González, R. G. (2023). Plant hormones: Revising of the concepts of biostimulation, elicitation and their application in a sustainable agricultural production. *Science of The Total Environment*, 894, 164883.
<https://doi.org/https://doi.org/10.1016/j.scitotenv.2023.164883>
- Gong, L., Xiao, Y., Xia, F., Wu, P., Zhao, T., Xie, S., Wang, R., Wen, Q., Zhou, W., Xu, H., Zhu, L., Zheng, Z., Yang, T., Chen, Z., & Duan, Q. (2019). The mevalonate coordinates energy input and cell proliferation. *Cell Death & Disease*, 10(4), 327.
<https://doi.org/10.1038/s41419-019-1544-y>
- Gryndler, M., Hřselová, H., Chvátalová, I., & Jansa, J. (1998). The effect of selected plant hormones on in vitro proliferation of hyphae of *Glomus fistulosum*. *Biologia Plantarum*, 41(2), 255–263. <https://doi.org/10.1023/A:1001874832669>
- Guenther, J. C., Hallen-Adams, H. E., Bücking, H., Shachar-Hill, Y., & Trail, F. (2009). Triacylglyceride Metabolism by *Fusarium graminearum* During Colonization and

- Sexual Development on Wheat. *Molecular Plant-Microbe Interactions*®, 22(12), 1492–1503. <https://doi.org/10.1094/MPMI-22-12-1492>
- Hamann, A., Osiewacz, H. D., & Teichert, I. (2022). *Sordaria macrospora* Sterile Mutant pro34 Is Impaired in Respiratory Complex I Assembly. *Journal of Fungi*, 8(10). <https://doi.org/10.3390/jof8101015>
- He, X., Wang, X., Fang, J., Chang, Y., Ning, N., Guo, H., Huang, L., Huang, X., & Zhao, Z. (2017). Structures, biological activities, and industrial applications of the polysaccharides from *Hericium erinaceus* (Lion's Mane) mushroom: A review. *International Journal of Biological Macromolecules*, 97, 228–237. <https://doi.org/https://doi.org/10.1016/j.ijbiomac.2017.01.040>
- Herbst, D. A., Esbin, M. N., Louder, R. K., Dugast-Darzacq, C., Dailey, G. M., Fang, Q., Darzacq, X., Tjian, R., & Nogales, E. (2021). Structure of the human SAGA coactivator complex. *Nature Structural & Molecular Biology*, 28(12), 989–996. <https://doi.org/10.1038/s41594-021-00682-7>
- Hinsch, J., Galuszka, P., & Tudzynski, P. (2016). Functional characterization of the first filamentous fungal tRNA-isopentenyltransferase and its role in the virulence of *Claviceps purpurea*. *New Phytologist*, 211(3), 980–992. <https://doi.org/https://doi.org/10.1111/nph.13960>
- Hinsch, J., Vrabka, J., Oeser, B., Novák, O., Galuszka, P., & Tudzynski, P. (2015). De novo biosynthesis of cytokinins in the biotrophic fungus *Claviceps purpurea*. *Environmental Microbiology*, 17(8), 2935–2951. <https://doi.org/https://doi.org/10.1111/1462-2920.12838>

- Hock, B., Bahn, M., Walk, R.-A., & Nitschke, U. (1978). The Control of Fruiting Body Formation in the Ascomycete *Sordaria macrospora* Auersw. by Regulation of Hyphal Development: An Analysis Based on Scanning Electron and Light Microscopic Observations. *Planta*, *141*(1), 93–103. <http://www.jstor.org/stable/23373480>
- Holk, R. U. P. andré, & Scherer, G. F. E. (1998). Fatty acids and lysophospholipids as potential second messengers in auxin action. Rapid activation of phospholipase A2 activity by auxin in suspension-cultured parsley and soybean cells. *The Plant Journal*, *16*(5), 601–611. <https://doi.org/https://doi.org/10.1046/j.1365-313x.1998.00333.x>
- Homrahud, D., Uraichuen, S., & Attathom, T. (2016). Cultivation of *Aschersonia placenta* Berkeley and Broom and its efficacy for controlling *Parlatoria ziziphi* (Lucas) (Hemiptera: Diaspididae). *Agriculture and Natural Resources*, *50*(3), 179–185. <https://doi.org/https://doi.org/10.1016/j.anres.2016.06.005>
- Janda, M., Planchais, S., Djafi, N., Martinec, J., Burketova, L., Valentova, O., Zachowski, A., & Ruelland, E. (2013). Phosphoglycerolipids are master players in plant hormone signal transduction. *Plant Cell Reports*, *32*(6), 839–851. <https://doi.org/10.1007/s00299-013-1399-0>
- Jones, D. E., Perez, L., & Ryan, R. O. (2020). 3-Methylglutaric acid in energy metabolism. *Clinica Chimica Acta*, *502*, 233–239. <https://doi.org/https://doi.org/10.1016/j.cca.2019.11.006>
- Kadlecová, A., Maková, B., Artal-Sanz, M., Strnad, M., & Voller, J. (2019). The plant hormone kinetin in disease therapy and healthy aging. *Ageing Research Reviews*, *55*, 100958. <https://doi.org/https://doi.org/10.1016/j.arr.2019.100958>

- Kasahara, H., Takei, K., Ueda, N., Hishiyama, S., Yamaya, T., Kamiya, Y., Yamaguchi, S., & Sakakibara, H. (2004). Distinct Isoprenoid Origins of cis- and trans-Zeatin Biosyntheses in Arabidopsis*. *Journal of Biological Chemistry*, 279(14), 14049–14054. <https://doi.org/10.1074/jbc.M314195200>
- Kessi-Pérez, E. I., González, A., Palacios, J. L., & Martínez, C. (2022). Yeast as a biological platform for vitamin D production: A promising alternative to help reduce vitamin D deficiency in humans. *Yeast*, 39(9), 482–492. <https://doi.org/10.1002/yea.3708>
- Kessner, D., Chambers, M., Burke, R., Agus, D., & Mallick, P. (2008). ProteoWizard: open source software for rapid proteomics tools development. *Bioinformatics*, 24(21), 2534–2536. <https://doi.org/10.1093/bioinformatics/btn323>
- Kim, Y.-H., Min, J., Bae, K.-D., Gu, M. B., & Lee, J. (2005). Biodegradation of dipropyl phthalate and toxicity of its degradation products: a comparison of *Fusarium oxysporum* f. sp. *pisi* cutinase and *Candida cylindracea* esterase. *Archives of Microbiology*, 184(1), 25–31. <https://doi.org/10.1007/s00203-005-0026-z>
- Kind, S., Hinsch, J., Vrabka, J., Hradilová, M., Majeská-Čudejková, M., Tudzynski, P., & Galuszka, P. (2018). Manipulation of cytokinin level in the ergot fungus *Claviceps purpurea* emphasizes its contribution to virulence. *Current Genetics*, 64(6), 1303–1319. <https://doi.org/10.1007/s00294-018-0847-3>
- Koivistoinen, O. M. (2013). *Catabolism of biomass-derived sugars in fungi and metabolic engineering as a tool for organic acid production*.
- Kojima, M., Kamada-Nobusada, T., Komatsu, H., Takei, K., Kuroha, T., Mizutani, M., Ashikari, M., Ueguchi-Tanaka, M., Matsuoka, M., Suzuki, K., & Sakakibara, H.

- (2009). Highly Sensitive and High-Throughput Analysis of Plant Hormones Using MS-Probe Modification and Liquid Chromatography–Tandem Mass Spectrometry: An Application for Hormone Profiling in *Oryza sativa*. *Plant and Cell Physiology*, 50(7), 1201–1214. <https://doi.org/10.1093/pcp/pcp057>
- Krzemińska, I., Szymańska, M., Ciempiel, W., & Piasecka, A. (2023). Auxin supplementation under nitrogen limitation enhanced oleic acid and MUFA content in *Eustigmatos calamaris* biomass with potential for biodiesel production. *Scientific Reports*, 13(1), 594. <https://doi.org/10.1038/s41598-023-27778-y>
- Kück, U., Pöggeler, S., Nowrousian, M., Nolting, N., & Engh, I. (2009). *Sordaria macrospora*, a Model System for Fungal Development. In T. Anke & D. Weber (Eds.), *Physiology and Genetics: Selected Basic and Applied Aspects* (pp. 17–39). Springer Berlin Heidelberg. https://doi.org/10.1007/978-3-642-00286-1_2
- Kulkarni, G. B., Sanjeevkumar, S., Kirankumar, B., Santoshkumar, M., & Karegoudar, T. B. (2013). Indole-3-Acetic Acid Biosynthesis in *Fusarium delphinoides* Strain GPK, a Causal Agent of Wilt in Chickpea. *Applied Biochemistry and Biotechnology*, 169(4), 1292–1305. <https://doi.org/10.1007/s12010-012-0037-6>
- Kumar, V., & Dwivedi, S. K. (2019). Hexavalent chromium reduction ability and bioremediation potential of *Aspergillus flavus* CR500 isolated from electroplating wastewater. *Chemosphere*, 237, 124567. <https://doi.org/https://doi.org/10.1016/j.chemosphere.2019.124567>
- Kunkel, B. N., & Harper, C. P. (2018). The roles of auxin during interactions between bacterial plant pathogens and their hosts. *Journal of Experimental Botany*, 69(2), 245–254. <https://doi.org/10.1093/jxb/erx447>

- LEE, B. O. (1961). Effect of Kinetin on the Fertility of some Strains of *Neurospora crassa*. *Nature*, *192*(4799), 288. <https://doi.org/10.1038/192288a0>
- Lelli, V., Belardo, A., & Timperio, A. M. (2021). From Targeted Quantification to Untargeted Metabolomics. In X. Zhan (Ed.), *Metabolomics* (p. Ch. 2). IntechOpen. <https://doi.org/10.5772/intechopen.96852>
- Leontovyčová, H., Trdá, L., Dobrev, P. I., Šašek, V., Gay, E., Balesdent, M.-H., & Burketová, L. (2020). Auxin biosynthesis in the phytopathogenic fungus *Leptosphaeria maculans* is associated with enhanced transcription of indole-3-pyruvate decarboxylase LmIPDC2 and tryptophan aminotransferase LmTAM1. *Research in Microbiology*, *171*(5), 174–184. <https://doi.org/https://doi.org/10.1016/j.resmic.2020.05.001>
- Lidoy, J., Berrio, E., García, M., España-Luque, L., Pozo, M. J., & López-Ráez, J. A. (2023). Flavonoids promote *Rhizophagus irregularis* spore germination and tomato root colonization: A target for sustainable agriculture. *Frontiers in Plant Science*, *13*. <https://doi.org/10.3389/fpls.2022.1094194>
- Lin, D.-L., Yao, H.-Y., Jia, L.-H., Tan, J.-F., Xu, Z.-H., Zheng, W.-M., & Xue, H.-W. (2020). Phospholipase D-derived phosphatidic acid promotes root hair development under phosphorus deficiency by suppressing vacuolar degradation of PIN-FORMED2. *New Phytologist*, *226*(1), 142–155. <https://doi.org/https://doi.org/10.1111/nph.16330>
- Liu, G., Zheng, X., Guan, H., Cao, Y., Qu, H., Kang, J., Ren, X., Lei, J., Dong, M.-Q., Li, X., & Li, H. (2019). Architecture of *Saccharomyces cerevisiae* SAGA complex. *Cell Discovery*, *5*(1), 25. <https://doi.org/10.1038/s41421-019-0094-x>

- Liu, Y.-Y., Chen, H.-W., & Chou, J.-Y. (2016). Variation in Indole-3-Acetic Acid Production by Wild *Saccharomyces cerevisiae* and *S. paradoxus* Strains from Diverse Ecological Sources and Its Effect on Growth. *PLOS ONE*, *11*(8), e0160524. <https://doi.org/10.1371/journal.pone.0160524>
- Ljungdahl, P. O., & Daignan-Fornier, B. (2012). Regulation of Amino Acid, Nucleotide, and Phosphate Metabolism in *Saccharomyces cerevisiae*. *Genetics*, *190*(3), 885–929. <https://doi.org/10.1534/genetics.111.133306>
- Lord, K. M., & Read, N. D. (2011). Perithecium morphogenesis in *Sordaria macrospora*. *Fungal Genetics and Biology*, *48*(4), 388–399. <https://doi.org/https://doi.org/10.1016/j.fgb.2010.11.009>
- Lozano-Juste, J., Masi, M., Cimmino, A., Clement, S., Fernández, M. A., Antoni, R., Meyer, S., Rodriguez, P. L., & Evidente, A. (2019). The fungal sesquiterpenoid pyrenophoric acid B uses the plant ABA biosynthetic pathway to inhibit seed germination. *Journal of Experimental Botany*, *70*(19), 5487–5494. <https://doi.org/10.1093/jxb/erz306>
- Lu, M., Flanagan, J. U., Langley, R. J., Hay, M. P., & Perry, J. K. (2019). Targeting growth hormone function: strategies and therapeutic applications. *Signal Transduction and Targeted Therapy*, *4*(1), 3. <https://doi.org/10.1038/s41392-019-0036-y>
- Lütkenhaus, R., Traeger, S., Breuer, J., Carreté, L., Kuo, A., Lipzen, A., Pangilinan, J., Dilworth, D., Sandor, L., Pöggeler, S., Gabaldón, T., Barry, K., Grigoriev, I. V., & Nowrousian, M. (2019). Comparative Genomics and Transcriptomics To Analyze Fruiting Body Development in Filamentous Ascomycetes. *Genetics*, *213*(4), 1545–1563. <https://doi.org/10.1534/genetics.119.302749>

- Maeda, T., Wakasawa, T., Shima, Y., Tsuboi, I., Aizawa, S., & Tamai, I. (2006). Role of Polyamines Derived from Arginine in Differentiation and Proliferation of Human Blood Cells. *Biological and Pharmaceutical Bulletin*, 29(2), 234–239. <https://doi.org/10.1248/bpb.29.234>
- Małkowski, E., Sitko, K., Szopiński, M., Gieroń, Ż., Pogrzeba, M., Kalaji, H. M., & Zieleźnik-Rusinowska, P. (2020). Hormesis in Plants: The Role of Oxidative Stress, Auxins and Photosynthesis in Corn Treated with Cd or Pb. *International Journal of Molecular Sciences*, 21(6). <https://doi.org/10.3390/ijms21062099>
- Malm, L., Palm, E., Souihi, A., Plassmann, M., Liigand, J., & Kruve, A. (2021). Guide to Semi-Quantitative Non-Targeted Screening Using LC/ESI/HRMS. *Molecules*, 26(12). <https://doi.org/10.3390/molecules26123524>
- Margulis, L., & Chapman, M. J. (2009). Chapter Four - KINGDOM FUNGI. In L. Margulis & M. J. Chapman (Eds.), *Kingdoms and Domains (Fourth Edition)* (pp. 379–409). Academic Press. <https://doi.org/https://doi.org/10.1016/B978-0-12-373621-5.00004-0>
- Markham, P., Robson, G. D., Bainbridge, B. W., & Trinci, A. P. J. (1993). Choline: Its role in the growth of filamentous fungi and the regulation of mycelial morphology. *FEMS Microbiology Reviews*, 10(3–4), 287–300. <https://doi.org/10.1111/j.1574-6968.1993.tb05872.x>
- Martínez-Medina, A., Del Mar Alguacil, M., Pascual, J. A., & Van Wees, S. C. M. (2014). Phytohormone Profiles Induced by Trichoderma Isolates Correspond with Their Biocontrol and Plant Growth-Promoting Activity on Melon Plants. *Journal of Chemical Ecology*, 40(7), 804–815. <https://doi.org/10.1007/s10886-014-0478-1>

- Masloff, S., Pöggeler, S., & Kück, U. (1999). The pro1+ Gene From *Sordaria macrospora* Encodes a C6 Zinc Finger Transcription Factor Required for Fruiting Body Development. *Genetics*, *152*(1), 191–199. <https://doi.org/10.1093/genetics/152.1.191>
- Meena, M., Prasad, V., Zehra, A., Gupta, V., & Upadhyay, R. (2015). Mannitol metabolism during pathogenic fungal–host interactions under stressed conditions. *Frontiers in Microbiology*, *6*. <https://www.frontiersin.org/articles/10.3389/fmicb.2015.01019>
- Mohanta, T. K. (2020). Fungi contain genes associated with flavonoid biosynthesis pathway. *Journal of Functional Foods*, *68*, 103910. <https://doi.org/10.1016/j.jff.2020.103910>
- Mollinedo, F. (2012). Lipid raft involvement in yeast cell growth and death. *Frontiers in Oncology*, *2*. <https://www.frontiersin.org/articles/10.3389/fonc.2012.00140>
- Morrison, E. N., Emery, R. J. N., & Saville, B. J. (2017). Fungal derived cytokinins are necessary for normal *Ustilago maydis* infection of maize. *Plant Pathology*, *66*(5), 726–742. <https://doi.org/https://doi.org/10.1111/ppa.12629>
- Morrison, E. N., Knowles, S., Hayward, A., Thorn, R. G., Saville, B. J., & Emery, R. J. N. (2015). Detection of phytohormones in temperate forest fungi predicts consistent abscisic acid production and a common pathway for cytokinin biosynthesis. *Mycologia*, *107*(2), 245–257. <https://doi.org/10.3852/14-157>
- Mousavi Basir Seyed and Sayfzadeh, S. and J. H. and V. A. S. and M. H. E. (2022). Effect of auxin foliar application on seed yield and fatty acids composition of two safflower genotypes under late-season drought. *Plant, Soil and Environment*, *68*(2), 82–88. <https://doi.org/10.17221/329/2021-PSE>

- Nagy, L. G., Vonk, P. J., Künzler, M., Földi, C., Virágh, M., Ohm, R. A., Hennicke, F., Bálint, B., Csernetics, Á., Hegedüs, B., Hou, Z., Liu, X.-B., Nan, S., Pareek, M., Sahu, N., Szathmári, B., Varga, T., Wu, H., Yang, X., & Merényi, Z. (2022). Lessons on fruiting body morphogenesis from genomes and transcriptomes of Agaricomycetes. *BioRxiv*, 2021.12.09.471732. <https://doi.org/10.1101/2021.12.09.471732>
- Nakamura, T., Kawanabe, Y., Takiyama, E., Takahashi, N., & Murayama, T. (1978). Effects of auxin and gibberellin on conidial germination in *Neurospora crassa*. *Plant and Cell Physiology*, 19(4), 705–709. <https://doi.org/10.1093/oxfordjournals.pcp.a075642>
- Nakatogawa, H. (2013). Two ubiquitin-like conjugation systems that mediate membrane formation during autophagy. *Essays in Biochemistry*, 55, 39–50. <https://doi.org/10.1042/bse0550039>
- Nanjundappa, A., Bagyaraj, D. J., Saxena, A. K., Kumar, M., & Chakdar, H. (2019). Interaction between arbuscular mycorrhizal fungi and *Bacillus* spp. in soil enhancing growth of crop plants. *Fungal Biology and Biotechnology*, 6(1), 23. <https://doi.org/10.1186/s40694-019-0086-5>
- Nasmin, G., & Rahman, M. (2009). CYTOKININ PRIMING AS A TOOL TO INDUCE IN VITRO GROWTH AND BIOMASS PRODUCTION OF SOME SOIL FUNGI. *Pakistan Journal of Botany*, 9.
- Nguyen, H. N., Nguyen, T. Q., Kisiala, A. B., & Emery, R. J. N. (2021). Beyond transport: cytokinin ribosides are translocated and active in regulating the development and environmental responses of plants. *Planta*, 254(3), 45. <https://doi.org/10.1007/s00425-021-03693-2>

- Niu, M., Steffan, B. N., Fischer, G. J., Venkatesh, N., Raffa, N. L., Wettstein, M. A., Bok, J. W., Greco, C., Zhao, C., Berthier, E., Oliw, E., Beebe, D., Bromley, M., & Keller, N. P. (2020). Fungal oxylipins direct programmed developmental switches in filamentous fungi. *Nature Communications*, *11*(1), 5158. <https://doi.org/10.1038/s41467-020-18999-0>
- Niwa, Y. S., & Niwa, R. (2014). Neural control of steroid hormone biosynthesis during development in the fruit fly *Drosophila melanogaster*. *Genes & Genetic Systems*, *89*(1), 27–34. <https://doi.org/10.1266/ggs.89.27>
- Nowrousian, M., Masloff, S., Pöggeler, S., & Kück, U. (1999a). Cell Differentiation during Sexual Development of the Fungus *Sordaria macrospora* Requires ATP Citrate Lyase Activity. *Molecular and Cellular Biology*, *19*(1), 450–460. <https://doi.org/10.1128/MCB.19.1.450>
- Nowrousian, M., Masloff, S., Pöggeler, S., & Kück, U. (1999b). Cell Differentiation during Sexual Development of the Fungus *Sordaria macrospora* Requires ATP Citrate Lyase Activity. *Molecular and Cellular Biology*, *19*(1), 450–460. <https://doi.org/10.1128/MCB.19.1.450>
- Oliw, E. H. (2021). Fatty acid dioxygenase-cytochrome P450 fusion enzymes of filamentous fungal pathogens. *Fungal Genetics and Biology*, *157*, 103623. <https://doi.org/https://doi.org/10.1016/j.fgb.2021.103623>
- Pal, P., Ansari, S. A., Jalil, S. U., & Ansari, M. I. (2023). Chapter 1 - Regulatory role of phytohormones in plant growth and development. In M. I. R. Khan, A. Singh, & P. Poór (Eds.), *Plant Hormones in Crop Improvement* (pp. 1–13). Academic Press. <https://doi.org/https://doi.org/10.1016/B978-0-323-91886-2.00016-1>

- Peraza Reyes, L., & Berteaux-Lecellier, V. (2013). Peroxisomes and sexual development in fungi. *Frontiers in Physiology*, 4. <https://www.frontiersin.org/articles/10.3389/fphys.2013.00244>
- Pfützner, A., Kubicek, C. P., & Röhr, M. (1987). Presence and regulation of ATP:citrate lyase from the citric acid producing fungus *Aspergillus niger*. *Archives of Microbiology*, 147(1), 88–91. <https://doi.org/10.1007/BF00492910>
- Phan, C.-W., Wang, J.-K., Cheah, S.-C., Naidu, M., David, P., & Sabaratnam, V. (2018). A review on the nucleic acid constituents in mushrooms: nucleobases, nucleosides and nucleotides. *Critical Reviews in Biotechnology*, 38(5), 762–777. <https://doi.org/10.1080/07388551.2017.1399102>
- Pöggeler, S., & Kück, U. (2004). A WD40 Repeat Protein Regulates Fungal Cell Differentiation and Can Be Replaced Functionally by the Mammalian Homologue Striatin. *Eukaryotic Cell*, 3(1), 232–240. <https://doi.org/10.1128/ec.3.1.232-240.2004>
- Pöggeler, S., Nowrousian, M., Jacobsen, S., & Kück, U. (1997). An efficient procedure to isolate fungal genes from an indexed cosmid library. *Journal of Microbiological Methods*, 29(1), 49–61. [https://doi.org/https://doi.org/10.1016/S0167-7012\(97\)00018-3](https://doi.org/https://doi.org/10.1016/S0167-7012(97)00018-3)
- Pollack, J. K., Harris, S. D., & Marten, M. R. (2009). Autophagy in filamentous fungi. *Fungal Genetics and Biology*, 46(1), 1–8. <https://doi.org/https://doi.org/10.1016/j.fgb.2008.10.010>
- Pons, S., Fournier, S., Chervin, C., Bécard, G., Rochange, S., Frei Dit Frey, N., & Puech Pagès, V. (2020). Phytohormone production by the arbuscular mycorrhizal fungus

- Rhizophagus irregularis. *PLOS ONE*, 15(10), e0240886-
<https://doi.org/10.1371/journal.pone.0240886>
- Rangasamy, D., & Ratledge, C. (2000). Compartmentation of ATP:Citrate Lyase in Plants 1. *Plant Physiology*, 122(4), 1225–1230. <https://doi.org/10.1104/pp.122.4.1225>
- Rao, R. P., Hunter, A., Kashpur, O., & Normanly, J. (2010). Aberrant Synthesis of Indole-3-Acetic Acid in *Saccharomyces cerevisiae* Triggers Morphogenic Transition, a Virulence Trait of Pathogenic Fungi. *Genetics*, 185(1), 211–220. <https://doi.org/10.1534/genetics.109.112854>
- REINEKE, G., HEINZE, B., SCHIRAWSKI, J. A. N., BUETTNER, H., KAHMANN, R., & BASSE, C. W. (2008). Indole-3-acetic acid (IAA) biosynthesis in the smut fungus *Ustilago maydis* and its relevance for increased IAA levels in infected tissue and host tumour formation. *Molecular Plant Pathology*, 9(3), 339–355. <https://doi.org/https://doi.org/10.1111/j.1364-3703.2008.00470.x>
- Reisdorph, N. A., Walmsley, S., & Reisdorph, R. (2020). A Perspective and Framework for Developing Sample Type Specific Databases for LC/MS-Based Clinical Metabolomics. *Metabolites*, 10(1). <https://doi.org/10.3390/metabo10010008>
- Reisz, J. A., Zheng, C., D'Alessandro, A., & Nemkov, T. (2019). Untargeted and Semi-targeted Lipid Analysis of Biological Samples Using Mass Spectrometry-Based Metabolomics. In A. D'Alessandro (Ed.), *High-Throughput Metabolomics: Methods and Protocols* (pp. 121–135). Springer New York. https://doi.org/10.1007/978-1-4939-9236-2_8
- Riquelme, M., Aguirre, J., Bartnicki-García, S., Braus, G. H., Feldbrügge, M., Fleig, U., Hansberg, W., Herrera-Estrella, A., Kämper, J., Kück, U., Mouriño-Pérez, R. R.,

- Takeshita, N., & Fischer, R. (2018). Fungal Morphogenesis, from the Polarized Growth of Hyphae to Complex Reproduction and Infection Structures. *Microbiology and Molecular Biology Reviews*, 82(2), 10.1128/membr.00068-17. <https://doi.org/10.1128/membr.00068-17>
- Roberts, L. D., Souza, A. L., Gerszten, R. E., & Clish, C. B. (2012). Targeted Metabolomics. *Current Protocols in Molecular Biology*, 98(1), 30.2.1-30.2.24. <https://doi.org/https://doi.org/10.1002/0471142727.mb3002s98>
- Roudier, F., Gissot, L., Beaudoin, F., Haslam, R., Michaelson, L., Marion, J., Molino, D., Lima, A., Bach, L., Morin, H., Tellier, F., Palauqui, J.-C., Bellec, Y., Renne, C., Miquel, M., DaCosta, M., Vignard, J., Rochat, C., Markham, J. E., ... Faure, J.-D. (2010). Very-Long-Chain Fatty Acids Are Involved in Polar Auxin Transport and Developmental Patterning in Arabidopsis . *The Plant Cell*, 22(2), 364–375. <https://doi.org/10.1105/tpc.109.071209>
- Rupali, G., Gautam, A., Lorena, P., Dana, L., Neta, K., Noa, S., Tal, Y., Ehud, G., & Maya, B. (2021). Cytokinin Inhibits Fungal Development and Virulence by Targeting the Cytoskeleton and Cellular Trafficking. *MBio*, 12(5), 10.1128/mbio.03068-20. <https://doi.org/10.1128/mbio.03068-20>
- Rush, T. A., Puech-Pagès, V., Bascaules, A., Jargeat, P., Maillet, F., Haouy, A., Maës, A. Q., Carriel, C. C., Khokhani, D., Keller-Pearson, M., Tannous, J., Cope, K. R., Garcia, K., Maeda, J., Johnson, C., Kleven, B., Choudhury, Q. J., Labbé, J., Swift, C., ... Ané, J.-M. (2020). Lipo-chitoooligosaccharides as regulatory signals of fungal growth and development. *Nature Communications*, 11(1), 3897. <https://doi.org/10.1038/s41467-020-17615-5>

- Saini, R. K., Prasad, P., Shang, X., & Keum, Y.-S. (2021). Advances in Lipid Extraction Methods—A Review. *International Journal of Molecular Sciences*, 22(24).
<https://doi.org/10.3390/ijms222413643>
- Sakakibara, H. (2006). CYTOKININS: Activity, Biosynthesis, and Translocation. *Annual Review of Plant Biology*, 57(1), 431–449.
<https://doi.org/10.1146/annurev.arplant.57.032905.105231>
- Sakamoto, N., Tsuyuki, R., Yoshinari, T., Usuma, J., Furukawa, T., Nagasawa, H., & Sakuda, S. (2013). Correlation of ATP Citrate Lyase and Acetyl CoA Levels with Trichothecene Production in *Fusarium graminearum*. *Toxins*, 5(11), 2258–2269.
<https://doi.org/10.3390/toxins5112258>
- Savidov, N., Glorizova, T. A., Poroikov, V. V., & Dembitsky, V. M. (2018). Highly oxygenated isoprenoid lipids derived from fungi and fungal endophytes: Origin and biological activities. *Steroids*, 140, 114–124.
<https://doi.org/https://doi.org/10.1016/j.steroids.2018.10.006>
- Schapira, M., Tyers, M., Torrent, M., & Arrowsmith, C. H. (2017). WD40 repeat domain proteins: a novel target class? *Nature Reviews Drug Discovery*, 16(11), 773–786.
<https://doi.org/10.1038/nrd.2017.179>
- Schimpf, U., & Schulz, R. (2016). Industrial by-products from white-rot fungi production. Part I: Generation of enzyme preparations and chemical, protein biochemical and molecular biological characterization. *Process Biochemistry*, 51(12), 2034–2046.
<https://doi.org/https://doi.org/10.1016/j.procbio.2016.08.032>
- Schmid, R., Heuckeroth, S., Korf, A., Smirnov, A., Myers, O., Dyrland, T. S., Bushuiev, R., Murray, K. J., Hoffmann, N., Lu, M., Sarvepalli, A., Zhang, Z., Fleischauer, M.,

- Dührkop, K., Wesner, M., Hoogstra, S. J., Rudt, E., Mokshyna, O., Brungs, C., ... Pluskal, T. (2023). Integrative analysis of multimodal mass spectrometry data in MZmine 3. *Nature Biotechnology*, *41*(4), 447–449. <https://doi.org/10.1038/s41587-023-01690-2>
- Schoor, S., Farrow, S., Blaschke, H., Lee, S., Perry, G., von Schwartzberg, K., Emery, N., & Moffatt, B. (2011). Adenosine Kinase Contributes to Cytokinin Interconversion in *Arabidopsis*. *Plant Physiology*, *157*(2), 659–672. <https://doi.org/10.1104/pp.111.181560>
- Sejdiu, B. I., & Tieleman, D. P. (2020). Lipid-Protein Interactions Are a Unique Property and Defining Feature of G Protein-Coupled Receptors. *Biophysical Journal*, *118*(8), 1887–1900. <https://doi.org/10.1016/j.bpj.2020.03.008>
- SEVINDIK, M. (2020). Antioxidant and antimicrobial capacity of *Lactifluus rugatus* and its antiproliferative activity on A549 cells. *Indian Journal of Traditional Knowledge*, *19*(2). <https://doi.org/10.56042/ijtk.v19i2.35356>
- Sheldrake, M. (2020). *Entangled life: How fungi make our worlds, change our minds and shape our futures*. Random House.
- Sherry, E. B., Lee, P., & Choi, I.-Y. (2015). In Vivo NMR Studies of the Brain with Hereditary or Acquired Metabolic Disorders. *Neurochemical Research*, *40*(12), 2647–2685. <https://doi.org/10.1007/s11064-015-1772-1>
- Sivaramakrishnan, R., & Incharoensakdi, A. (2020). Plant hormone induced enrichment of *Chlorella* sp. omega-3 fatty acids. *Biotechnology for Biofuels*, *13*(1), 7. <https://doi.org/10.1186/s13068-019-1647-9>

- Spiess, G. M., & Zolman, B. K. (2013). Peroxisomes as a Source of Auxin Signaling Molecules. In L. A. del Río (Ed.), *Peroxisomes and their Key Role in Cellular Signaling and Metabolism* (pp. 257–281). Springer Netherlands. https://doi.org/10.1007/978-94-007-6889-5_14
- Steffens, E. K., Becker, K., Krevet, S., Teichert, I., & Kück, U. (2016). Transcription factor PRO1 targets genes encoding conserved components of fungal developmental signaling pathways. *Molecular Microbiology*, *102*(5), 792–809. <https://doi.org/https://doi.org/10.1111/mmi.13491>
- Sugimoto, K., Allmann, S., & Kolomiets, M. V. (2022). Editorial: Oxylipins: The Front Line of Plant Interactions. *Frontiers in Plant Science*, *13*. <https://doi.org/10.3389/fpls.2022.878765>
- Takpho, N., Watanabe, D., & Takagi, H. (2018). Valine biosynthesis in *Saccharomyces cerevisiae* is regulated by the mitochondrial branched-chain amino acid aminotransferase Bat1. *Microbial Cell*, *5*(6), 293–299. <https://doi.org/10.15698/mic2018.06.637>
- Tao, L., Zhang, Y., Fan, S., Nobile, C. J., Guan, G., & Huang, G. (2017). Integration of the tricarboxylic acid (TCA) cycle with cAMP signaling and Sfl2 pathways in the regulation of CO₂ sensing and hyphal development in *Candida albicans*. *PLOS Genetics*, *13*(8), e1006949-. <https://doi.org/10.1371/journal.pgen.1006949>
- Teichert, I., Pöggeler, S., & Nowrousian, M. (2020). *Sordaria macrospora*: 25 years as a model organism for studying the molecular mechanisms of fruiting body development. *Applied Microbiology and Biotechnology*, *104*(9), 3691–3704. <https://doi.org/10.1007/s00253-020-10504-3>

- Tomita, K., Murayama, T., & Nakamura, T. (1984). Effects of Auxin and Gibberellin on Elongation of Young Hyphae in *Neurospora crassa*. *Plant and Cell Physiology*, *25*(2), 355–358. <https://doi.org/10.1093/oxfordjournals.pcp.a076722>
- Tran, L. P., & Pal, S. (2014). *Phytohormones: A Window to Metabolism, Signaling and Biotechnological Applications*. Springer: New York.
- Trdá, L., Barešová, M., Šašek, V., Nováková, M., Zahajská, L., Dobrev, P. I., Motyka, V., & Burketová, L. (2017). Cytokinin Metabolism of Pathogenic Fungus *Leptosphaeria maculans* Involves Isopentenyltransferase, Adenosine Kinase and Cytokinin Oxidase/Dehydrogenase. *Frontiers in Microbiology*, *8*. <https://www.frontiersin.org/articles/10.3389/fmicb.2017.01374>
- Tsavkelova, E., Oeser, B., Oren-Young, L., Israeli, M., Sasson, Y., Tudzynski, B., & Sharon, A. (2012). Identification and functional characterization of indole-3-acetamide-mediated IAA biosynthesis in plant-associated *Fusarium* species. *Fungal Genetics and Biology*, *49*(1), 48–57. <https://doi.org/https://doi.org/10.1016/j.fgb.2011.10.005>
- Verschueren, K. H. G., Blanchet, C., Felix, J., Dansercoer, A., De Vos, D., Bloch, Y., Van Beeumen, J., Svergun, D., Gutsche, I., Savvides, S. N., & Verstraete, K. (2019). Structure of ATP citrate lyase and the origin of citrate synthase in the Krebs cycle. *Nature*, *568*(7753), 571–575. <https://doi.org/10.1038/s41586-019-1095-5>
- Vetter, J. (2023). The Mushroom Glucans: Molecules of High Biological and Medicinal Importance. *Foods*, *12*(5). <https://doi.org/10.3390/foods12051009>
- Voglmayr, H., Mayer, V., Maschwitz, U., Moog, J., Djieto-Lordon, C., & Blatrix, R. (2011). The diversity of ant-associated black yeasts: insights into a newly discovered world

- of symbiotic interactions. *Fungal Biology*, 115(10), 1077–1091.
<https://doi.org/https://doi.org/10.1016/j.funbio.2010.11.006>
- Voigt, O., & Pöggeler, S. (2013). Autophagy genes *Smatg8* and *Smatg4* are required for fruiting-body development, vegetative growth and ascospore germination in the filamentous ascomycete *Sordaria macrospora*. *Autophagy*, 9(1), 33–49.
<https://doi.org/10.4161/auto.22398>
- Wang, J., Kambhampati, S., Allen, D. K., & Chen, L.-Q. (2022). Comparative Metabolic Analysis Reveals a Metabolic Switch in Mature, Hydrated, and Germinated Pollen in *Arabidopsis thaliana*. *Frontiers in Plant Science*, 13.
<https://www.frontiersin.org/articles/10.3389/fpls.2022.836665>
- Wang, J., Su, Y., Kong, X., Ding, Z., & Zhang, X. S. (2020). Initiation and maintenance of plant stem cells in root and shoot apical meristems. *ABIOTECH*, 1(3), 194–204.
<https://doi.org/10.1007/s42994-020-00020-3>
- Wang, J., Wang, S., Zhang, Z., Hao, Z., Shi, X., Li, L., Zhu, X., Qiu, H., Chai, R., Wang, Y., Li, L., Liu, X., Feng, X., Sun, G., & Lin, F. (2021). MAT Loci Play Crucial Roles in Sexual Development but Are Dispensable for Asexual Reproduction and Pathogenicity in Rice Blast Fungus *Magnaporthe oryzae*. *Journal of Fungi*, 7(10).
<https://doi.org/10.3390/jof7100858>
- Wang, L., Chen, W., Feng, Y., Ren, Y., Gu, Z., Chen, H., Wang, H., Thomas, M. J., Zhang, B., Berquin, I. M., Li, Y., Wu, J., Zhang, H., Song, Y., Liu, X., Norris, J. S., Wang, S., Du, P., Shen, J., ... Chen, Y. Q. (2011). Genome Characterization of the Oleaginous Fungus *Mortierella alpina*. *PLOS ONE*, 6(12), e28319-
<https://doi.org/10.1371/journal.pone.0028319>

- Wang, P., Shen, L., Guo, J., Jing, W., Qu, Y., Li, W., Bi, R., Xuan, W., Zhang, Q., & Zhang, W. (2019). Phosphatidic Acid Directly Regulates PINOID-Dependent Phosphorylation and Activation of the PIN-FORMED2 Auxin Efflux Transporter in Response to Salt Stress. *The Plant Cell*, *31*(1), 250–271. <https://doi.org/10.1105/tpc.18.00528>
- Wang, Y., Ma, R., Li, S., Gong, M., Yao, B., Bai, Y., & Gu, J. (2018). An alkaline and surfactant-tolerant lipase from *Trichoderma lentiforme* ACCC30425 with high application potential in the detergent industry. *AMB Express*, *8*(1), 95. <https://doi.org/10.1186/s13568-018-0618-z>
- Want, E. J. (2018). LC-MS Untargeted Analysis. In G. A. Theodoridis, H. G. Gika, & I. D. Wilson (Eds.), *Metabolic Profiling: Methods and Protocols* (pp. 99–116). Springer New York. https://doi.org/10.1007/978-1-4939-7643-0_7
- Weete, J. D., Abril, M., & Blackwell, M. (2010). Phylogenetic Distribution of Fungal Sterols. *PLOS ONE*, *5*(5), e10899-. <https://doi.org/10.1371/journal.pone.0010899>
- Wen, Z., Liao, W., & Chen, S. (2005). Production of cellulase/ β -glucosidase by the mixed fungi culture *Trichoderma reesei* and *Aspergillus phoenicis* on dairy manure. *Process Biochemistry*, *40*(9), 3087–3094. <https://doi.org/https://doi.org/10.1016/j.procbio.2005.03.044>
- Westergaard, M., & Mitchell, H. K. (1947). NEUROSPORA V. A SYNTHETIC MEDIUM FAVORING SEXUAL REPRODUCTION. *American Journal of Botany*, *34*(10), 573–577. <https://doi.org/https://doi.org/10.1002/j.1537-2197.1947.tb13032.x>

- Wu, W., Du, K., Kang, X., & Wei, H. (2021). The diverse roles of cytokinins in regulating leaf development. *Horticulture Research*, 8(1), 118. <https://doi.org/10.1038/s41438-021-00558-3>
- Xiao-Hong, L., Jian-Ping, L., Lei, Z., Bo, D., Hang, M., & Fu-Cheng, L. (2007). Involvement of a Magnaporthe grisea Serine/Threonine Kinase Gene, MgATG1, in Appressorium Turgor and Pathogenesis. *Eukaryotic Cell*, 6(6), 997–1005. <https://doi.org/10.1128/ec.00011-07>
- Xie, M. (2019). Phospholipids. In L. Melton, F. Shahidi, & P. Varelis (Eds.), *Encyclopedia of Food Chemistry* (pp. 214–217). Academic Press. <https://doi.org/https://doi.org/10.1016/B978-0-08-100596-5.21597-7>
- Xu, J., Audenaert, K., Hofte, M., & De Vleeschauwer, D. (2013). Abscisic Acid Promotes Susceptibility to the Rice Leaf Blight Pathogen Xanthomonas oryzae pv oryzae by Suppressing Salicylic Acid-Mediated Defenses. *PLOS ONE*, 8(6), e67413-. <https://doi.org/10.1371/journal.pone.0067413>
- Xue, A. G., Guo, W., Chen, Y., Siddiqui, I., Marchand, G., Liu, J., & Ren, C. (2017). Effect of seed treatment with novel strains of Trichoderma spp. on establishment and yield of spring wheat. *Crop Protection*, 96, 97–102. <https://doi.org/https://doi.org/10.1016/j.cropro.2017.02.003>
- Yang, T., Li, H., Tai, Y., Dong, C., Cheng, X., Xia, E., Chen, Z., Li, F., Wan, X., & Zhang, Z. (2020). Transcriptional regulation of amino acid metabolism in response to nitrogen deficiency and nitrogen forms in tea plant root (Camellia sinensis L.). *Scientific Reports*, 10(1), 6868. <https://doi.org/10.1038/s41598-020-63835-6>

- Yasmin, S., Alcazar-Fuoli, L., Gründlinger, M., Puempel, T., Cairns, T., Blatzer, M., Lopez, J. F., Grimalt, J. O., Bignell, E., & Haas, H. (2012). Mevalonate governs interdependency of ergosterol and siderophore biosyntheses in the fungal pathogen *Aspergillus fumigatus*. *Proceedings of the National Academy of Sciences*, *109*(8), E497–E504. <https://doi.org/10.1073/pnas.1106399108>
- Zhang, K., Zhang, B., & Yang, S.-T. (2013). Production of Citric, Itaconic, Fumaric, and Malic Acids in Filamentous Fungal Fermentations. In *Bioprocessing Technologies in Biorefinery for Sustainable Production of Fuels, Chemicals, and Polymers* (pp. 375–398). <https://doi.org/https://doi.org/10.1002/9781118642047.ch20>
- Zhang, S., Wakai, S., Sasakura, N., Tsutsumi, H., Hata, Y., Ogino, C., & Kondo, A. (2020). Pyruvate metabolism redirection for biological production of commodity chemicals in aerobic fungus *Aspergillus oryzae*. *Metabolic Engineering*, *61*, 225–237. <https://doi.org/https://doi.org/10.1016/j.ymben.2020.06.010>
- Zhang, W., Zhang, X., Feng, D., Liang, Y., Wu, Z., Du, S., Zhou, Y., Geng, C., Men, P., Fu, C., Huang, X., & Lu, X. (2023). Discovery of a Unique Flavonoid Biosynthesis Mechanism in Fungi by Genome Mining. *Angewandte Chemie*, *135*(12). <https://doi.org/10.1002/ange.202215529>
- Zhang, X., Chen, Y., Lin, X., Hong, X., Zhu, Y., Li, W., He, W., An, F., & Guo, H. (2013). Adenine Phosphoribosyl Transferase 1 is a Key Enzyme Catalyzing Cytokinin Conversion from Nucleobases to Nucleotides in Arabidopsis. *Molecular Plant*, *6*(5), 1661–1672. <https://doi.org/https://doi.org/10.1093/mp/sst071>
- Zhao, B., Liu, Q., Wang, B., & Yuan, F. (2021). Roles of Phytohormones and Their Signaling Pathways in Leaf Development and Stress Responses. *Journal of*

Agricultural and Food Chemistry, 69(12), 3566–3584.

<https://doi.org/10.1021/acs.jafc.0c07908>

Zhou, Q., Yu, L., Ying, S.-H., & Feng, M.-G. (2021). Comparative roles of three adhesin genes (*adh1–3*) in insect-pathogenic lifecycle of *Beauveria bassiana*. *Applied Microbiology and Biotechnology*, 105(13), 5491–5502.

<https://doi.org/10.1007/s00253-021-11420-w>

Zied, D. C., Dourado, F. A., Dias, E. S., & Pardo-Giménez, A. (2017). First study of hormesis effect on mushroom cultivation. *World Journal of Microbiology and Biotechnology*, 33(11), 195. <https://doi.org/10.1007/s11274-017-2342-2>

APPENDIX I

Supplementary data Overview

Figures S1 to S21 showcase the image results for "**Chapter 2. The Metabolome of *Sordaria macrospora*,**" providing confirmation of the developmental stages in both the wild type and mutants (spt3, smatg4, pro1, pro11, per5, smgpi1). To achieve these results, the strains were cultivated in *Sordaria macrospora* minimal media (SMM) as detailed in the "Materials and Methods" section. The images were captured using an inverted microscope.

Figures S22 and S 23 showcase the statistical analysis for lipidomic of *S. macrospora* between stage 2 and stage 3 (Figure S22) and between the wild type and per 5 in stage 3 (Figure S23).

Finally, a folder zip containing the images for Chapter 3- "The effects of cytokinins on *S. macrospora* growth and development", the folder "experiment 1" contains the inverted microscope images after 8 days of growing *S. macrospora* in SMM supplemented with cis-Zeatin (cZ) and Kinetin Riboside (KR) 0.1 μ M applied at the beginning of *S. macrospora* life cycle. The folder "experiment 2" contains the inverted microscope images after 8 days of growing *S. macrospora* in SMM supplemented with cZ, KR, isopentyl-adenine (iP), and IP riboside (iPR) from 0.01 to 100 μ M applied at the ascospore-genesis stage of *S. macrospora* life cycle, and the control group images.

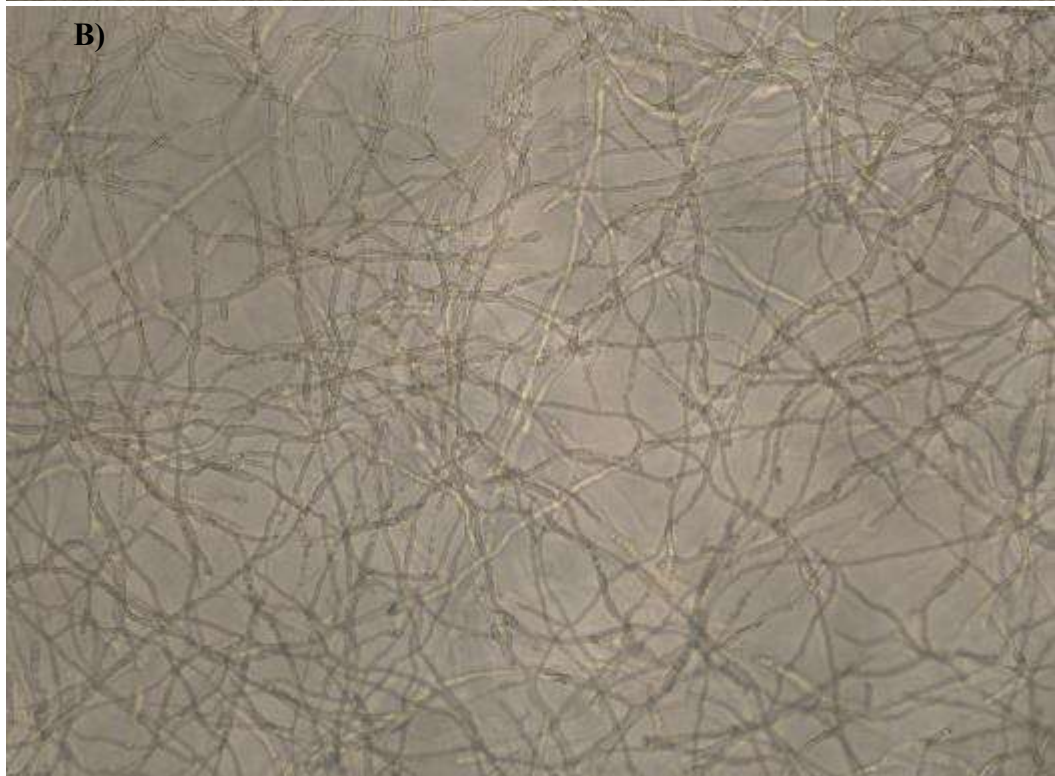
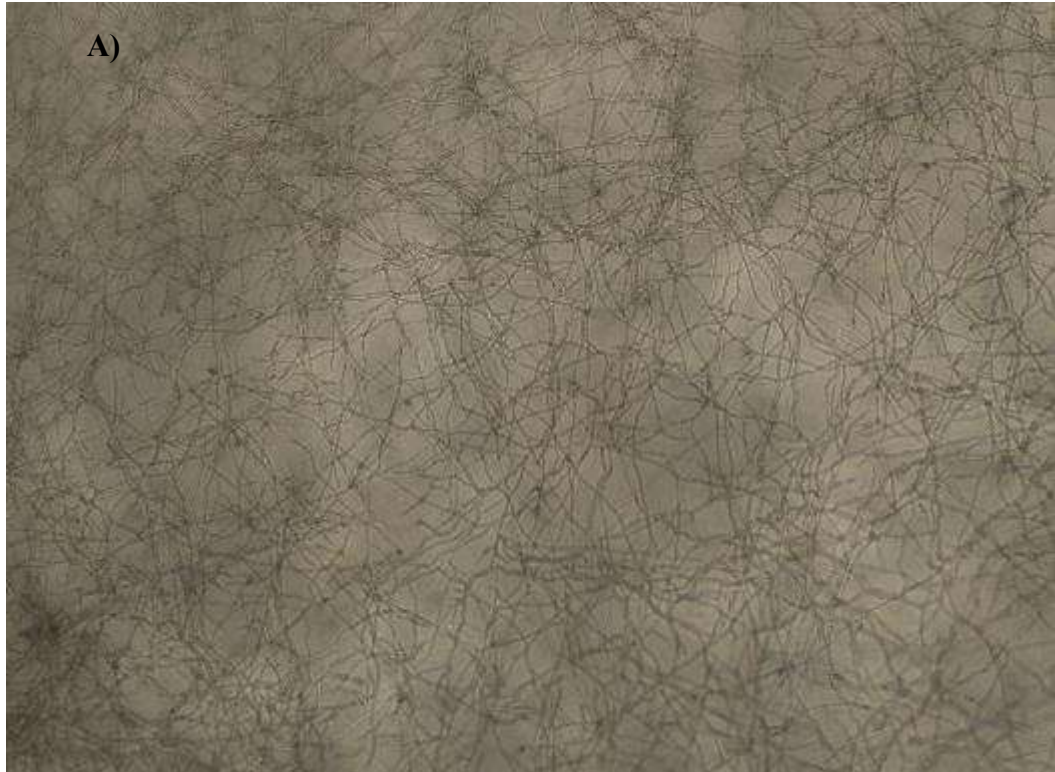


Figure S1. *Sordaria macrospora spt3* at day 2, stage 1. Growth in SMM media, inverted microscope at A) 10X and B) 40X magnitude.

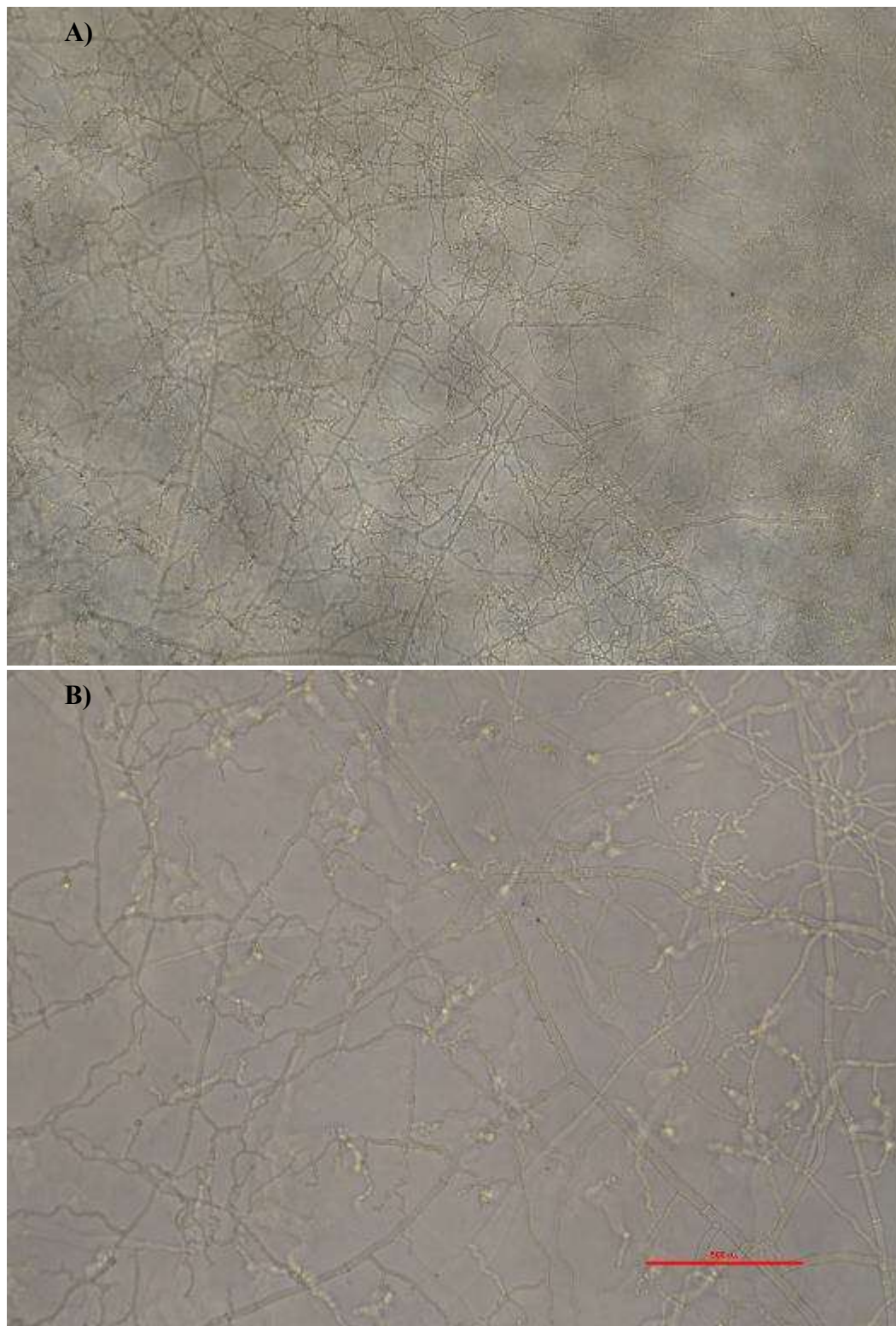


Figure S2. *Sordaria macrospora smatg4* at day 2, stage 1. Growth in SMM media, inverted microscope at A) 10X and B) 40X magnitude.



Figure S3. *Sordaria macrospora pro1* at day 2, stage 1. Growth in SMM media, inverted microscope at A) 10X and B) 40X magnitude.

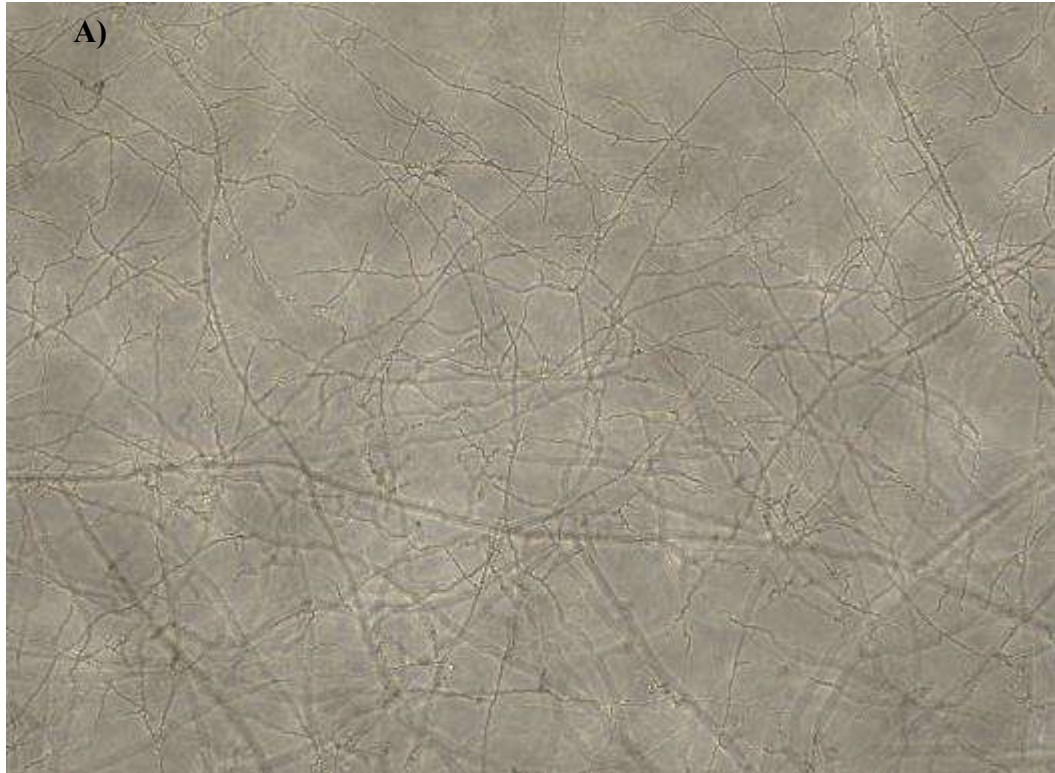


Figure S4. *Sordaria macrospora pro11* at day 2, stage 1. Growth in SMM media, inverted microscope at A) 10X and B) 40X magnitude.

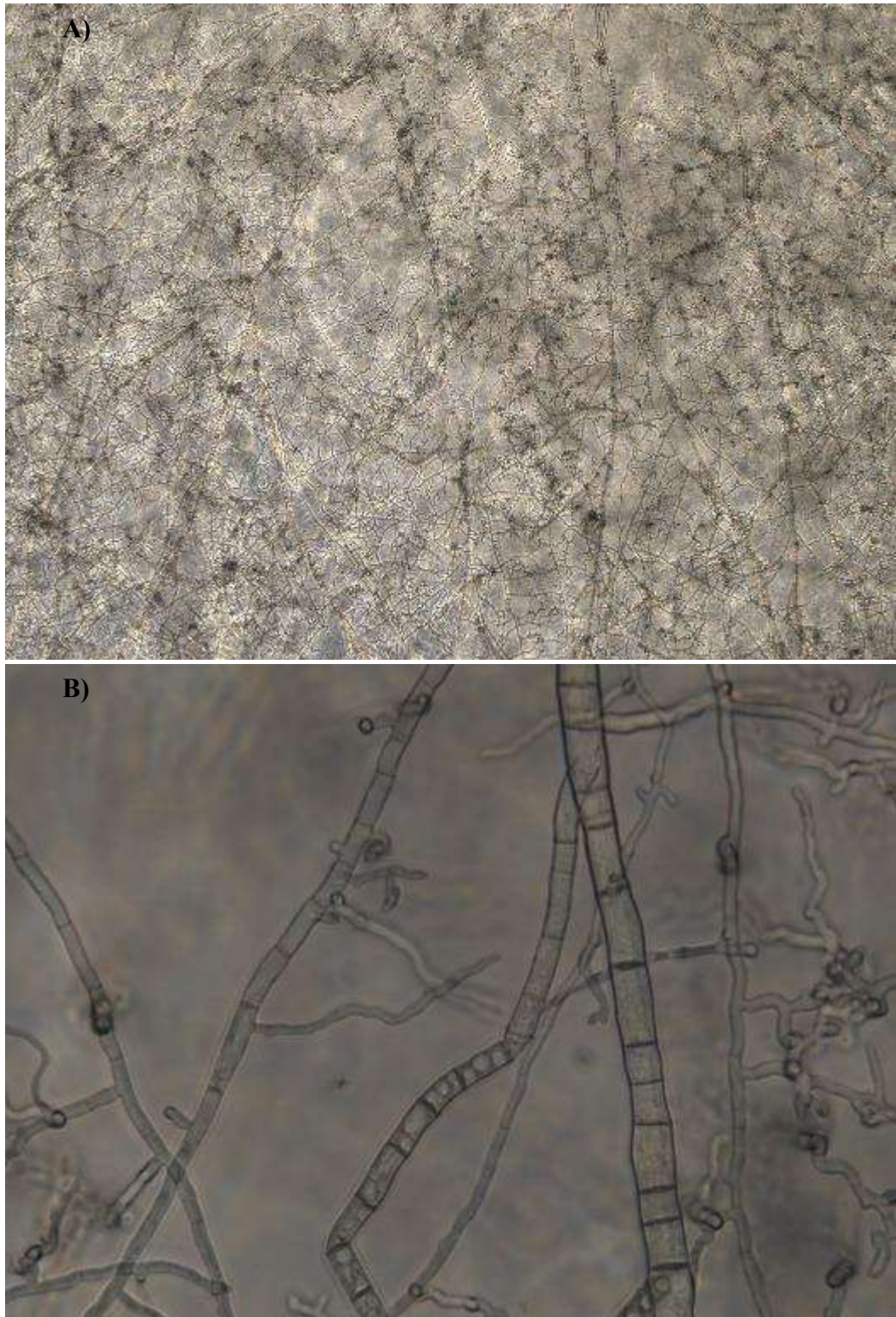


Figure S5. *Sordaria macrospora per5* at day 2, stage 1. Growth in SMM media, inverted microscope at A) 10X and B) 40X magnitude.

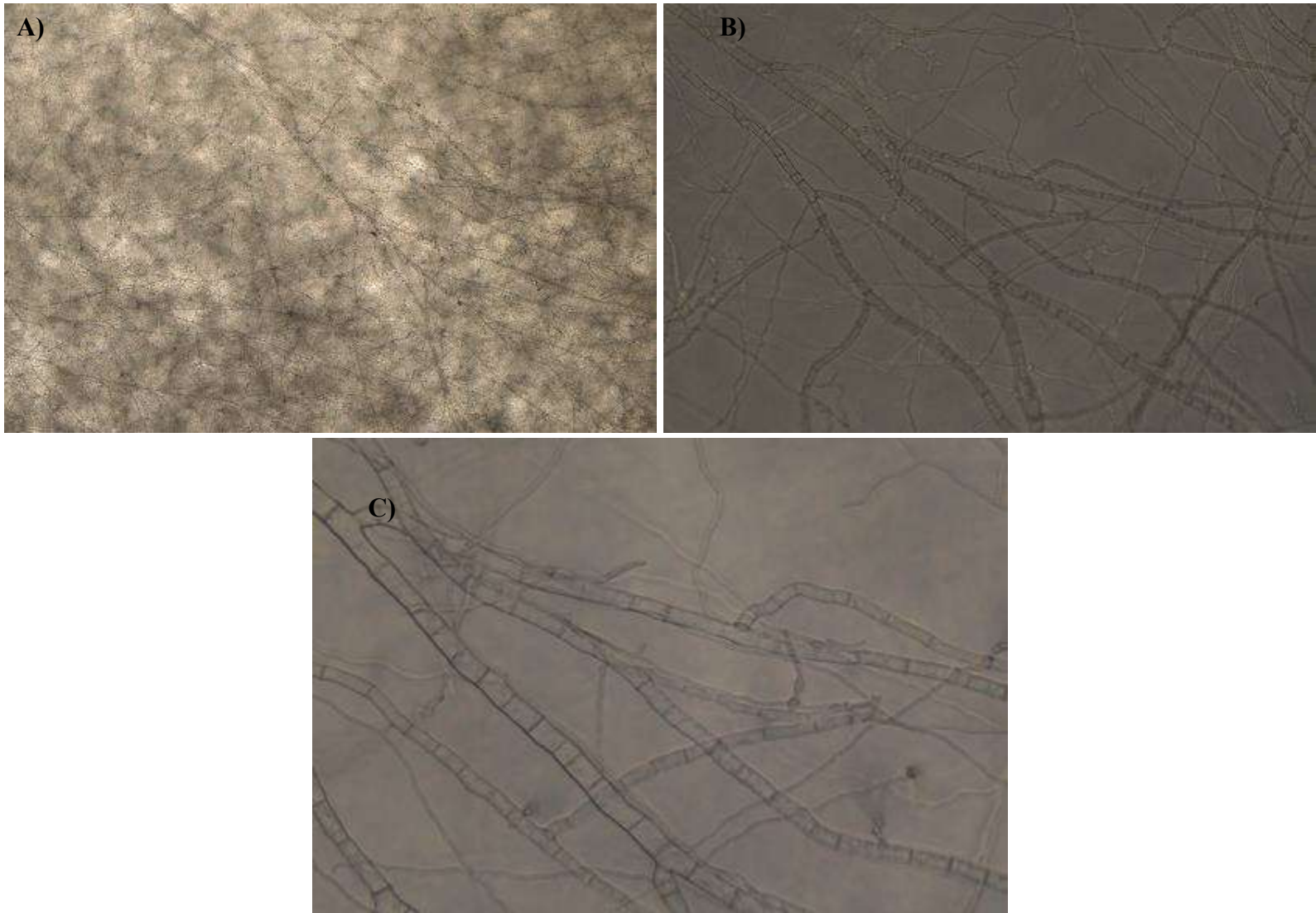


Figure S6. *Sordaria macrospora smgpi1* at day 2, stage 1. Growth in SMM media, inverted microscope at A) 10X, B) 30X, and C) 40X magnification

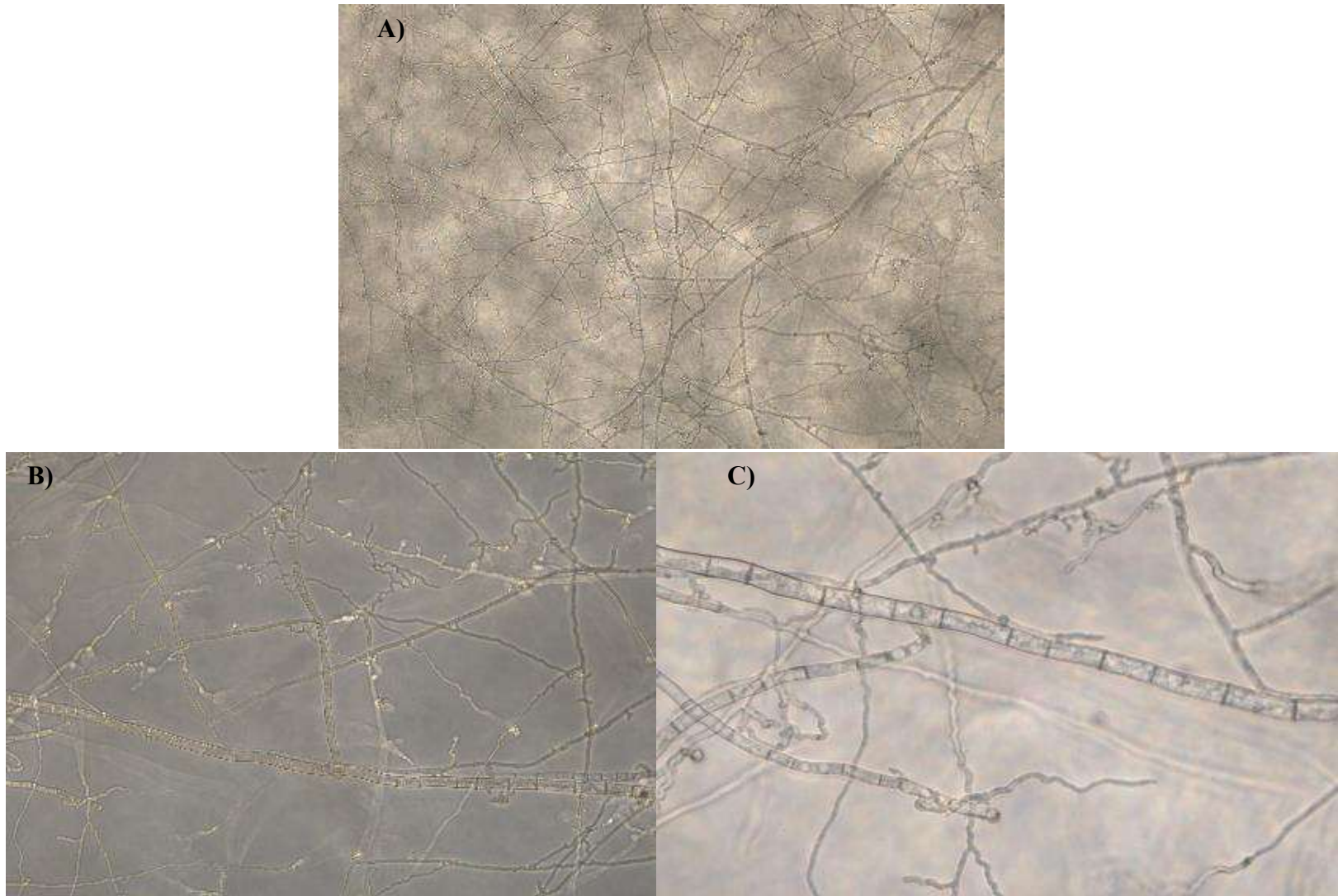


Figure S7. *Sordaria macrospora* WT at day 2, stage 1. Growth in SMM media, inverted microscope at A) 10X, B) 30X, and C) 40X magnification.

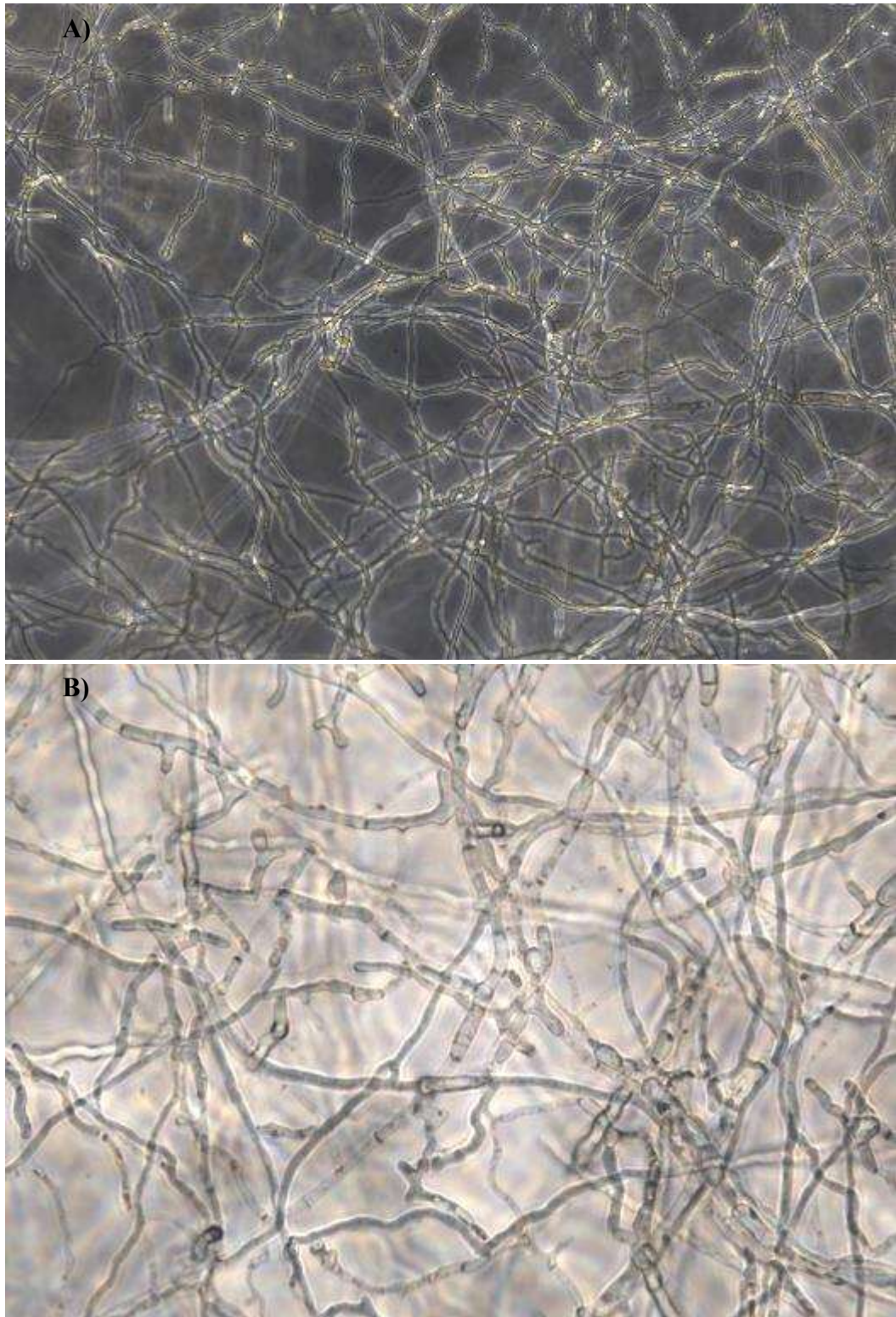


Figure S8. *Sordaria macrospora spt3* at day 4, stage 2. Growth in SMM media, inverted microscope at A) 10X and C) 40X magnitude.

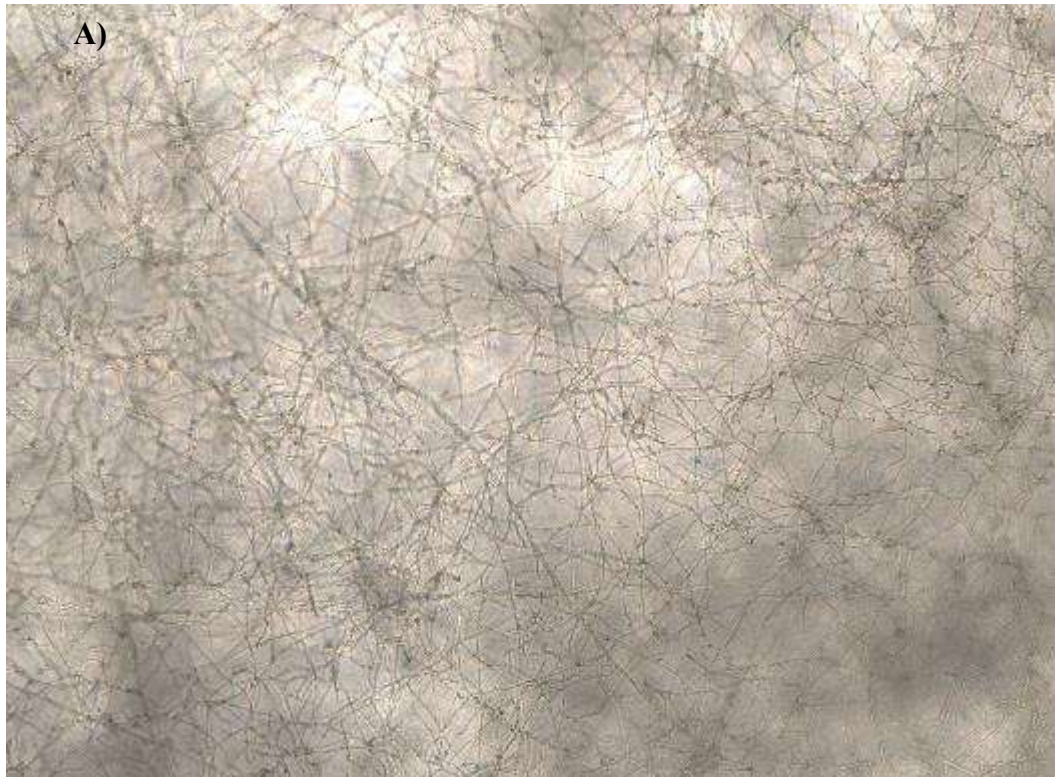


Figure S9. *Sordaria macrospora smatg4* at day 4, stage 2. Growth in SMM media, inverted microscope at A) 10X and C) 40X magnitude

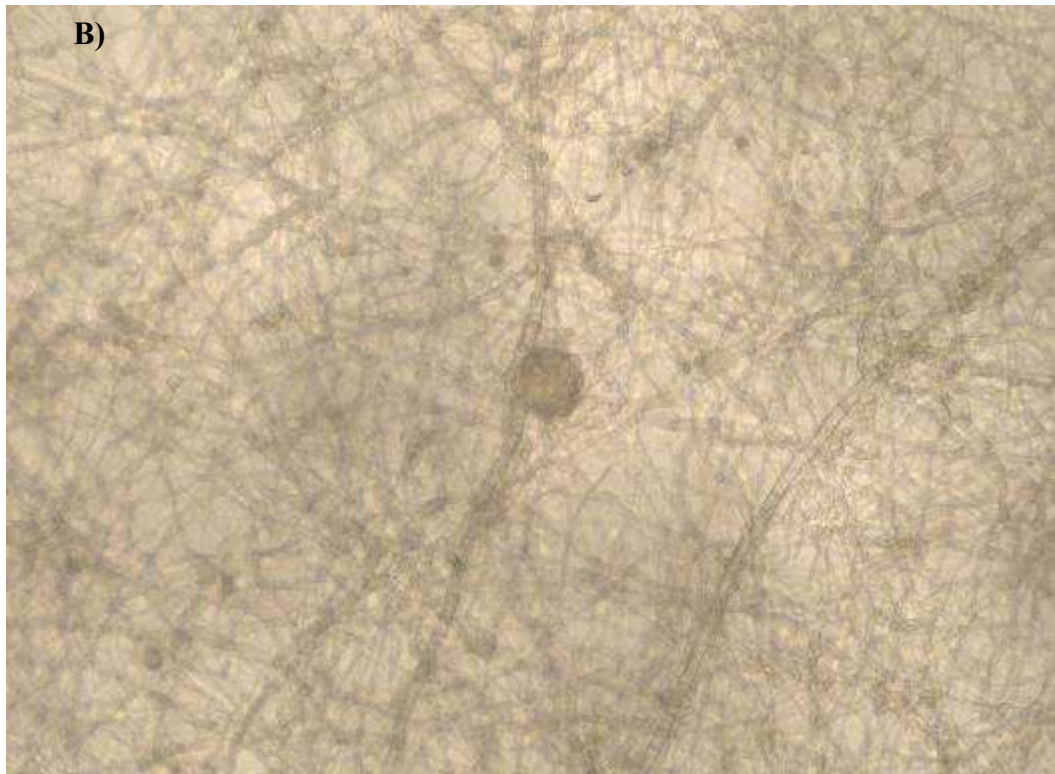
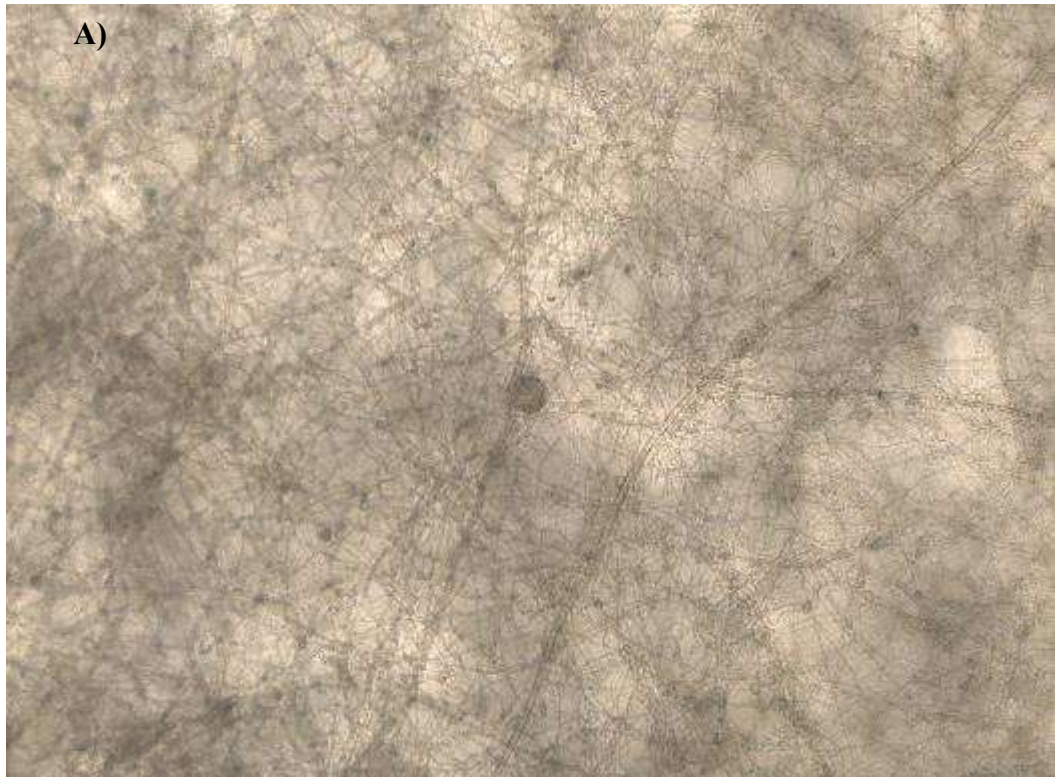


Figure S10. *Sordaria macrospora pro1* at day 4, stage 2. Growth in SMM media, inverted microscope at A) 10X and C) 20X magnitude

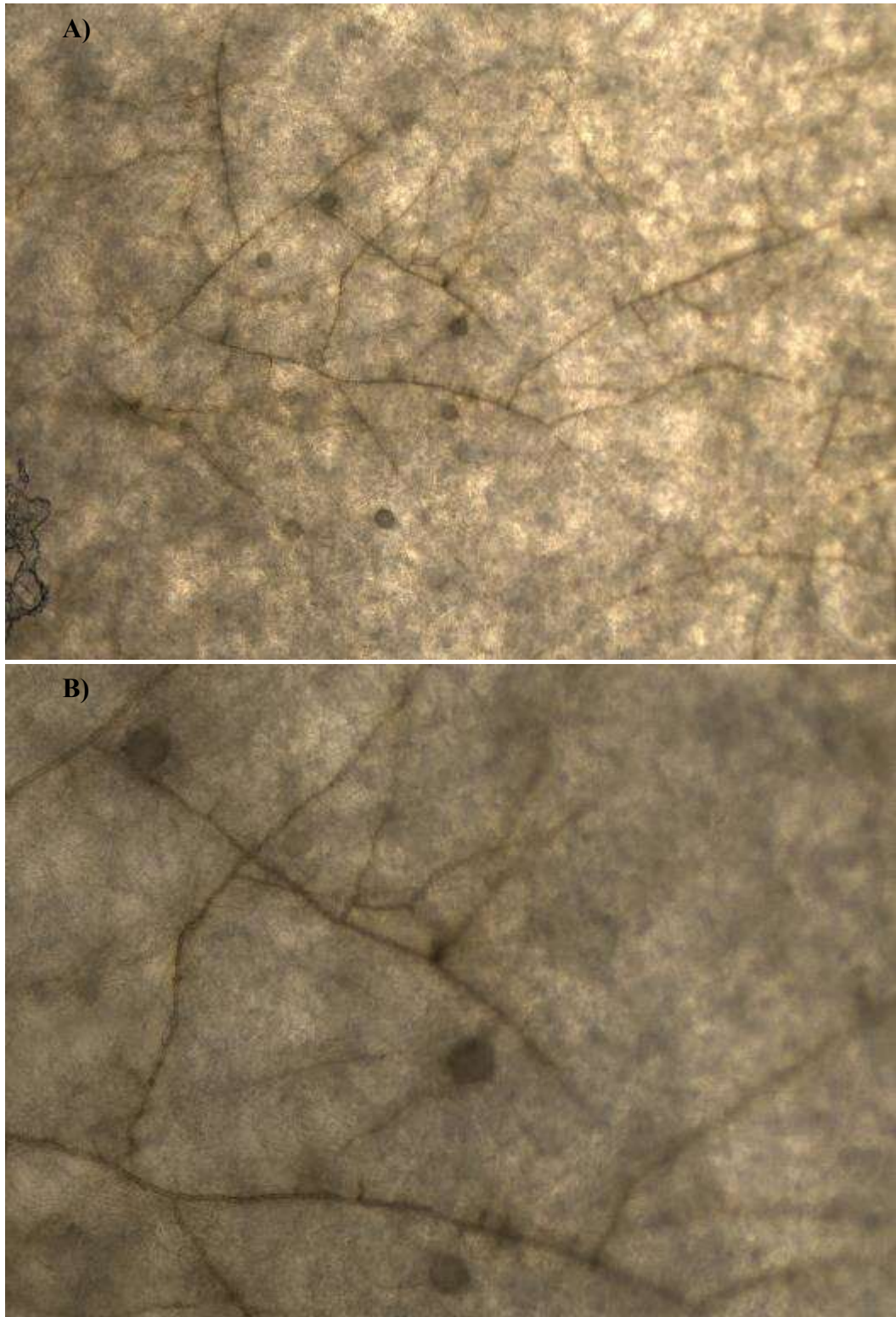


Figure S11. *Sordaria macrospora pro11* at day 4, stage 2. Growth in SMM media, inverted microscope at A) 10X and C) 20X magnitude

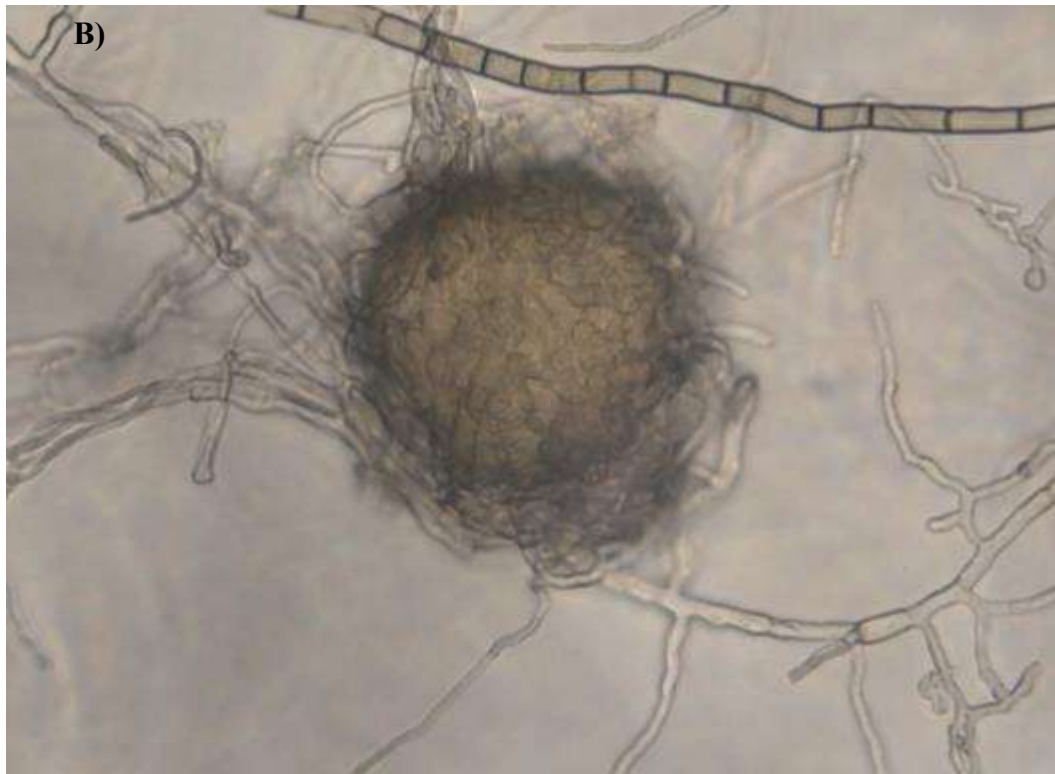
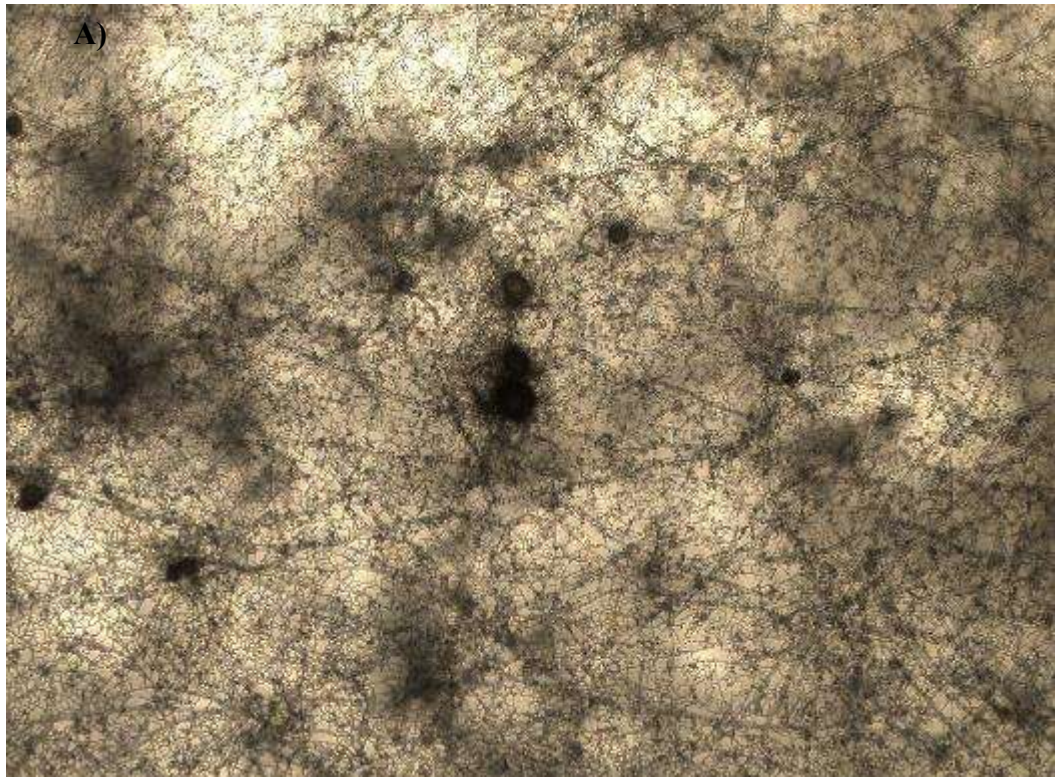


Figure S12. *Sordaria macrospora per5* at day 4, stage 2. Growth in SMM media, inverted microscope at A) 4X and C) 40X magnitude

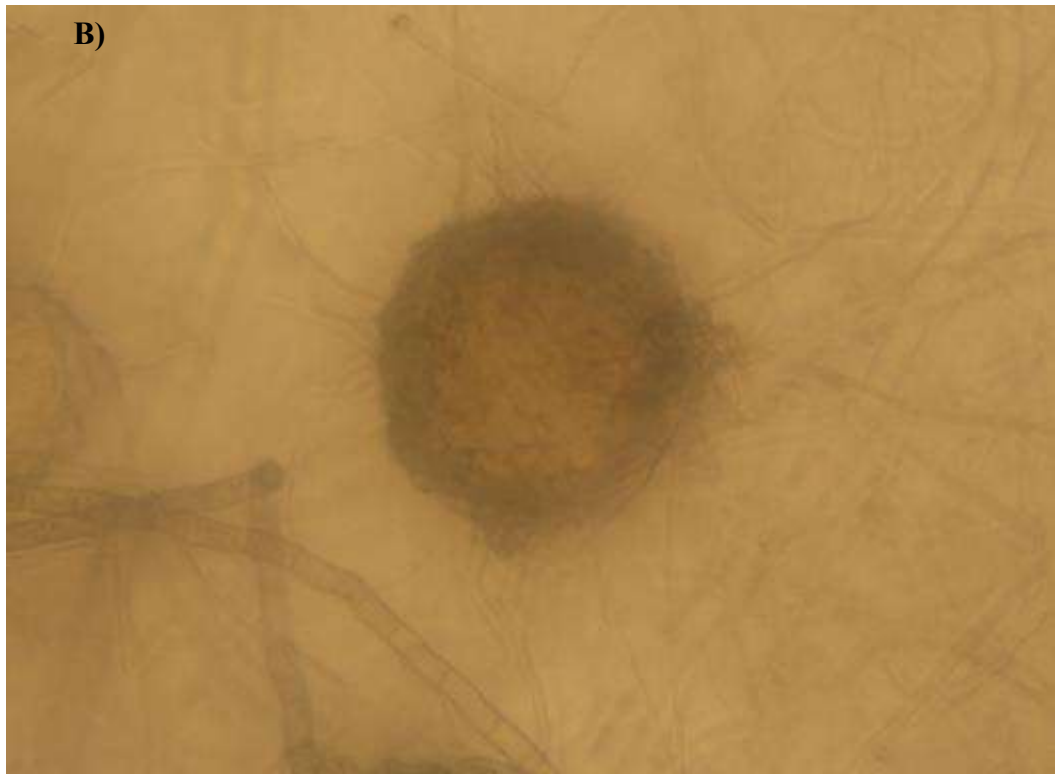
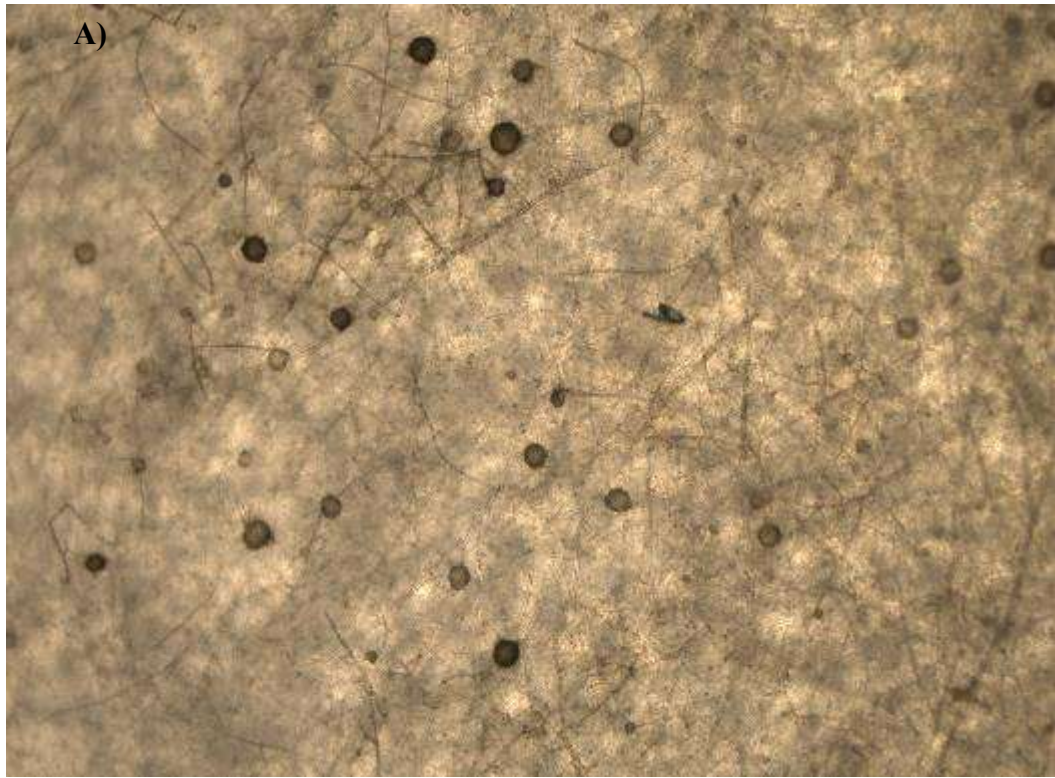


Figure S13. *Sordaria macrospora smgpi1* at day 4, stage 2. Growth in SMM media, inverted microscope at A) 4X and C) 40X magnitude

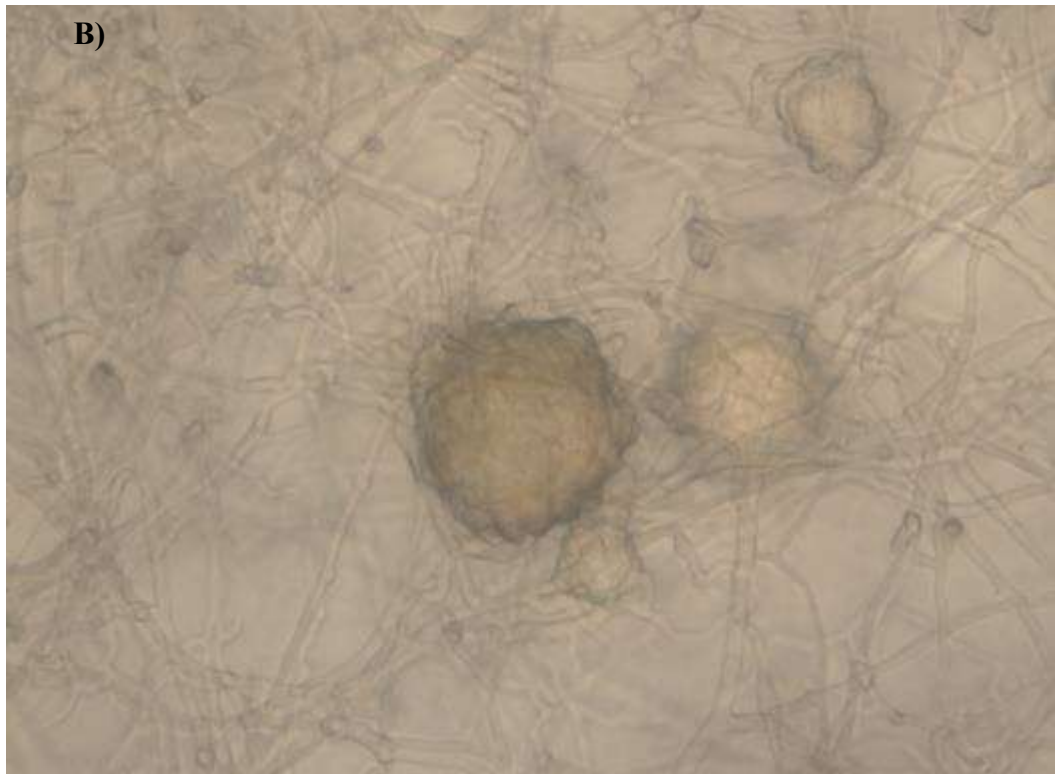
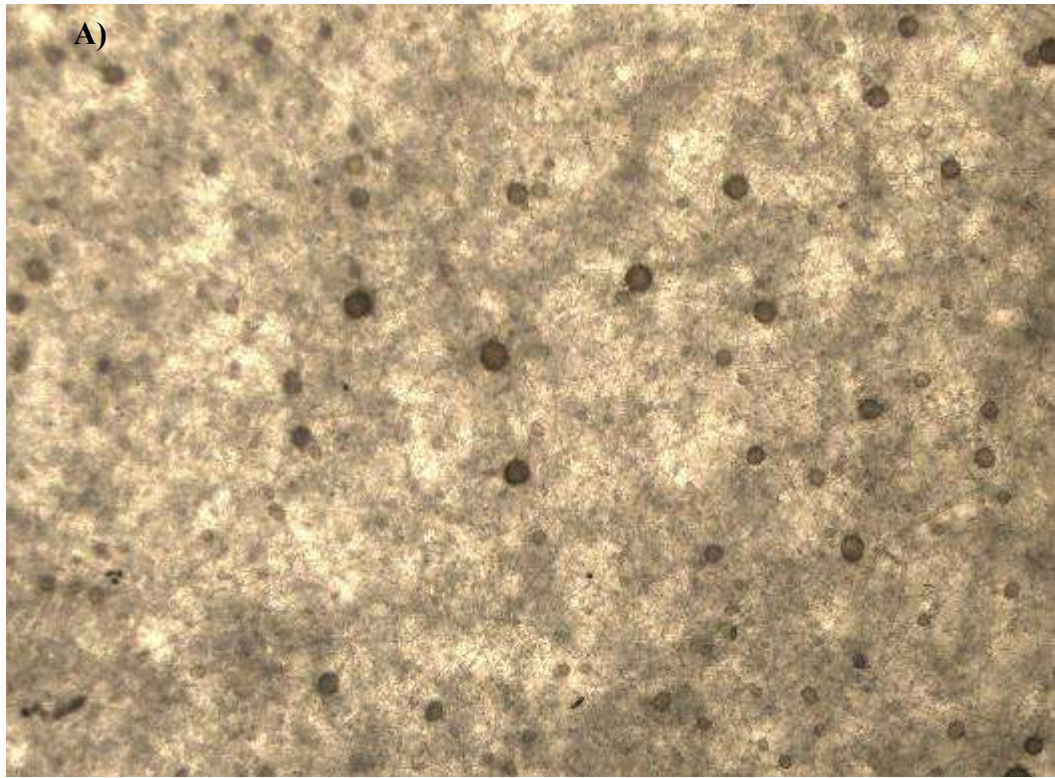


Figure S14. *Sordaria macrospora* wildtype at day 4, stage 2. Growth in SMM media, inverted microscope at A) 4X and C) 40X magnitude

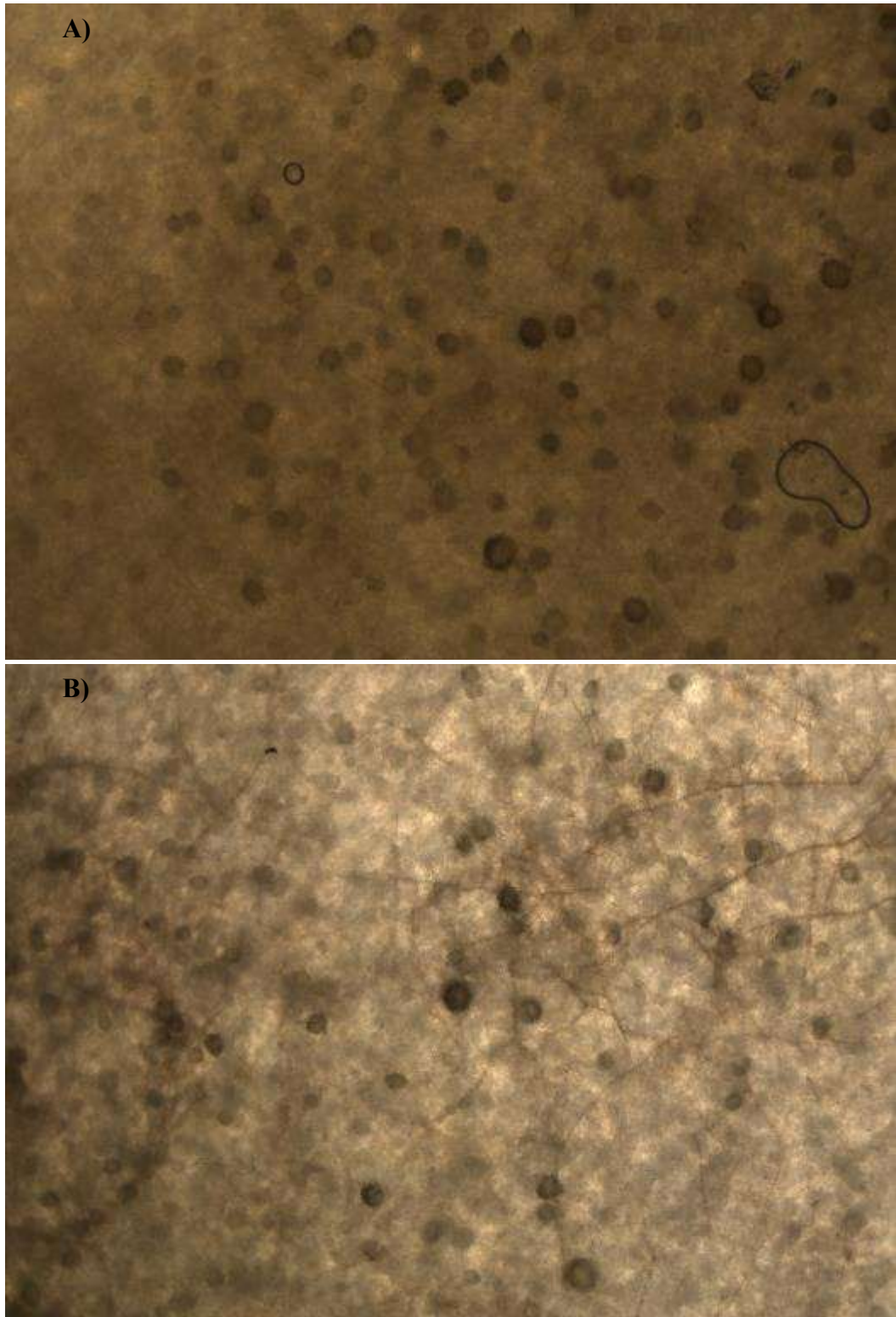


Figure S15. *Sordaria macrospora* day 6, stage 3. Growth in SMM media, inverted microscope at A) 4X for the strain pro1 and C) 4X magnitude for the strain pro11



Figure S16. *Sordaria macrospora per5* at day 6, stage 3. Growth in SMM media, inverted microscope at A) 4X and B) 40X magnitude

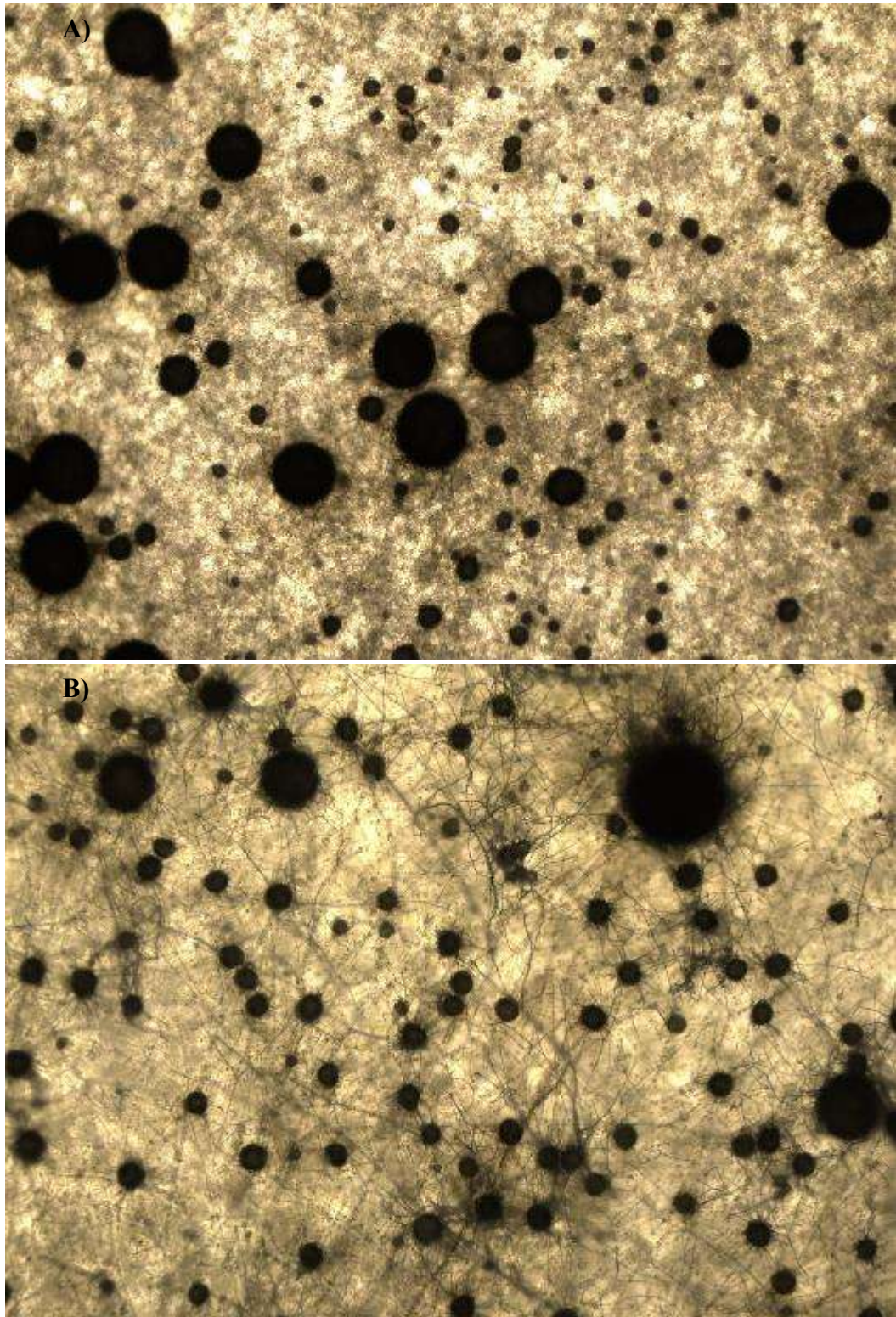


Figure S17. *Sordaria macrospora smgp1* at day 6, stage 3. Growth in SMM media, inverted microscope at A) 4X and B) 4X magnitude

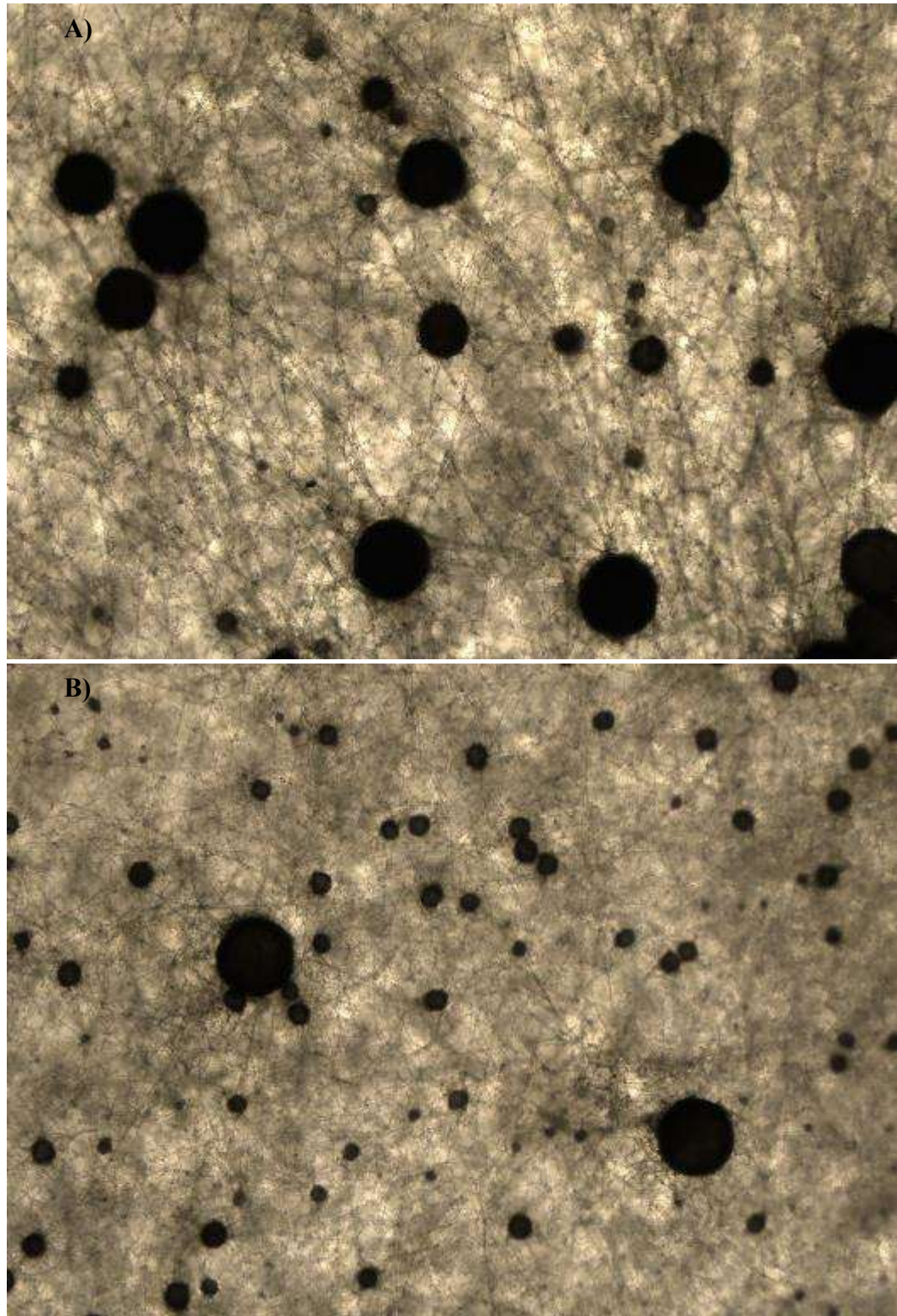


Figure S18. *Sordaria macrospora* wildtype at day 6, stage 3. Growth in SMM media, inverted microscope at A) 10X and B) 4X magnification.

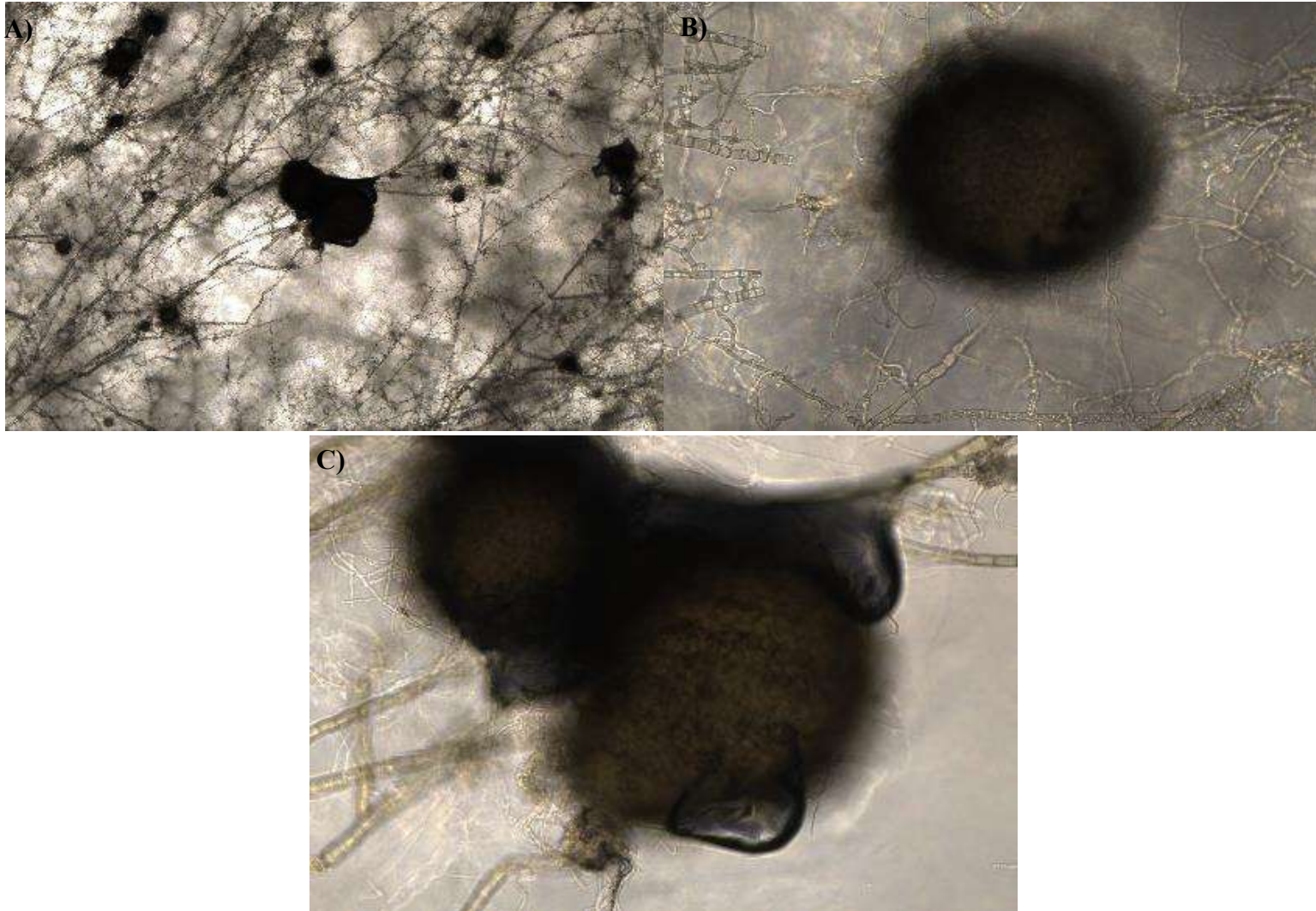


Figure S19. *Sordaria macrospora per5* at day 8, stage 4. Growth in SMM media, inverted microscope at A) 4X, B) 40X, and C) 40X magnification

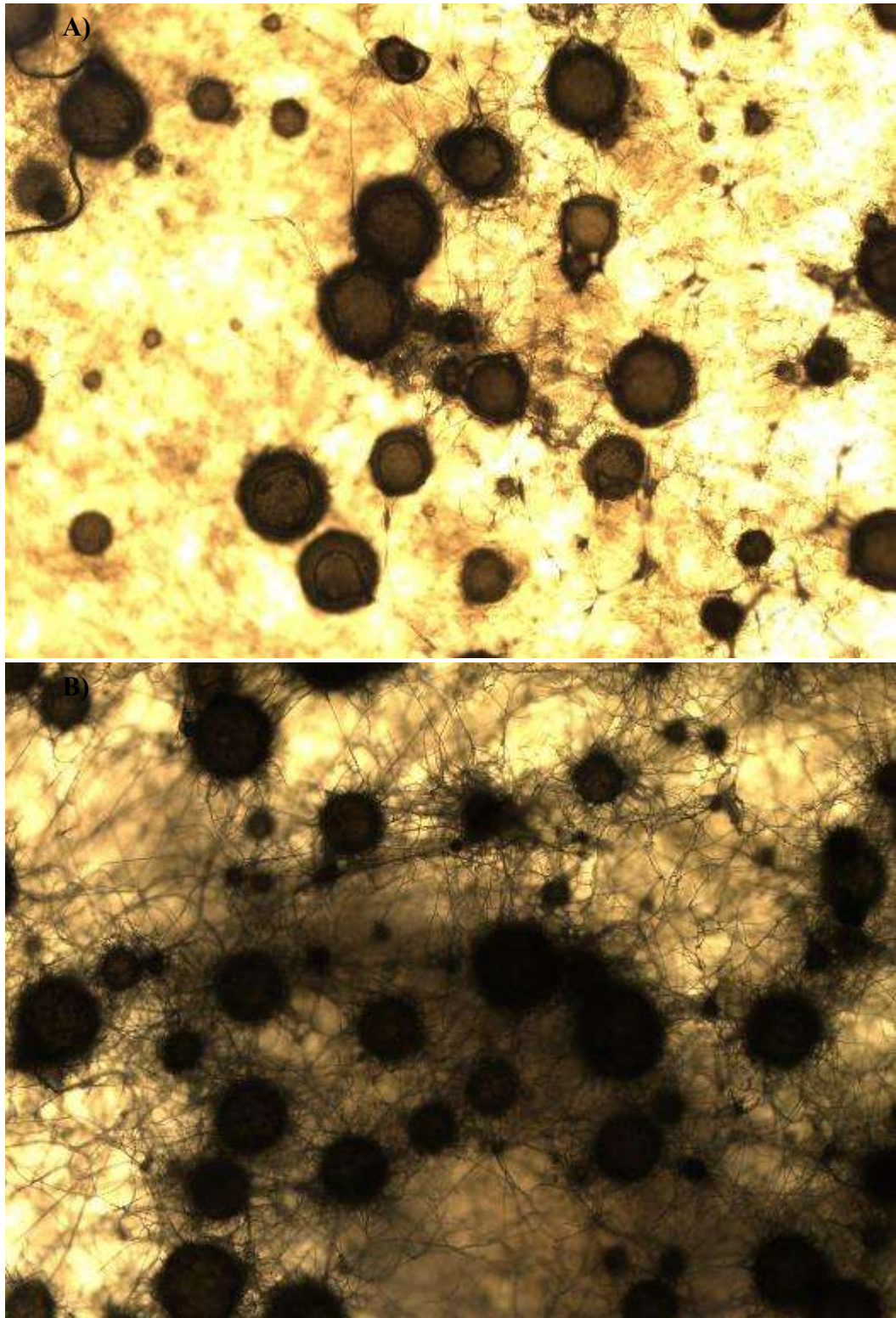


Figure S20. *Sordaria macrospora smgpi1* at day 8, stage 4. Growth in SMM media, inverted microscope at A) 4X and B) 10X magnification.

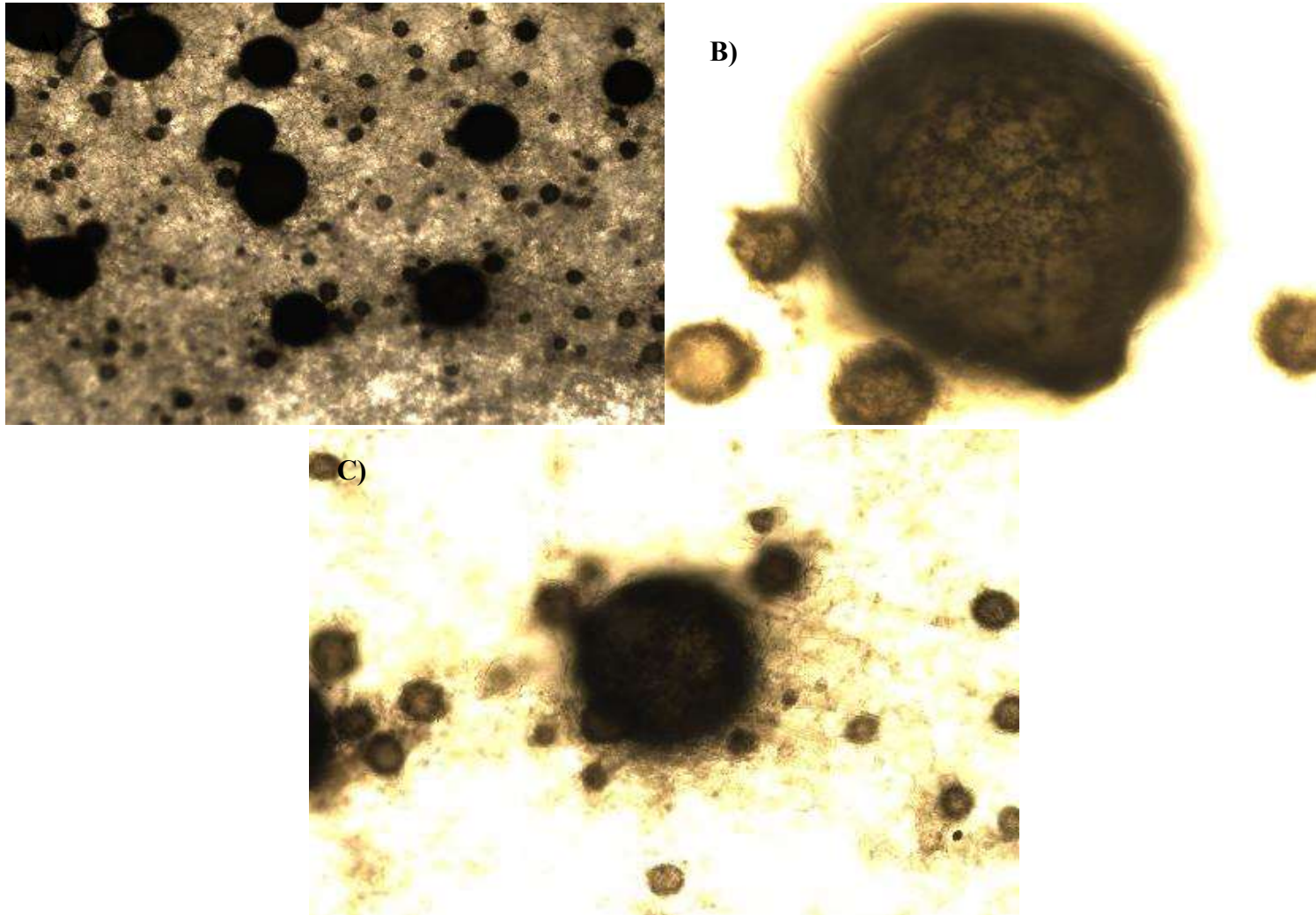


Figure S21. *Sordaria macrospora* wildtype at day 8, stage 4. Growth in SMM media, inverted microscope at A) 4X, B) 20X, and C) 10X magnification..

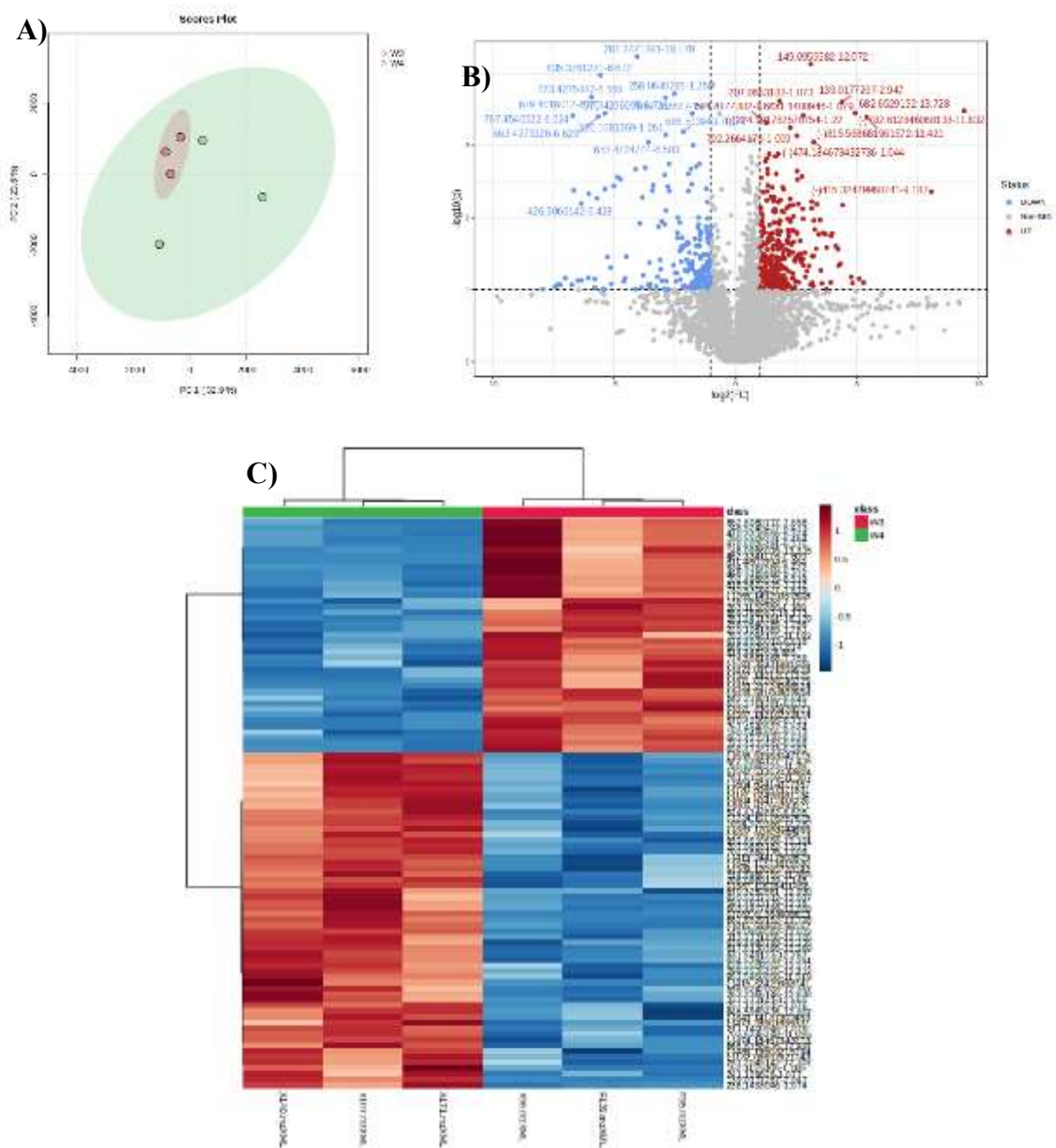


Figure S22. Statistical analysis for lipidomic of *S. macrospora* between stage 2 and stage 3. A) PCA score plot (red stage 2, green stage 3), B) Volcano plot ($p < 0.1$ and $FC > 2$ or < -2), and C) Heatmap (t-Test) for the top 150 top features (red stage 2, green stage 3)

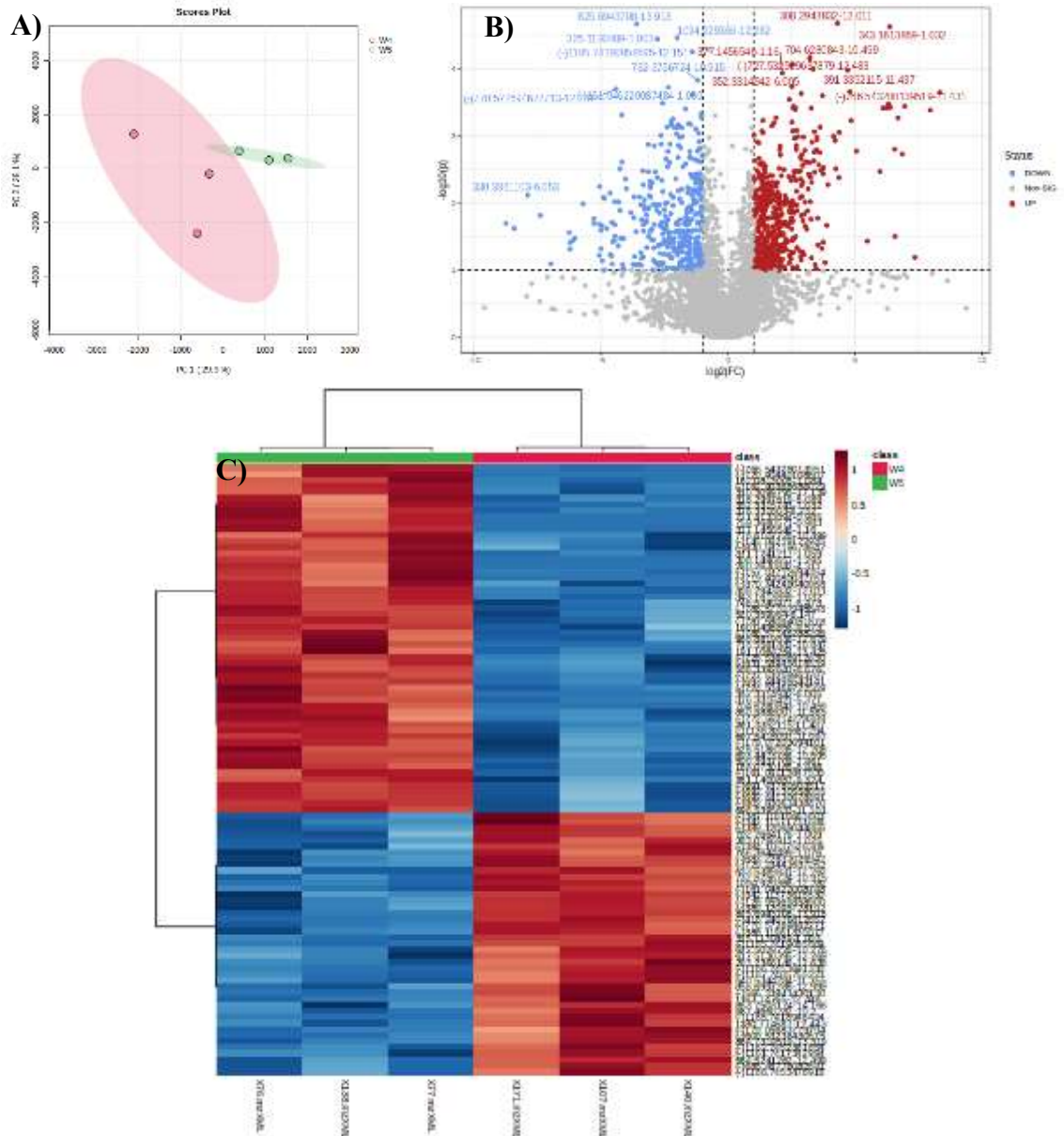


Figure S23. Statistical analysis for lipidomic of *S. macrospora* at stage 3 between wild type and the mutant strain per5 . A) PCA score plot (red stage 2, green stage 3), B) Volcano plot ($p < 0.1$ and $FC > 2$ or < -2), and C) Heatmap (t-Test) for the top 150 top features (red stage 2, green stage 3)